Antibody Responses to Recombinant Oligopeptides of *Pf*EMP1 Isolated From Children Infected With *Plasmodium falciparum*

Thesis

Antibody Responses to recombinant oligopeptides of *Pf*EMP1 isolated from children infected with *Plasmodium falciparum.*

A thesis submitted for the degree of Doctor of Philosophy

Life and Biomolecular Sciences

Open University

Affiliated Research Centre

KEMRI-Wellcome Trust Research Programme, Kilifi, Kenya

James Ogwindi Tuju

March 2013

DATE OF SUBMISSION : 5 APRIL 2013

DATE OF AWARD : 30 OCTOBER 2013

ProQuest LLC.
789 East Eisenhower Parkway
P.O. Box 1346
Ann Arbor, MI 48106 – 1346

ABSTRACT

Individuals living in malaria endemic areas acquire immunity against clinical disease through repeated encounters with the *Plasmodium falciparum* parasite during their childhood. As a result, the majority of severe cases of malaria are restricted to younger children. Naturally acquired immunity is thought to be partly mediated by antibodies directed at parasite derived antigens on the surface of red blood cells infected with mature forms of *P. falciparum* called variant surface antigens (VSA). Of these, *P. falciparum* erythrocyte membrane protein 1 is well characterized and associated with pathology and immune evasion. Sera obtained from young children living in endemic areas show limited recognition of *Pf*EMP1 unlike immune adult sera that exhibit recognition of a wide range of *Pf*EMP1. It is not yet clear whether this wide recognition of PfEMP1 by adult immune sera is exclusively a product of variant specific response accumulated over many exposures or whether it includes a cross-reactive response that recognizes a diverse set of antigens.

Here, I have used the recombinant DBLα-tag region of *Pf*EMP1 generated from parasites isolated from children infected with malaria to show that individuals develop a strong variant-specific response to their infecting isolate, accompanied by partly cross-reactive response. Based on antigenic and genetic similarities between different DBLα-tag variants, I identified potential epitope regions in this study that may account for the cross reactive responses. However, these appear to be conformational and predominantly lie towards the N-terminal end. Once verified, such regions may form good candidates for inclusion in a multi-epitope vaccine construct that affords broad protection against malaria.

ACKNOWLEDGEMENTS

I just want to say that I have learned so much in the past 4 years. I have thoroughly enjoyed my journey to this PhD and writing this thesis. It has been challenging and it would not have been possible if I wasn't surrounded by an excellent scientific community that ensured I had all the support and guidance needed. For that, I would like to sincerely like to thank colleagues at the Kemri-Wellcome Trust Research Programme who in one way or another made this happen.

My deepest gratitude goes out to my supervisory team; Dr. Britta Urban, Dr. Peter Bull and Prof. Kevin Marsh for the excellent supervision, for their patience and for holding my hand and pointing me in the right direction whenever I was lost (many times!). To Dr. Margaret Mackinnon who took me under her wing and selflessly made it her business to teach me all matters statistics, I want to say I big thank you. I would also want to thank Prof Derek Smith and Dr. Collin Russell for taking time off their busy schedule to meet me, for their invaluable advice and for allowing me access to their antigenic cartography software.

I am heavily indebted to my teachers in the lab: Moses Mosobo and Jennifer Musyoki who taught me how to culture parasites; Dr. George Warimwe who taught me most of the Molecular Biology techniques; Alex Macharia and Dr. Isabella Ochola-Oyier for the DNA sequencing lessons and Eva Kimani for the protein expression assay.

I am hugely grateful for the support from the Britta Urban group especially Dr. Evelyn Gitau for ensuring we never lacked in reagents. I will forever be indebted to Henry Karanja for the herculean effort we put in protein expression and for all the discussion we had in the lab.

Special gratitude goes to Dr. Sam Kinyanjui and Liz Murabu from the training department for your assistance with administrative issues ;to the librarian, Alex Maina, for access with publications and to my third party monitor, Dr. Sassy Molyneux for the pastoral care throughout this study.

Last, I want to thank my family, especially my loving wife Domtila, for the support and understanding during this period.

This work was only possible because of the world class facilities at the KEMRI-Wellcome Trust Research Programme and funding from the Wellcome Trust.

DEDICATION

Soli Deo Gloria

Contents

LIST OF FIGURES

LIST OF TABLES

LIST OF ABBREVIATIONS

HIV/AIDS	Human Immunodeficiency Virus/Acquired Immune Deficiency Syndrome
WHO	World Health Organization
DDT	Dichlorodiphenyltrichloroethane
MHC	Major histocompatibility complex
RBCs	Red blood cells
SICA	Schizont-infected cell agglutination
VSA	Variant surface antigens
*Pf*EMP 1	*Plasmodium falciparum* erythrocyte membrane protein 1
RIFINS	Repetitive interspersed family proteins
STEVORS	Subtelomeric variable open reading frame proteins
SURFINS	Surface-associated interspersed family proteins
CD36	Cluster of Differentiation 36
CSA	Chondroitin Sulphate A
ICAM-1	Intercellular Cytoadhesion Molecule-1
CR1	Complement Receptor 1
DBL	Duffy Binding Like
CIDR	Cysteine Rich Interspersed Domain Region
PECAM	Platelet endothelial cell adhesion molecule
PoLV	Position of limited variability
Cys	Cysteine
RNA	Ribonucleic acid
DNA	Deoxyribonucleic acid
cDNA	Complimentary DNA
DEPC	Diethylpyrocarbonate

TE	Tris-EDTA
TBE	Tris Borate EDTA
Rpm	revolutions per minute
LB	Luria-Bertani
PCR	Polymerase chain reaction
dNTP	Deoxyribonucleotide triphosphate
SDS-PAGE	Sodium dodecyl sulfate polyacrylamide gel electrophoresis
ELISA	Enzyme-linked immunosorbent assay
PBS-T	Phosphate buffered saline-Tween
PBS	Phosphate buffered saline
KDa	Kilodaltons
bp	base pairs
ANOVA	Analysis of variance
HI	Hemagglutination inhibition
MN	Microneutralization
OD	Optical Density
OPD	O-phenylenediamine dihydrochloride
HRP	Horse radish peroxidase

LIST OF PUBLICATIONS

Gitau, E. N., **Tuju, J.**, Stevenson, L., Kimani, E., Karanja, H., Marsh, K., Bull, P. C., et al. (2012). T-cell responses to the DBLα-tag, a short semi-conserved region of the Plasmodium falciparum membrane erythrocyte protein 1. *PloS one, 7*(1), e30095. doi:10.1371/journal.pone.0030095

Chapter 1

Literature review

Introduction

1.1 Malaria

Malaria is a major global health problem that has afflicted humans throughout history. It is a disease that is widespread throughout the tropical and subtropical regions of the world where it remains a killer of hundreds of thousands even today (World Malaria Report 2011). The control of malaria, together with HIV/AIDS and other diseases is crucial to the achievement of several of the millennium development goals set by the United Nations by 2015 (United Nations Millennium Declaration,2000). The past decade has witnessed progress in the fight against human malaria. The scaling up of available interventions for the prevention and control of the disease has resulted in decreases in the recorded incidence of the disease in many endemic regions (World Malaria Report 2011). The WHO malaria report estimates that there was a decrease of more than 50% in malaria cases between 2000 and 2010 in 43 of the 99 countries with on-going malaria transmission. This was accompanied by a reduction in malaria mortality of 25% globally and 33% specifically in Africa. These interventions include increased use of effective treatment with artemisinin-based combination therapies (ACTs), long lasting insecticidal nets, rapid diagnostic tests and indoor residual spraying. Improved socio-economic levels may have contributed to this decline.

Despite this apparent evidence that the battle is being won, the war is far from over. The number of malaria cases and deaths, especially among young children in Africa, remain high. In 2010 alone, 216 million cases of malaria were reported worldwide with 81% of these

occurring in sub Saharan Africa resulting in 655,000 deaths globally. An estimated 596,000 of these deaths are reported to have occurred in Africa and were mainly restricted to children under 5 years of age (World Malaria Report 2011). These statistics, from a disease that can be effectively treated when promptly diagnosed, are demoralising. This is further compounded by recent reports of emerging resistance of parasites to artemisinin based therapies and of vectors to insecticides in several endemic areas (Wongsrichanalai & Meshnick 2008; Noedl et al. 2008; Dondorp et al. 2009).

There still remains an urgent need for more investment in vaccine development and drug discovery to come up with better methods for malaria control and eventual elimination and eradication.

The development and deployment of vaccines has played a big role in the fight against infectious agents in the past 6 decades. Vaccination programmes against polio, *H. influenza*, small pox among other diseases have been successful in significantly decreasing the incidence of most of these disease to levels close to eradication (Hebert et al. 2012). Despite the best effort over the past few decades, there is no licensed effective malaria vaccine. The main problem confronting malaria vaccine development has been a poor understanding of the targets and mechanism of protection of the naturally acquired immune response.

Malaria is caused by the protozoan parasites from the *Plasmodia* genus. Members of this genus have evolved to form numerous species that affect almost all vertabrates. Of these, only five cause disease in human: *P. falciparum*, *P. malariae*, *P. vivax*, *P. ovale* and *P. knowlesi*. The most virulent of these species is *P. falciparum* and is responsible for the majority of severe malaria cases and deaths. In the past few years, *P. vivax* has also been recognised as an important public health concern.

1.2 Lifecycle of *P. falciparum*

P. falciparum has a complex lifecycle that involves sexual reproduction in the Anopheles mosquito and asexual reproduction in the human host with several developmental stages that are morphologically and antigenically distinct. Female anopheles mosquitoes inject sporozoites into the skin (Reveiewed by Yamauchi et al. 2007) from where they traverse cells and enter into the peripheral circulation and find their way to the liver. The sporozoites migrate through Kupffer cells and several hepatocytes before finally infecting a hepatocyte (Ishino et al. 2004). In the hepatocyte, the sporozoites differentiate asexually to form schizonts that rupture to release merozoites into the blood stream and infect red blood cells and begin the erythrocytic stage of asexual development. During a 48 hour period, the parasites differentiate within the red blood cells from the young ring stage, to mature trophozoites and finally to schizonts that rupture to release merozoites that re-infect red blood cells to initiate another round of asexual replication (Reveiwed by Kyes et al. 2001). The cyclical fevers that characterize malaria infection are caused by pyrogenic substances that are released into circulation when schizonts rapture (Clark et al. 1987; Clark et al. 1981; Sherry et al. 1995; Karunaweera et al. 1992). After several rounds of asexual reproduction, a few of the merozoites differentiate into male and female gametocytes that are ingested by a feeding mosquito to initiate sexual development.

In the midgut, the male and female gametes are released and fuse to form a diploid zygote that differentiates to form an ookinete that traverses the gut of the mosquito and further differentiates into an oocsyt that undergoes asexual reproduction to produce haploid sporozoites. Once they mature, oocsyts rupture to release thousand of sporozoites that

migrate to the salivary glands from where they are transmitted to humans during a blood meal (Sinnis & Coppi 2007).

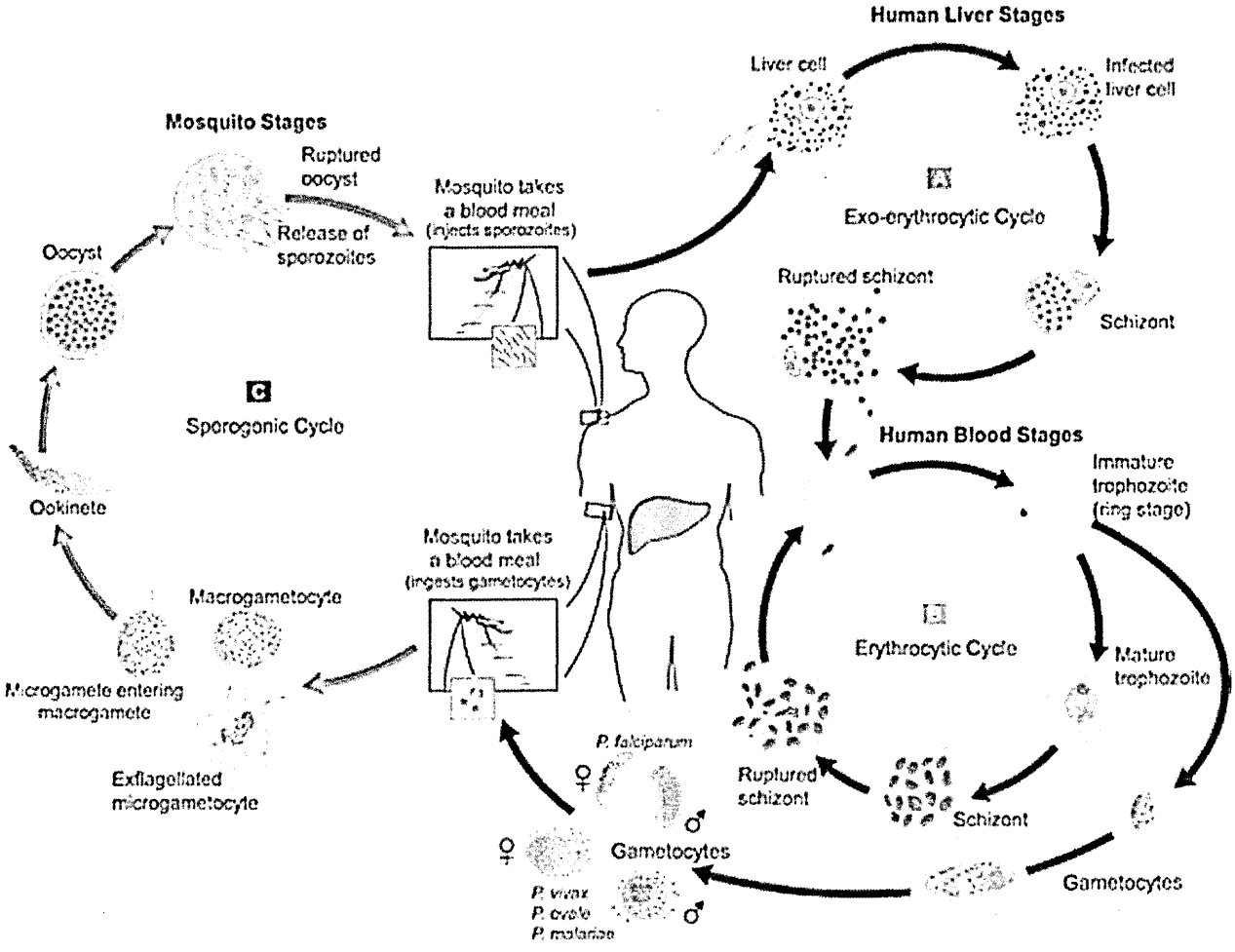

Figure 1.1 Life cycle of *Plasmodium falciparum*. The diagram shows the different stages of development of the parasite in the asexual stages, i.e., red blood cells (A) and the liver (B) that take place in the human host, and the sexual stages (C) that happen in the mosquito vector.
(Adapted from www.dpd.cdc.gov/dpdx).

1.3 Naturally acquired immunity to malaria

That people become immune to malaria in endemic areas is not in doubt. In areas of high malaria endemicity, individuals are continuously infected by *P. falciparum* but only infants,

young children and malaria-naïve visitors suffer from clinical disease; the majority of the older children and adults enjoy protection against severe morbidity and mortality. The ability of older residents to resist disease is what constitutes naturally acquired immunity (Reveiwed by Doolan et al. 2009). It is the beacon that gives malaria vaccinologists hope that the development of a malaria vaccine is feasible. Development of strategies that mimic the adult like immune status among high-risk infants in malaria endemic regions will greatly diminish malaria related morbidity and mortality. A vaccine based on this approach would be an attractive option as it would afford children protection from disease and the additional benefit of natural boosting from continuous exposure.

1.3.1 Features of naturally acquired immunity

Naturally acquired immunity is acquired after a prolonged period of intense uninterrupted exposure to the parasite and at a rate that is determined by the degree of exposure. Individuals living in areas with intense transmission develop this protection faster compared to their age-matched counterparts in areas with less intense transmission. As a result the proportion of people who are susceptible to disease in high intense transmission areas is smaller compared to regions where transmission is decreased (Snow et al. 1997).

The continuous intense exposure is required not only for the development but also for the maintenance of this immunity. Protection is diminished or lost when individuals move to non-malarious areas (Jelinek et al. 2002; Matteelli et al. 1999). This has profound implications for interventions that aim to decrease the level of transmission in these settings as was discussed by Snow and colleagues (Snow et al. 1997). Interventions that eliminate exposure or decrease it to levels that cannot maintain naturally acquired immunity should

be carefully designed to be highly effective, long-acting or sustainable for a long period and have absolute coverage of the endemic areas when implemented. Failure to this will result in epidemic malaria as such interventions prevent non-immune individuals from acquiring natural immunity and re-introduces susceptibility to severe disease in previously immune people.

This was best observed in the malaria epidemic that occurred in the highlands of the Madagascar in the 1980s (Reviewed by Mouchet et al. 1997). After a successful period of control in the 1950s in which the highlands were rendered malaria-free by DDT spraying and free distribution of anti-malarials for chemotherapy, an abandonment of the control efforts in the 60's and 70's resulted in rebound malaria infections that caused the deaths of more than 40,000 people across all age groups (Reveiwed by Mouchet et al. 1997). This observation is of particular importance today as the recent decline in malaria has partly been contributed to by vector control programs and widespread distribution of long lasting insecticide treated nets that prevent people from developing natural immunity (Lengeler 2004).

Naturally acquired immunity develops relatively rapidly against severe malaria perhaps after only a few episodes of disease during childhood then gradually against mild malaria. Sterilizing immunity against infection is maybe never acquired and asymptomatic parasitemia is common among clinically immune adults. Older children and adults protected from disease in areas with stable transmission will often have asymptomatic parasitemia (Reveiwed by Doolan et al. 2009; Marsh & Kinyanjui 2006.; Baird 1998). These low level

parasites are thought to mediate protection via a poorly studied mechanism called premunition (Sergent & Parrot 1935).

1.3.2 Targets and mechanism of natural acquired immunity

The underlying mechanisms of the acquired protection and the molecular targets remain unresolved. It is known, however, that humoral immunity is a key component of this protection. This was demonstrated by early experiments in which passive transfer of antibodies purified from the sera of malaria immune adults to sick children resulted in resolution of both disease and parasitemia (Sabchareon et al. 1991; Edozien et al. 1962; Cohen et al. 1961).

The resolution of parasitemia by passively transferred antibodies and the prolonged period of exposure characterized by repeated infections for onset of protective immunity when taken together point to a cumulative acquisition of antibodies to a diverse repertoire of asexual stage antigens. During the asexual stage, the merozoites that invade red cells develop into young ring stage trophozoites to the more mature trophozoites and schizonts stages as discussed earlier. At each of these stages, the parasite presents the immune system with a myriad of antigens. In an area with stable transmission, exposed individuals continually make antibody responses to these antigens. Not all of these responses are important for protection. Identifying the antigens that are targets of clinical immunity, and the mechanism by which it is effected, remains a top priority of malaria immunology. Although acquisition of antibodies to antigens expressed by merozoites may play an important role in naturally acquired immunity to malaria (Ramasamy et al. 2001; Doolan et al. 2009), the scope of this literature review and the studies conducted in this thesis are limited to a family of antigens expressed on the mature stages of the parasite.

1.4 The intra erythrocytic stage

The red blood cells form a safe niche that allows parasites to hide from the surveillance of the adaptive immune system during development of the blood asexual stages. Red blood cells lack MHC molecules on their surfaces and thus cannot present antigens to the immune system (Brown et al. 1979). However, as *P. falciparum* parasites mature within the red blood cells they present what, at face value, appears to be a suicidal development by exporting antigens to the surface of the infected red cells. These antigens allow the parasite to interact with receptors on endothelial surfaces and sequester away from circulation as one of their functions (Reveiwed by Kyes et al. 2001).

The presence of parasite antigens on the surface of infected red blood cells was demonstrated by Eaton who pioneered the use of micro agglutination serological assays in the late 1930s. In his experiments, Eaton observed that an agglutination reaction occurred when red blood cells infected with mature forms of *P. knowlesi* where mixed with sera obtained from rhesus monkeys previously infected with the same parasite. The agglutination was not observed when red blood cells infected with young merozoites or sera obtained from non immune monkeys were used (Eaton 1938). This indicated that the mature forms of the parasites introduced foreign components on the surface of the red cell that were recognizable by the immune responses against the *P. knowlesi*.

In subsequent experiments, it was demonstrated that during chronic *P. knowlesi* infection in rhesus monkeys, the parasite was able to change the antigens inserted on the surface of the red cells resulting in a series of immunologically distinct variants within the courses of a single infection (Brown & Brown 1965). This change in antigenic phenotype was thought to

be a mechanism by which the parasite escaped from the antibody response and allowed it to maintain chronic infection. This was the earliest demonstration of the concept of antigenic variation in a malaria model. This phenomenon was confirmed in a later conclusive study that reproduced the same results using clonal lines of *P. knowlesi* (Barnwell et al. 1983). The conclusion from these early experiments was that naturally acquired immunity was a product of the accumulation of antibodies to these antigens in a variant specific manner; a view that is consistent with the long period of continuous exposure required for the onset of clinical immunity. Similar observations were made in squirrel monkeys that infected with *P. falciparum* (Hommel et al. 1982).

The ability to culture *P. falciparum* paved the way for the development of similar agglutination studies in humans. From these studies, it was observed that, as with *P. knowlesi,* agglutination only occurred between red blood cells infected with mature trophozoites and immune sera (Sherwood et al. 1985; Marsh et al. 1986); clonal populations of *P. falciparum* in continuous culture undergo changes in the antigenic and adhesive phenotype at the red cell surface and that agglutination is largely variant specific (Udeinya et al. 1983; Smith et al. 1995). Agglutination studies done using clinical isolates indicate that after infection, individuals developed an antibody response that was predominantly isolate-specific (Marsh & Howard 1986; Newbold et al. 1992; Bull et al. 1998; Giha et al. 1999; Forsyth et al. 1989; Iqbal et al. 1983; Southwell et al. 1989).

1.5 A case for strain-transcending immunity

In their landmark study demonstrating antigenic variation in *P. knowlesi* (Brown & Brown 1965), Brown and Brown reported that although the immune responses to the schizont-

infected cell agglutination (SICA) antigens was acquired largely in a variant specific manner, it was accompanied by the development of a strain transcending antibody response; a part of their work that is rarely acknowledged. In their experiments, Marsh and Howard, showed that isolate-specific antibodies were capable of agglutinating a panel of heterologous *P. falciparum* infected red blood cells (Marsh & Howard 1986). In addition, they also observed strain transcending responses, and as with Brown and Brown, this is often overlooked. A subsequent study that tested the ability of sera to co-agglutinate pairs of differentially stained *P. falciparum* infected red blood cells observed only single colour agglutinates indicating that immune responses were largely variant specific (Newbold et al. 1992). Chattopadhay and colleagues exploited the same test in a larger sample of parasite pairs against sera obtained from adults who had experienced single monoclonal *P. falciparum* episodes and observed both single- and mixed-color agglutinates indicating both variant-specific and strain transcending responses were present (Chattopadhyay et al. 2003). The frequencies with which the variant surface antigens are recognized by sera in a population vary (Bull et al. 1999). Parasites isolated from severely ill children have variant surface antigens that are more frequently recognized by plasma from semi-immune children and are preferentially expressed in non-immune host as compared to parasites isolated from uncomplicated or asymptomatic infections (Bull et al. 1999; Bull et al. 2000; Nielsen et al. 2002; Lindenthal et al. 2003). The high frequency of recognition is a common phenotype of parasites infecting young (non-immune) children. The differences in these early studies could be explained by the choice and number of parasite pairs used in the test as well as differences in age and exposure of the host.

In a different study, Aguiar and colleagues observed that sera collected from different geographical regions agglutinated parasites isolated from sick children in Tanzania and Gambia, indicating the presence of either identical or cross reactive antigenic variants circulating in different places (Aguiar et al. 1992). The acquisition of strain-transcending immunity after a single infection has been observed in other studies using different methodologies (Elliott et al. 2007). In this study, serum collected from previously malaria naïve travelers who were diagnosed with malaria after visiting malaria endemic areas was used. Heterologous recognition of the antigens on the surface of the infected red cells as measured by flow cytometry was observed in 11 of the 14 sera tested.

This broad specificity of immune sera from adults indicates that the antigenic repertoire is limited. Although this is mainly a product of multiple specificities to many variants acquired after prolonged exposure, there is some level of cross reactive responses generated. The contribution of these responses to natural immunity is poorly defined. The studies described in this thesis, explore the extent to which such responses are generated against DBL-α tag a recombinant segment of one of the main antigens expressed on the surface of the infected red blood cells using a subset of parasites isolated from children admitted to hospital with disease.

1.6 Antibodies on the surface of the infected red cells are targets of naturally acquired immunity

Antibodies to the variant surface antigens (VSA) introduced at the surface of the red blood cells (RBC) by the infecting parasites are thought to be an important component of naturally acquired immunity. In a study done in the Gambia, Marsh and Howard showed that children

develop antibodies to the parasite antigens on the surface of the red cell after exposure (Marsh & Howard 1986). A study done in Kenya showed that parasites isolated at the time of acute disease are likely to express antigens on the red blood cells that cannot be recognized by pre-existing antibodies in children at the time of disease (Bull et al. 1998). In this large prospective study, Bull and colleagues obtained sera from children at the beginning of the malaria season and followed them up for disease for the next 8 months. Parasites obtained from children who fell ill during this period were tested for reactivity by the agglutination reaction with homologous sera obtained from the sick children at the beginning of the malaria season, at the time of infection as well as to sera obtained from community age-matched controls. The homologous sera obtained before the malaria season was less likely to recognize the homologous isolate compared to the sera obtained from age-matched controls. Taken together, this implies that malaria is caused by parasite expressing variants of antigens on the surface of red blood cells to which the host lacks antibodies. Further support for this comes from studies done in Sudan that show a decreased likelihood of infection with homologous parasites to which individuals have a pre-existing humoral response (Giha et al. 2000; Dodoo et al. 2001).

1.7 Antigens on the surface of the *P. falciparum* infected red blood cell

A number of antigens have been identified on the surface of the infected red blood cell. These include the *Plasmodium falciparum* erythrocyte membrane protein (*Pf*EMP1) (Leech et al. 1984), subtelomeric variable open reading frame proteins (STEVORS) (Carcy et al. 1994) and surface-associated interspersed family proteins (SURFINS) (Winter et al. 2005).

The group A subtype of repetitive interspersed family proteins (RIFINS) have also been shown to be on the surface of infected red blood cell (Kyes et al. 1999; Kyes et al. 2000; Petter et al. 2007) *Pf*EMP1 is the most extensively studied of these and is thought to be the major target of the VSA-specific antibodies. All these proteins are encoded by multi-gene families and are co-expressed together on the surface of an infected red blood cell making it difficult to directly determine the specific role of each family in the development of naturally acquired immunity.

Chan and colleagues have recently developed an ingenious strategy that allowed them to generate genetically modified *P. falciparum* parasite lines in which expression of PfEMP1 was silenced. The genes encoding *Pf*EMP1 are under a mutually exclusive transcription that is partly controlled by their promoters. In this study, a drug selectable marker under the control of a promoter from a gene encoding native *Pf*EMP1 was transfected into parasites. When the parasites were grown under drug pressure, expression of the marker allowed the transfectants to grow and silenced endogenous *Pf*EMP1 transcription. Using 2 parasite lines they observed significant reduction in the recognition of red cells infected with PfEMP1-silenced parasites line by sera obtained from immune adults (Chan et al. 2012). In addition, the PfEMP1-silenced parasites showed significant decreased opsonic phagocytosis and binding to host receptors in vitro. All together, these data point to a role of PfEMP1 in cytoadhesion and as the major target of naturally acquired antibodies that target the surface of infected red blood cells. There has been increased interest in the non-PfEMP1 surface antigens in the recent past and early reports implicating RIFINs and STEVORs in the development of acquired immunity. It is possible that the parasite lines used by Chan and colleagues in their investigations were expressing poor immunogenic forms of the non-

PfEMP1 surface antigens and this would exaggerate the role of PfEMP1 in humoral immunity. More extensive studies that include many infected red blood cells expressing different variants of these antigens are required before a conclusive argument can be made.

1.8 *Pf*EMP 1

*Pf*EMP 1 is a family of high molecular weight polymorphic proteins of parasite origin that are inserted on the surface of *P. falciparum* infected red blood cells at the mature stages where they mediate adhesion to host receptors on endothelial cells (Leech et al. 1984; Baruch et al. 1995; Smith et al. 1995; Su et al. 1995). This sequesters the parasite away from circulation and as a result, only erythrocytes infected with very young *P. falciparum* trophozoites (ring stages) circulate in the peripheral blood, but nearly all infected red blood cells containing mature trophozoites and schizonts are sequestered in the capillary vessels of different organs. This is thought to be a mechanism by which parasites avoid splenic clearance. This is supported by the observation that infection of individuals with no spleen results in the circulation of the mature forms of the parasites that are usually sequestered (Bach et al. 2005; Bachmann et al. 2009; Demar et al. 2004; Looareesuwan et al. 1993). Repeated passage of adherent parasites in splenectomized monkeys and in mice resulted in a phenotype in which parasites no longer expressed variant surface antigens which this was restored when the parasites were used to infect animals that had a spleen (Barnwell et al. 1982; Barnwell et al. 1983; Handunnetti et al. 1987).

The adherence of infected red blood cells to host tissues and to other cells is thought to be the major factor that makes *P. falciparum* more virulent than other human malaria parasites. The cytoadherent properties of infected red blood cells arise mainly from the

introduction of *Pf*EMP 1 at the erythrocyte surface. *Pf*EMP 1 can bind to a diverse range of host receptors that include CD36 (Baruch et al. 1997), Intercellular Cytoadhesion Molecule-1 (ICAM-1) (Berendt et al. 1989), Chondroitin Sulphate A (CSA) (Rogerson et al. 1995) and Complement Receptor 1(CR1) (Rowe et al. 1997).

Most of these receptors exhibit heterogeneity in phenotype and levels of expression in different organs while PfEMP1 variants differ in their affinity to these receptors. This results in the accumulation of parasites expressing certain variants in specific organs. This is partly responsible for the different clinical manifestation of the disease. Adhesion to ICAM-1, a receptor enriched on brain endothelial surfaces, has been associated with cerebral malaria (Fernandez-Reyes et al. 1997; Turner et al. 1994; Newbold et al. 1997)whereas rosetting (Udomsangpetch et al. 1989), a phenotype where infected red blood cells bind non infected red blood cells, is associated with severe anaemia and generally severe disease (MacPherson et al. 1985; Rowe et al. 1995; Carlson et al. 1990). By contrast, parasites from children with mild disease tend to bind better to CD36 (Newbold et al. 1997; Rogerson et al. 1999; Ochola et al. 2011).

The association between the adhesion phenotype of particular PfEMP1 variants and disease is best exemplified by parasites causing placental malaria. The clinical immunity developed against disease by women living in malaria endemic areas is suddenly breached by parasites during their early pregnancies (McGregor 1984). This arises because the development of the placenta presents a novel ecological niche that sequesters parasites away from circulation. Parasites bind to CSA and hyaluronic acid expressed on the placenta in a process mediated by PfEMP1 (Fried & Duffy 1996; Beeson et al. 2000). Studies have identified var2csa as the specific PfEMP1 responsible for this phenotype (Salanti et al. 2003) and it forms a promising

vaccine candidate against placental malaria. In addition to sequestration, *Pf*EMP 1 mediates antigenic variation as described earlier. It is therefore conceivable that in the absence of negative selection by immune responses, availability of particular receptors or polymorphic variants of receptors may favor the binding of particular PfEMP1 variants. As a result, parasites expressing such variants can evade immune clearance in the spleen and will dominate that infection.

Malaria parasites are adapted to invade and propagate within the red blood cells. As a result, human genetic polymorphisms in red blood cell components critical for the optimal survival of parasites will modify risk of developing malaria. Hemoglobin, found within the red blood cells, is the main oxygen carrier in the body. Genetic resistance to malaria has been demonstrated for polymorphisms that affect the structures of the human B-globin gene, i.e., heterozygous hemoglobin S (sickle cell trait, HbAS) (Allison 1954), homozygous hemoglobin C (HbCC) (Agarwal et al. 2000) and haemoglobin E (HbE) (Flatz et al. 1965). In addition, the inability to express optimum levels of the globin chains (α & β-thalassaemias) (Flint et al. 1986; Yenchitsomanus et al. 1986; Willcox et al. 1983) as well as deficiencies in glucose-6-phospate (ALLISON & CLYDE 1961) and pyruvate kinase dehydrogenases (Durand & Coetzer 2008) have been implicated in providing innate resistance to disease. Other human genetic conditions that affect the risk of disease include the South-East Asia ovalocytosis (Castelino et al. 1981) and Duffy antigen/chemokine receptor (Miller et al. 1976). The uneven distribution of these traits in malaria endemic area is thought to be the result of evolutionary selection pressure from malaria.

1.9 *Pf*EMP 1 variants isolated from severe cases are serologically conserved

There is increasing evidence that the expression of *Pf*EMP1 in non-immune hosts is not random. Although more work needs to be done in epidemiological settings, limited data from lab isolates selected with sera from severe cases support the hypothesis that parasites infecting non-immune hosts tend to express a restricted sub-group of these antigens that are also implicated in causing severe malaria (Staalsoe et al. 2003; Jensen et al. 2004). This suggests that parasites isolated from severe malaria express a sub-group of PfEMP1 that have a survival advantage over parasites isolated from mild malaria cases in the non-immune host. This advantage however may come at the expense of epitope diversity as immunity to severe, non-cerebral malaria develops much quicker compared to immunity to mild malaria (Gupta et al. 1999). In addition, parasites isolated from severe malaria cases express PfEMP1 variants which are more frequently recognized by immune sera than those expressed by parasites isolated from uncomplicated (Bull et al. 2000; Nielsen et al. 2002). This high frequency of recognition is a common phenotype of parasites infecting young (non-immune) children (Bull et al. 2000; Nielsen et al. 2002). The high frequency of recognition may be due to restricted epitope diversity brought about by functional constraints as exemplified by parasites causing pregnancy associated malaria (Fried et al. 1998).

1.10 *var* genes

PfEMP1 molecules are encoded by a multi-gene family called the *var* genes (Su et al. 1995; Baruch et al. 1995; Smith et al. 1995). Each parasite contains between 50-60 copies of these

genes in their genome (Gardner et al. 2002). The majority of these genes are found in subtelomeric regions of the chromosomes where they cluster together with genes encoding members of the *rif* and *stevor* gene families. With a few exceptions, members of this multi-gene family exhibit extreme polymorphism both within and between genomes resulting in almost unlimited numbers in a parasite population (Barry et al. 2007).

In order to maintain chronic infection, the parasites maintain a tight control in the expression of *var* genes in an immune environment. At any point, the parasites expresses only one *var* gene while the rest are silenced in what is termed mutual exclusive expression (Chen, V Fernandez, et al. 1998; Scherf et al. 1998; Kyes et al. 2000) although expression of two different PfEMP1 on infected erythrocytes has been described (Joergensen et al. 2010). This ensures the parasite does not expose its entire repertoire of variant antigens all at once to the immune system. However, recent work shows that this does not prevent this from happening at the population level (Warimwe et al. 2013). Expression appears to be regulated at the transcription level in an epigenetically controlled process that involves promoter-promoter interactions. Each *var* gene has a 5'-upstream promoter that is transcribed to produce mRNA that is translated into protein and an intronic promoter that is transcribed to produce "sterile" mRNAs that do not form protein. Mutually exclusive expression requires the pairing of the 5'-upstream and the intronic promoters and removing the latter results in constitutive transcription of the gene controlled by the 5'-upstream. In addition, reversible acetylation and methylation of histones and sub-nuclear localization are known to shift the genes on and off between transciptionally active states (Tonkin et al. 2009; Duraisingh et al. 2005).

All *var* genes have the same basic structure consisting of two exons separated by an intron. The first exon encodes the extracellular portion that is divided into distinct domains (N-terminal sequence, Duffy Binding Like domains (DBL) and Cysteine Rich Interspersed Domain Regions (CIDR)). The second exon encodes the intercellular and relatively conserved acidic terminal sequence (Gardner et al. 2002; Smith et al. 2000). The DBL domains have been classified into 5 major homology groups based on sequence alignment i.e. DBLα, β, γ, δ, and ε. Similarly, the CIDR domains are classified into 3 main classes i.e. CIDRα, β and γ (Smith et al. 2000; Rask et al. 2010). Binding of PfEMP1 to particular host receptors has been mapped to specific PfEMP1 domains: DBLα has been associated with binding to heparin sulfate (HS) (Chen, Barragan, et al. 1998), blood group A antigen and complement receptor 1 (CR1) (Rowe et al. 1997), DBLβ with binding to ICAM-1 (Smith et al. 2000), DBLδ with binding to PECAM-1 on platelets whereas binding of CD36 has been associated with CIDRα domains (Baruch et al. 1997).

In addition to sequence polymorphisms, *Pf*EMP1 members vary in the number and composition of DBL and CIDR domains. In spite of this conserved pairing of certain domains is observed across multiple genomes (Rask et al. 2010). In particular, the overall structural organization of the N-terminal half of most *Pf*EMP1 molecules studied so far is relatively conserved (Chen et al. 2000). It is made up of the N-terminal sequence, DBLα and CIDRα domains together forming a conserved head structure. Despite considerable sequence heterogeneity, the DBLα domain is the most conserved domain within and between parasite isolates. It contains short stretches of conserved sequence that have been used to design universal primers with which DBLα tags from field and lab isolates can be sampled (Taylor et al. 2000). Bull et al have exploited distinct sequence features within these tags to classify

these DBLα tag sequences into 6 groups. This classification is based on short blocks of sequences showing limited variability (PoLV) and the number of Cysteine residues (Cys) (Bull et al. 2007).

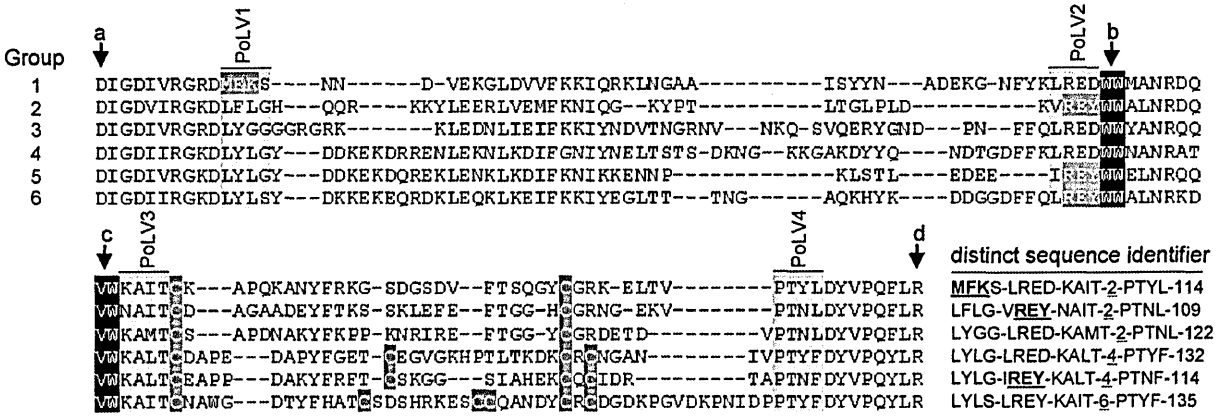

Fig 1.2 Classification of DBL*α* tag sequences. The classification system relies on the number of Cysteine residues and the four positions of limited variability marked PoLV 1-4. The PoLVs are located in the sequences using anchor points a, b , c and d. The 6 sequences are representative of the 6 DBL*α* tag sequence groups and indicated the PoLV motifs associated with each group. Figure adapted from (Bull et al. 2007)

The PoLV/Cys classifications groups have been shown to independently associate with immune status of the patient, disease syndromes as well as parasite phenotype. A small study by Bull and colleagues involving 12 parasites showed that parasites isolated from children with poor agglutinating antibody responses were likelier to express Cys2 DBL-α tags with MFK motif at PoLV1 (Bull et al. 2005) . In addition, this group reported an association between PoLV group 2 sequence tags and the rosetting phenotype. In a separate study done in Mali, Kyriacou and colleagues observed that parasites isolated from children with cerebral malaria predominantly expressed cys2 DBL-α tags (Kyriacou et al. 2006). A recent study by Warimwe and colleagues sampled 14,516 DBL-α tags from 217 clinical isolates from Kenyan children observed an association between cys2 DBL-α tags with severe malaria anemia and impaired consciousness (Warimwe et al. 2009).

Other investigators have grouped *var* genes in the 3D7 genome into 3 major groups (A, B and C) and two intermediate groups (B/A and B/C) that represent transitions between the three major groups. This classification considers the chromosomal location, the direction of transcription, domain architecture of the encoded proteins and sequence similarity in non-coding promoter regions (Gardner et al. 2002; Voss et al. 2000). DBLα-tags isolated from group A type *var* genes are predominantly of the cys2 type described earlier (Bull et al. 2007).

1.11 Thesis objectives

As described above, clinical immunity to malaria is a function of antibody responses to a wide range of different variants of PfEMP1 as well as other polymorphic parasite antigens. While this protection is acquired largely in a variant specific manner, it may be accompanied by responses that are partly cross reactive. This thesis aims to look at the extent of variant-specific and cross-reactive antibody responses against different DBL-α tag fragments from *Pf*EMP1 variants.

Aims:

1) To improve the recombinant expression of *Pf*EMP1 peptides in *E. coli*

The expression of plasmodial proteins in *E. coli* is a trial and error process characterized by tailor made conditions that are optimal for the particular protein of interest. In this work, I wanted to express variant forms of the DBLa tag region from *Pf*EMP1 isolated from parasites obtained from clinical isolates. I tested various *E. coli* cell lines supplemented with solubility enhancing characteristics as well as different bacterial culture conditions that aim to improve protein expression.

2) To determine the degree to which cross-reactive responses are generated between variants of DBL-α tags isolated from clinical isolates

P. falciparum displays immense variability in the immunologically important antigen *Pf*EMP1. This molecule varies between clonal parasite populations as well as in a single isogenic clone over time. This allows it to escape humoral responses. While the antibody response generated after infection will react strongest to the expressed *Pf*EMP1 variant

of the infecting parasite isolate, there is evidence that shows appreciable serological recognition of other variants that the host was not exposed to. The role of such heterologous responses against *Pf*EMP1 antigen family is poorly defined. Using DBLα tag antigen as a model antigen, I wanted to identify variants of *Pf*EMP1 that would cross react with each other and quantify the "antigenic distance" between them. I used ELISA to estimate the serological distances and refined the serological relationships by antigenic cartography.

3) To screen for potential epitope regions within the DBL-α tags gene targeted by the cross reactive responses

Antibodies that recognize multiple *Pf*EMP1 variants can protect the host from multiple *P. falciparum* serotypes. Vaccines against antigenically variable targets are typically designed to provide such broad spectrum protection. However, the targets of such cross reactive responses are poorly defined for *Pf*EMP1. In this PhD, I carried out an integrated fine-grain analysis genetic and antigenic data to identify potential regions in the DBLα tag antigen that may be targets of cross reactive responses.

Chapter 2

Materials and methods

2.1 Study site

The samples used in this study were obtained from children attending the Kilifi District Hospital, located approximately 60km to the North of coastal town of Mombasa in Kenya. It is the main hospital for Kilifi district and a serves population of about 680,000 that is mainly rural (Central Bureau of Statistics-Kenya, 2007). Malaria is endemic with peaks in transmission between May-August and December-January (Snow et al., 1993). This follows the two rainy seasons that occur from April to June and October-November. A recent reduction in malaria transmission in this area has resulted in a decrease in malaria related hospital admissions from 18.43 per 1000 children in 2003 to 3.43 per 1000 in 2007 (O'Meara et al. 2008).

Study Cohort

Children attending the Kilifi District Hospital with acute malaria and their parents were invited to take part in the study, and after providing informed consent, a 3 ml venous blood sample was collected on admission. Clinical malaria was defined as microscopic determined parasitemia of greater than 2500 parasite per μL with fever. All children and their parents were invited to attend follow-up appointments 4 weeks and 16 weeks after discharge. At these appointments, children were examined by a clinical officer and a 3 ml blood samples was taken for full white blood cell count, microscopy for parasites and storage of plasma and PBMCs.

Samples used in this study were selected from a biobank of stored samples from children attending Kilifi District Hospital with acute malaria collected between 2006 and 2009. Criteria for selection of samples were a full set of stored PBMCs and plasma from all time

points and RBCs and parasite RNA from admission samples. Among the children represented in this study, four suffered from severe respiratory distress (deep breathing), three from cerebral malaria (Blantyre coma score <3) and six from impaired consciousness (Blantyre coma score <5). There was an overlap of these symptoms in some of the patients with altogether nine children suffering from one or more symptoms of severe malaria. None of the children died. Baseline characteristics of the patients recruited in this study are given in table 2.1.

Table 2.1. The baseline characteristics of the patients at admission.

Patient	Age at admission (months)	Parasites/ml	Hemoglobin	Blantyre comma score	Severe respiratory distress
6387	6.93	137280	6.4	5	0
6398	46.23	190080	10.2	5	0
6408	8.97	125120	7.2	5	0
6429	58.77	247520	7.2	5	0
6430	52.9	148240	11.8	5	0
6433	60.63	73980	8.9	5	0
6485	29.73	218880	9.7	5	0
6964	47.97	134720	8.2	5	0
7045	21.23	38586	7	3	0
7069	24	927080	11.5	5	0
7084	28.8	56242	10.3	5	0
7116	37.17	155100	6.5	5	1
7134	128.2	74502	8.4	5	0
7157	40.47	803400	9.4	5	1
7160	44.97	231804	7.9	5	0
7183	4.1	67160	9.5	1	0
7198	10.6	63000	11.9	5	0
7204	34	257304	8.6	5	0
7249	53.6	719440	8.3	3	1
7250	46.07	294060	9.4	2	0
7323	32.9	430000	11.1	5	0
7337	84.63	147376	8.7	5	0
7391	23.37	98659	9.6	5	0
7410	9.8	10958.5	9.2	5	0

7506	70.67	87208	7.6	5	0
7530	63.6	1696800	9.8	5	0
7630	86.7	263900	10.1	5	0
7781	32.23	126210	8.9	5	0
7799	42.17	369720	6	5	1
7860	77.9	204870	7.1	5	0
7864	45.73	966520	7.9	1	0
8204	27.33	202080	11.1	4	0
8344	18.1	100100	8.9	5	0
8349	74.53	386640	10		0
8383	71.63	263840	7.6	5	0
8472	16.77	22792	7.3	5	0
8477	50.57	200200	7.4	5	0
8482	56	156480	9.1	5	0
8585	29.83	166820	10.7	5	0
8618	38.37	22064	10.3	5	0
8706	43.77	326400	9.4	5	0

2.2 Ethical approval

The study was approved by the Kenyan National Ethics Review Committee (protocol no. 1131) and the Oxford Tropical Research Ethics Committee (protocol no. 30-06)

2.3 Processing of the blood sample

At all time points, 3 ml of blood was collected in heparinised polypropylene tubes (Falcon) and spun at 2000rpm for 5 minutes to separate plasma from blood cells. The plasma was collected and stored at -80^{o}C till further use. The blood cells were then resuspended in 5mls of RPMI 1640 medium (Gibco) supplemented with 25μg/ml D-glucose(Gibco), 1mM L-glutamine (Gibco) and 25μg/ml gentamicin (Gibco) and carefully layered onto an equal volume of Lymphoprep (Axis-shield) and spun at 1800rpm for 20 minutes with the slowest deceleration settings to separate peripheral blood mononuclear cells from other cells. PBMCs were frozen in fetal calf serum/10% DMSO in liquid nitrogen. The remaining cells

were washed twice in 5mls of RPMI 1640 medium (Gibco) then layered onto Plasmion (Bellon) at 37°C for 15 minutes in order to separate granulocytes from the red blood cells (RBCs). At the acute time-point, the infected red blood cells were then washed twice in 5mls of RPMI 1640 medium (Gibco) after which 100µl packed cells were resuspended in 1ml of Trizol and stored at -80°C for RNA isolation as described below.

2.4 RNA extraction

To extract RNA, 200µl of Chloroform (Sigma-Aldrich) was added to thawed samples of 1100µl Trizol lysates. The lysates previously stores at -80°C, contained 100µl packed cell volume of infected red blood cells. The samples were shaken vigorously and allowed to stand for 3 minutes before they were spun at 4200rpm for 35 minutes at 4°C in a microfuge to separate the RNA rich aqueous layer from the protein rich organic layer. To maximize the yield of the aqueous layer, the samples were allowed to stand for 2 minutes in the sample rack after centrifugation. 500µl of the upper aqueous layer was then harvested taking care not to disturb the lower organic layer and transferred into fresh tubes to which 2µl of Glycoblue dye (Ambion) had previously been added.

The RNA was then precipitated with an equal volume of isopropanol (Sigma-Aldrich) for 2 hours at 4°C then spun at 13000rpm for 30 minutes. The supernatant was discarded while the pellet was washed once with 500µl of ice-cold 75% ethanol by gentle inversion and collected by a gentle spin at the bottom the tube after the alcohol was carefully poured out. Any residual alcohol was aspirated using a pipette and the pellet was air dried for 5 minutes. To re-suspend the RNA, 20µl of RNAsecure (Invitrogen) was added to the pellet and

incubated at 60°C for 10 minutes then mixed gently with a pipette. The RNA samples were stored at -80°C awaiting cDNA synthesis (Bull et al. 2005).

2.5 cDNA synthesis

2μl of the isolated parasite RNA sample was retrieved and transferred into 0.6ml test tubes for cDNA synthesis. To digest any contaminating DNA, the sample was treated with 1μl of DNAse1 (Ambion) in total reaction volume of 30μl that had 3μl DNAse1 buffer and 24μl of RNAse free DEPC water and incubated at 30°C for 20 minutes. To prevent DNAse1 from affecting downstream processes, 3μl of DNAse inactivation reagent was added and incubated for 2 minutes at room temperature after which the mix was spun at 10,000rpm for 2 minutes to pellet the inactivation slurry.

For each sample, two 8μl aliquots of the DNAse digested total RNA sample were then transferred into 0.2ml strip tubes. 1 μl of Random hexamers and 1μl of dNTPs were added to the samples before they were incubated in a thermocycler at 65°C for 5 minutes to denature the RNA followed by 4°C for 1 minute for the hexamers to anneal. A cDNA synthesis mix that had 2μl of 10X reverse transcriptase buffer,4μl of 25mM $MgCl_2$, 2μl of 0.1M dithiothreital and 1μl of RNAseOUT (40U/μl) (all Invitrogen) was added to all tubes. For each sample, 1μl of superscript III transciptase (200U/μl, Invitrogen) was then added to one tube and a 1μl of DEPC water (Ambion) added to the second tube to form the negative control sample. The samples were then incubated in a thermocycler under the following conditions: 25°C for 10minutes, 42°C for 50 minutes, 10°C for 10 minutes and 4°C for minute for cDNA synthesis. The RNA was then digested from the cDNA:RNA hybrid using

0.25µl of RNase H at 37°C for 20 minutes. The cDNA was stored at 4°C till required (Bull et al. 2005).

2.6 Amplification of the DBL-α tag region

DBL-α tags were amplified from cDNA by PCR using the universal degenerate DBLαAF' (5'-GCACG(A/C)AGTTT(C*/T)GC-3') and DBLαBR (5'-GCCCATTC(G/C)TCGAACCA-3') described by Bull et al 2005 in a 25µl reaction volume containing 2.5µl of 10X PCR buffer, 3mM $MgCl_2$,1.25mM of each primer and 2 units of Amplitaq Gold polymerase enzyme (Applied Biosystems) in a thermocycler under the following conditions: initial denaturation at 95°C for 5 min followed by 35 cycles of denaturation at 94°C for 30 seconds followed by annealing at 42°C for 30 seconds and extension at 42°C for 45 seconds. A final incubation at 65°C was added at the end of the last cycle.

2.7 Agarose gel electrophoresis

2g of agarose (Promega) was boiled in 0.5x TBE buffer then pour into a gel chamber (Biorad) and allowed to set. 5µl of PCR products were mixed with 1µl of the 6x DNA loading buffer (30% glycerol, a tip of spatula bromphenol blue and xylene cyanol, 70% TE) and loaded onto a gel. Gel electrophoresis was run at constant 90V for 90 minutes after which the gel was dipped in a staining buffer (0.5X TBE, 0.125µg/ml ethidium bromide) for 30 minutes and visualized under ultra-violet light.

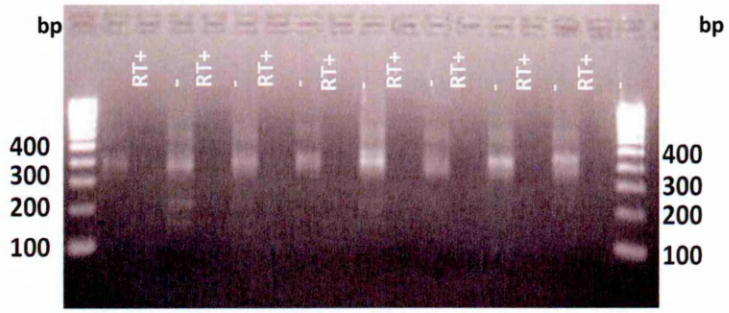

Fig 2.1 Ethidium bromide stain 0f 2% agarose gel PCR products from cDNA samples (RT+) with their corresponding negative control reaction run without the reverse transcriptase. There was no genomic DNA contamination during preparation in all of the cDNA samples generated.

2.8 Purification of PCR products

700µl of Sephacryl S-400 matrix (Amersham Biosciences) was added into empty microspin columns (Amersham Biosciences) and spun at 2800rpm for 2 minutes to pack the column. The matrix was then equilibrated twice with 200µl of 1X TE buffer and spun at 2800rpm for 1 minute each time. The PCR products were then loaded into the pre-equilibrated columns and spun at 2800rpm for 2 minutes to collect the purified PCR products.

2.9 Cloning of DBL-α tags

2µl of the purified PCR product was ligated to pCR 2.1 TOPO cloning vector (Invitrogen) in a 6µl reaction containing 1µl salt solution (1.2M NaCl,0.06M $MgCl_2$), 0.5 µl of the vector and 2.5µl of water. The reaction was incubated at room temperature for 5 minutes to allow for ligation to occur. 2µl of the cloning reaction was gently mixed with 25µl of One Shot TOP10 competent *E. coli* cells (Invitrogen) and incubated on ice for 30 minutes. The cells were then rapidly transferred to a preheated water bath at 42°C for 30 seconds before being transferred back to ice for 3 minutes. 250µl of pre-warmed SOC medium was then added to the cells and incubated in a shaking incubator at 200rpm and 37°C for 1 hour. 20µl of the

transformation reaction was then plated on pre-warmed selective LB agar plates containing 50μg/ml ampicillin (Sigma-Aldrich) and cultured overnight at 37°C in an incubator.

For each sample, 10-20 single bacterial colonies were randomly picked from each plate using sterile toothpicks and grown overnight in 5ml of LB broth (Invitrogen) containing 100μg/ml ampicillin in a shaking incubator at 200rpm and 37°C. Plamids were extracted from I.5ml of the overnight bacterial culture using the Perfect prep plasmid purification (mini) kit (Promega) according to manufacturer's instructions.

2.10 Sequencing

Subsequently, plasmids from the 10-20 colonies were sequenced to determine the dominant DBL-α tag transcript. The sequencing reaction was prepared in Micro Amp 96 well optical reaction plates (Applied Biosystems) using the BIG DYE terminator v3.1 cycle sequencing kit (Applied Biosystems) as follows: 0.25μl of the Big Dye reaction mix, 1.75μl of Big Dye terminator v1.1, v3.1 5X sequencing buffer(Applied Biosystems), 0.5μM M13 forward primer(5′-GTAAAACGACGGCCAG-3′) and 75ng of template in a 10μl reaction. The reaction mix was taken through cycle PCR in a thermocycler under the following conditions: initial denaturation at 96°C for 5 min followed by 25 cycles of denaturation at 96°C for 10 seconds followed by annealing at 42°C for 5 seconds and extension at 60°C for 4 minutes.

The cycle PCR products were precipitated by adding 50μl of a precipitation solution (made by mixing 3.3μl of 3M sodium acetate, 62.5μl of 95% ethanol and 24.2μl water) into each reaction and incubating on ice for 35 minutes. The plates were spun at 4000rpm for 30 minutes at 4°C in a biofuge and the supernatant discarded by inverting the plate over a pad of tissue. The PCR products were then washed twice with 150μl of 70% ice-cold ethanol and

spun at 4000rpm for 10minutes at 4°C each time. The plate was left to air dry for 30 minutes at room temperature before 10μl of Hi-Di Formamide was added to each well. The plate was heated at 96°C for 3 minutes in a thermocyler to resuspend the PCR products and then place on ice for 5 minutes to cool. Capillary electrophoresis and detection of the cycle PCR products was carried out in a 3130XL sequencer machine (Applied Biosytem) with a 50cm capillary.

The sequences were then classified according to the Cysteine/PoLV grouping system described by Bull and colleagues (Bull et al. 2007) using a Perl script developed by this group. This classification assigns the tags one of six groups based on the number of cysteines and sequence motifs (Fig 1.2)

2.11 Selection of dominant DBL-α tag transcript

The sequences were aligned by clustal in Bioedit using the defaults settings after the vector sequences had been cleaved off. The sequence that was most abundant among the 10-20 sequenced was selected for expression (Table 2.2 and Fig. 2.2).

Table 2.2 Frequencies of dominant DBL-α tag selected for expression

Tag	Number of identical DBLα-tag sequences	Total number of DBLα-tags sequenced	Proportion
6387	7	12	0.58
6408	8	18	0.44
6429	4	10	0.40
6430	14	20	0.70
6433	8	19	0.42
6485	3	15	0.20
6964	13	20	0.65
7045	4	9	0.44
7069	5	9	0.56
7116	6	16	0.38
7134	4	15	0.27
7157	5	10	0.50
7160	4	10	0.40
7183	5	17	0.29
7198	4	10	0.4
7204	5	18	0.28
7249	6	12	0.5
7250	5	13	0.38
7323	3	12	0.25
7337	11	21	0.52
7391	11	17	0.65
7410	6	14	0.43
7506	5	10	0.5
7530	5	11	0.45
7630	3	14	0.21
7781	4	13	0.31
7799	6	15	0.4
7864	9	14	0.64
8204	4	17	0.24
8349	5	10	0.5
8344	5	10	0.5
8383	7	15	0.47
8477	5	14	0.36
8482	6	11	0.55
8585	5	14	0.36
8706	5	13	0.38

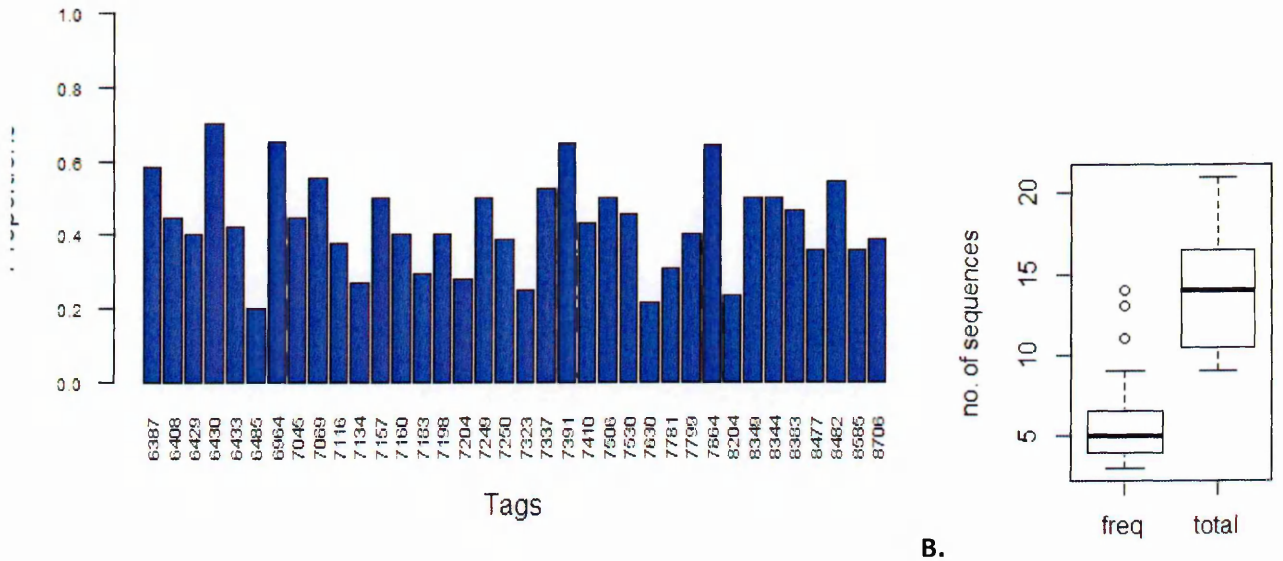

Fig 2.2. Proportion of the dominant DBL–α tags selected for expression for each of the 36 tags (A), and the distribution of the frequencies of the selected sequences and the total number of clones selected for sequencing (B).

It was isolated from the cloning plasmid using the the DBLαAF′ primer and a modified DBLαBR primer containing a 3′-stop codon (5′-TTAGCCCATTC(G/C)TCGAACCA-3′) under the following PCR conditions: initial denaturation at 95C for 5 min followed by 35 cycles of denaturation at 94°C for 30 seconds followed by annealing at 42°C for 30 seconds and extension at 65°C for 30 seconds. A final incubation at 65°C was added at the end of the last cycle. The PCR reaction contained 2.5µl of 10X reaction buffer, 3mM $MgCl_2$, 0.8mM dNTP mix,0.4µM of each primer and 2 units of Amplitaq Gold polymerase enzyme (Applied Biosystems) in a 25µl reaction. The amplified products were separated by agarose gel electrophoresis as previously described.

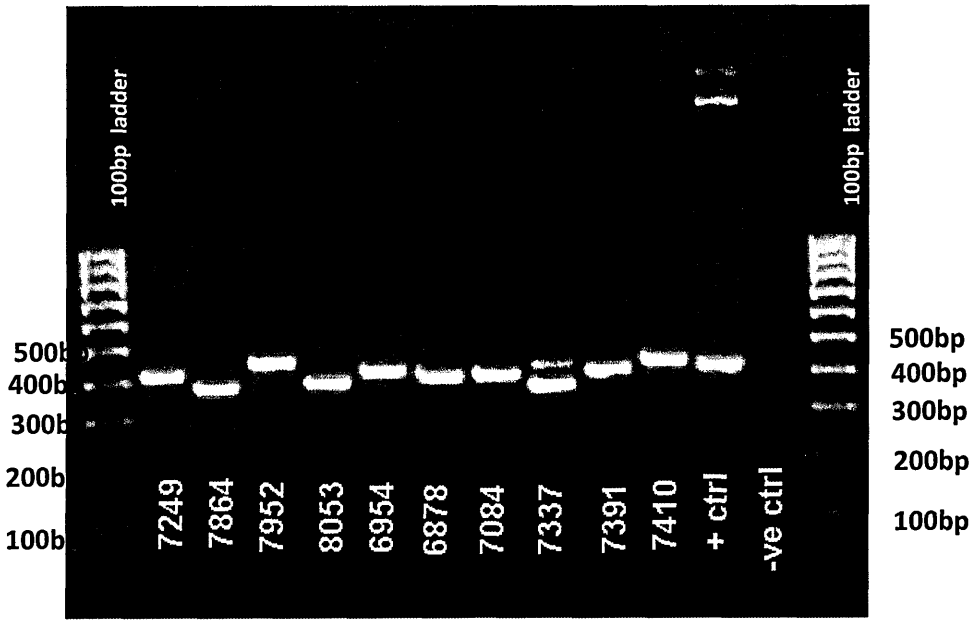

Fig 2.3 A 2% ethidium stained agarose gel showing DBL-α tags amplified with a modified DBLαBR reverse primer that had a stop codon included at the 3' end.

The amplified DBL-α tag was excised from the gel, weighed and purified using the Perfectprep Gel Cleanup kit (Eppendorf) according to manufacturer's protocol.

2.12 Protein Expression

The dominant transcript was cloned as earlier described into the expression vector pEXP5-NT/TOPO (Invitrogen) that contains an N- terminal histidine tag for purification. The cloned fragments are then transformed into One Shot TOP10 competent *E. coli* cells (Invitrogen) as earlier described and grown overnight in selective LB Agar plates containing 100μg/ml ampicillin (Sigma-Aldrich).

From each LB agar plate, 8 single bacterial colonies were randomly picked using sterile toothpicks and grown overnight in 5ml of LB broth (Invitrogen) containing 100μg/ml ampicillin in a shaking incubator at 200rpm and 37C.

The colonies were then screened by PCR for inserts with the correct orientation by PCR using the T7 forward primer and the DBLαBR primer. As templates, crude plasmid preparations were made by diluting 10μl of the overnight bacterial culture with sterile water and boiling for 5 minutes. 5μl of the crude plasmid sample was used as template in a that reaction contained 2.5μl of 10X NH_4^+ reaction buffer, 3mM $MgCl_2$, 0.8mM dNTP mix,0.4μM of each primer and 2 units of Taq polymerase enzyme (Bioline) in a 25μl reaction . After an initial denaturation (5 min 94°C) the PCR cycle was as follows: 30 seconds annealing at 42°C, 30 seconds elongation at 65°C and 45 seconds melting at 94°C, 35 cycles.

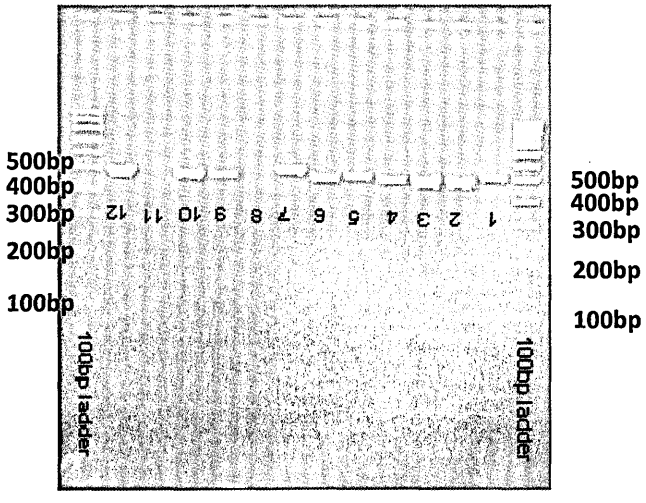

Fig 2.4 Screening of 12 pEXP5-NT/TOPO expression vectors for recombinants in which the DBL-α tags were inserted in the right orientation. Lanes 1,2,3,4,5,6,7,8,10 and 12 had the inserts in the correct orientation while lanes 8 and 11 had the insert in the wrong orientation.

Plasmids were extracted from the overnight bacterial culture that had a PCR product of the desired orientation using the Perfect prep plasmid purification (mini) kit (Promega) according to manufacturer's instructions. Subsequently, the plasmids were sequenced as earlier described to confirm that the insert was in the correct orientation and of the proper reading frame for protein translation.

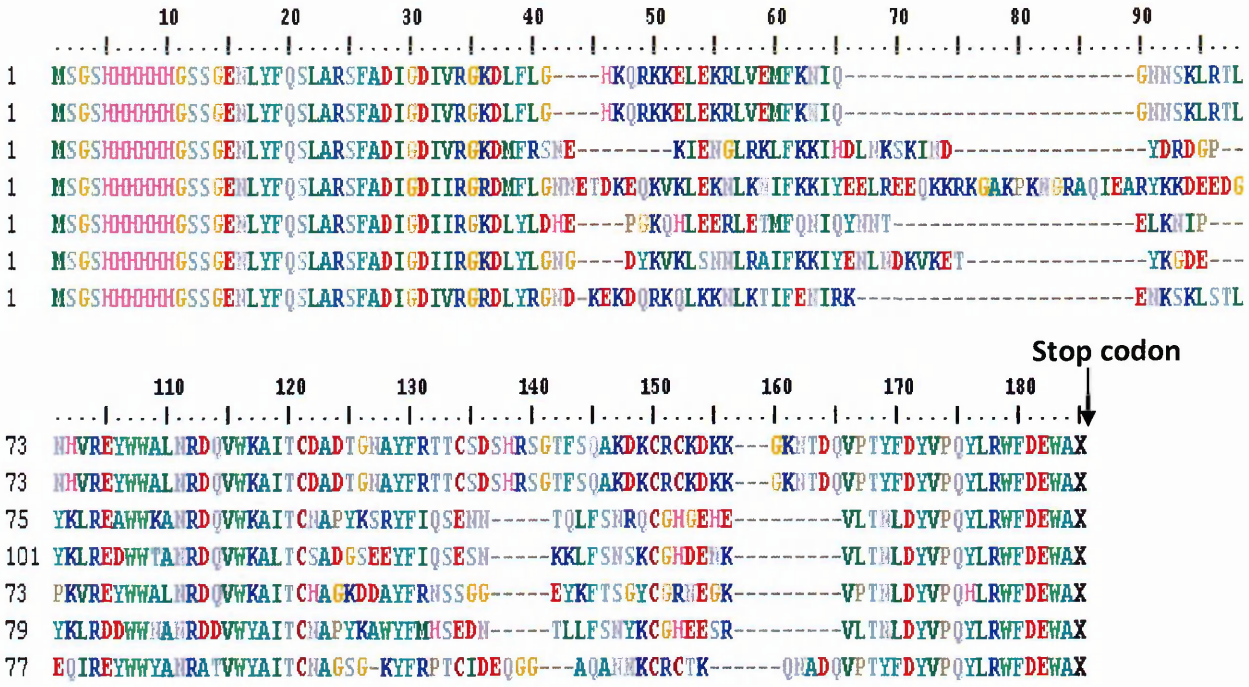

Fig 2.5 Sequences of DBL-α tag transcript inserted into the expression pEXP5-NT/TOPO vector that introduces a histidine tag at the N terminal end. The stop codon introduced at the C terminal end is indicated by **X** in the alignment. The sequences were aligned by clustal in Bioedit using the default settings.

The purified plasmids were transformed into BL21 (DE3) pLysS *E.coli* cells (Invitrogen) as described earlier and cultured overnight in 5ml LB broth containing 100μg/ml ampicillin and 34μg/ml chloramphenical (both Sigma-Aldrich). The 5ml overnight cultures of the recombinant BL21 (DE3) pLysS *E.coli* cells were diluted 1:10 with fresh 50ml LB Broth bacterial culture medium containing the antibiotics ampicillin (100μg/m) and chloramphenical (34μg/ml) and incubated in a shaking incubator at 37^{o}C. The growth of bacteria was periodically monitored by OD at 600 nm and was induced to express protein at OD_{600} of 0.4 with a final concentration of 1mM IPTG. 1 ml of the bacterial culture was sampled as the un-induced control just before adding IPTG. After 6 hours, 1 ml of the bacterial was similarly sampled as the induced control for comparison. The remainder of

the culture was harvested by centrifugation at 12,000 rpm for 20 minutes and stored at -20^{0}C until further use.

The un-induced and induced samples were spun at 13,000rpm and the supernatants discarded. 50μl of Laemmli sample buffer (Biorad) supplemented with β-mercaptoethanol was added to the pellets and boiled and then analysed by sodium dodecyl sulphate electrophoresis-polyacrylamide gel electrophoresis SDS-PAGE (described below).

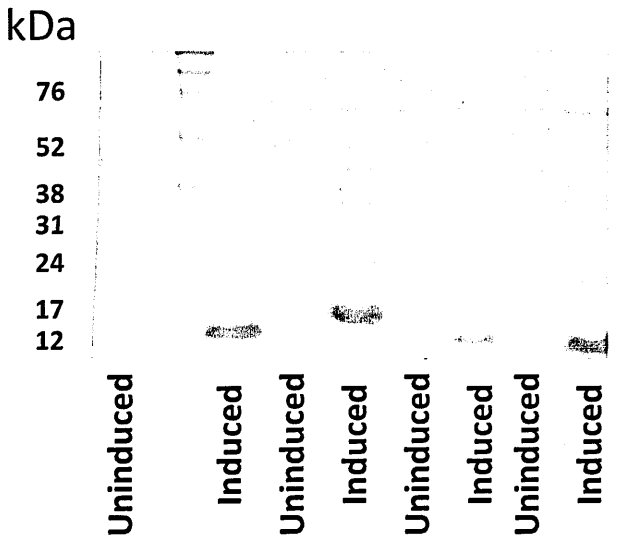

Fig. 2.6 Production of recombinant DBL-α tags using *E. coli* 10μl of bacterial pellet from paired IPTG induced and uninduced sample were run on a 12% SDS-Polyacrylamide gel and stained with Coomassie blue stain. Molecular mass standards are shown outside the panel.

2.13 Bacterial cell lysis

The bacterial pellet was lysed in 2.5ml Bugbuster lysis solution (Novagen) supplemented with 0.1μl benzonase nuclease (250U/ml,Novagen) and incubated at 4^{0}C for 20 minutes with gentle rotation. The benzonase nuclease reduces viscosity due to chromosomal DNA released by cell lysis. The suspension was spun at 12000 rpm for 30 minutes at 4^{0}C in a biofuge. The supernatant was aspirated and the pellet was washed in 1X PBS and

resuspended in 2.5ml of urea buffer (8M Urea, 200mM NaCl, 10mM Tris, pH 7.8). 20µl of both the supernatant and the resuspended pellet were mixed with 20µl of Laemmli sample buffer (Biorad) supplemented with β-mercaptoethanol, boiled for 5 minutes then analysed by SDS-PAGE.

2.14 Purification of recombinant DBL-α tags

1 ml of Probond resin was packed in a tube by spinning at 1000rpm for 5 minutes at 4°C. The resin was washed twice with 10ml of water then equilibrated twice with 10ml denaturing binding buffer (8M urea, 20mM NaPO4, 500mM NaCl, pH 7.8). At each of these steps, the resin was rotated gently for 2 minutes then spun at 1000rpm for 5 minutes at 4°C in a biofuge. The resuspended pellet was diluted with the denaturing binding buffer in a ratio of 1:3 and mixed with the pre-equilibrated resin. The resin was gently rotated at 4°C for 30 minutes to allow the recombinant proteins to bind. The resin was spun at 1000rpm for 5 minutes at 4°C before being washed 5 times with 5ml of wash buffer (8M urea, 20mM NaPO4, 500mM NaCl, pH 6.0). The proteins were eluted from the beads with low pH elution buffer (8M urea, 20mM NaPO4, 500mM NaCl, pH 4.0). 20ul of the flow through, washes and elutes were mixed with 20µl of Laemmli sample buffer (Biorad) supplemented with β-mercaptoethanol, boiled for 5 minutes then analysed by SDS-PAGE. The quantity of the recombinant proteins was measured by the BCA assay according to manufacturer's instructions.

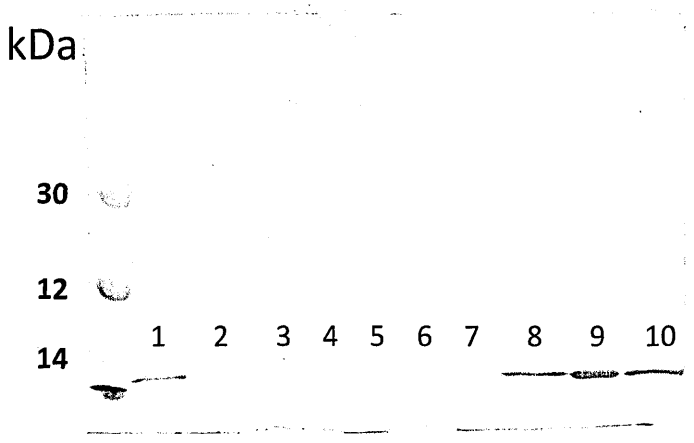

Fig. 2.7 Purified recombinant DBL-α tag. Lane 1 contains the flow through; the protein purification resin was washed 5 times, lanes 2-7. The proteins were eluted 3 times in Urea buffer, pH 4, lanes 8-10.

2.15 ELISA of DBLα-tags with human sera

Maxisorb 96 well ELISA plates (Nunc) were coated over night at 4°C with 1µg/ml recombinant protein in 1x PBS. Plates were washed three times in an ELISA washer and blocked for 2 hours at room temperature with 100ul 3% BSA in PBS 0.01% tween 20 (PBS-T). Then, plates were washed again and incubated with human sera diluted 1:200 in 1% non-fat milk powder in PBS-T. After incubation for 2 hours at room temperature, the plates were washed twice in the ELISA washer and then incubated with the secondary antibody (mouse anti-human IgG alkaline phosphatase labeled (1:5000) in 1% non-fat milk powder in PBS-T for one hour at room temperature. After washing, the plate was developed with OPD and measured in an ELISA reader at 490nm.

Non-immune sera were obtained from European donors with no history of malaria or travel to malaria endemic areas were used as negative control samples. For each antigen, background absorbance against 10 non-immune sera was subtracted from each value. In addition, each antigen was tested against a pool of hyper immune sera obtained from

clinically immune adults living in a malaria endemic area. All samples were run in duplicates and a mean for each sample was calculated.

Chapter 3

Recombinant expression of DBL-α tag from clinical isolates

Expression of recombinant proteins is commonly used to generate antigens for immunological characterization and vaccine production. Plasmodial proteins are typically difficult to express in heterologous systems. Differences in protein translational mechanisms coupled with a characteristic high AT rich genome and frequent Lysine and Arginine repeats make expression of plasmodium proteins in *E. coli* particularly difficult. The lack of a universal method applicable to the expression of plasmodial protein means that each protein is handled on a case by case basis. In this study, I tested different *E. coli* cell lines and various bacterial growth conditions that favour soluble protein expression of variants of the DBL-α tag isolated from parasites obtained from children diagnosed with malaria. These methods, though successful for other plasmodial proteins, did not result in improved solubility of the expressed protein. In all cases, the expressed product was in a precipitated insoluble form. The proteins were recovered by denaturing them in urea and gradually renaturing them by dialysis in a process that was sensitive to pH and glycerol. The recombinant variants of DBLa tags were then used as molecular tools to quantify cross-reactive antibody responses and antigenic relationships between them.

3.1 Introduction

Immunological, structural or functional characterization of proteins requires that they are first expressed in large quantities as purified recombinant forms in their native conformation. This is commonly achieved using heterologous expression systems that include bacteria, yeast, insect cells, mammalian cells and recently cell-free expression systems. The *E. coli* expression system is the most attractive and widely used because it is a cheap method that produces high protein yields in short time using simple laboratory equipment. This system, though attractive, typically results in poor quality proteins that are improperly folded often forming inclusion bodies and lacking in post-translational modifications (Carrió & Villaverde 2002). These limitations are primarily due to differences in features of the translational machinery between *E. coli* and the organism from which the recombinant gene to be expressed is sourced. These include differences in codon usage and bias , abundance of certain amino acids and tRNAs, GC content among other factors (Sayers et al. 1995; Rogers 1996).

Plasmodium proteins are difficult to express in heterologous systems, particularly in *E. coli*. This is thought to be due to various reasons: a high AT-rich genome (80%) of Plasmodium compared to *E. coli* (50%), codon bias that is different from *E. coli*, proteins rich in arginine and lysine residues as well as high molecular weights of many plasmodial proteins (Gardner et al. 2002; Schneider et al. 2005; Sayers et al. 1995; Saul & Battistutta 1988; Singer & Hickey 2000). Heterologous expression of plasmodial proteins in *E. coli* is typically characterised by failure of expression or in the expression of precipitated forms of the protein that aggregate to form inclusion bodies (Mehlin et al. 2006; Aguiar et al. 2004; Vedadi et al. 2007). This was highlighted by an extensive study carried out by Mehlin et al in

which 1000 open reading frames from a sequenced genome of a *P. falciparum* strain were cloned for expression in *E. coli*. The authors were able to successfully express only 337 as recombinant proteins. Only 63 of the expressed proteins were in soluble form, the rest formed inclusion bodies. In that study, proteins that either had higher molecular weight, high isoelectric point or distant homology to *E. coli* proteins, were less well expressed in *E. coli*. In addition, among the 337 that were successfully expressed, the soluble ones were likely to have higher isoelectric points. More importantly, the authors observed that there was no universal applicable method for the expression of plasmodial proteins. In a similar study, up to 30% of 1008 genes obtained from four apicomplexan parasites were successfully expressed in soluble recombinant form using a strain of bacteria supplemented with additional tRNA. Of the 1008 genes, 400 were obtained from *P. falciparum* (Vedadi et al. 2007).

Over production of proteins in *E. coli* exerts immense metabolic stress beyond what the endogenous translational mechanism in *E. coli* can cope with. Strategies that supplement the deficiencies in the endogenous translational mechanism or those that lower the rate of translational process have resulted in improved solubility of expressed products. The extreme AT rich genome results in a codon bias that is different from *E. coli*. The codons AGA and AGG that encode arginine, are particularly rare in *E. coli* but are over-represented in *P. falciparum* (Sayers et al. 1995). During translation, the limited numbers of tRNAs in the host cell are unable to cope with the demands of codons that are over represented in the host cell resulting in unwanted substitutions, translational stalling and termination (Schneider et al. 2005). The accumulation of such truncated misfolded protein contributes to inclusion body formation. Two different strategies have been used to overcome codon

bias in the expression of *P. falciparum* proteins in *E. coli*, i.e., the supplementing the translational machinery with additional copies of rare tRNAs (Baca & Hol 2000; Rogers 1996) or harmonizing the codons of the target genes to suit the codon usage in *E.coli* (codon optimisation) (Yadava & Ockenhouse 2003; Zhou et al. 2004; Angov et al. 2008; Yazdani et al. 2006). Alternative conditions that lower the growth rate of bacteria have also been used to enhance soluble expression in bacteria (Gräslund et al. 2008; Flick et al. 2004). Flick and colleagues were able to dramatically improve solubility of recombinant *Pf*EMP1 domains expressed in *E.coli* by delaying the induction of expression to the lag phase where bacterial growth is slow. The slowing down of metabolic processes is thought to allow the protein translational mechanism time to properly fold the expressed proteins. Growing bacterial at low temperatures and use of weak promoters to reduce the metabolic stress on *E. coli* have been proposed as attractive alternatives. Despite the availability of all these strategies, expression of soluble protein remains a trial and error process as there is no universal method applicable to *P. falciparum* antigens. Conditions have to be optimized on a case by case basis.

Initial attempts at expressing the DBL-α tags as recombinant antigens resulted in formation of inclusion bodies. I tested several of the above strategies with an aim of developing a method best suited for the expression of most DBLα-tags in soluble form.

3.2 Results

3.2.1 The effect of different *E. coli* strains on expression of DBLα-tags

Four strains of *E. coli* were tested for expression of soluble DBL-α tag antigens: the BL21(DE3)pLysS that contains a plasmid that limits the basal expression of the target gene; BL21trxB(DE3)pLysS that is supplemented with the thioredoxin to enhance disulphide bond formation; the origami(DE3)pLysS strain that is supplemented by the thioredoxin and glutathione reductase genes to greatly enhance disulphide bond formation and the BL21 (DE3) CodonPlus-RIL strain that is supplemented with rare tRNAs to allow for expression of genes with rare codons. The BL21(DE3)pLysS was used as a comparator for better expression.

Briefly, 50ml LB Broth bacterial culture medium containing the antibiotics ampicillin the appropriate antibiotic were inoculated with 5ml overnight culture of either BL21 (DE3) pLysS, BL21trxB(DE3)pLysS, BL21 (DE3) CodonPlus-RIL or origami(DE3)pLysS *E.coli* cells transformed with recombinant pEXP5-NT/TOPO with a DBL-α tag fragment. The cultures were incubated at 37°C and induced with a final concentration of 1mM IPTG when OD_{600} was 0.4. Four hours later the bacteria were harvested by centrifugation at 12,000rpm for 20minutes. The bacterial pellet was lysed in Bugbuster lysis solution supplemented with benzonase nuclease. The insoluble proteins were separated by centrifugation at 12000rpm for 30minutes. The pellet was washed in PBS and resuspended in Urea buffer (8M Urea, 200mM NaCl, 10mM Tris, pH 7.8). 10ul of the supernatant (soluble) and resuspended pellet

(insoluble) fractions were run on a 12% SDS poly acrylamide gel and stained with Coomassie blue dye.

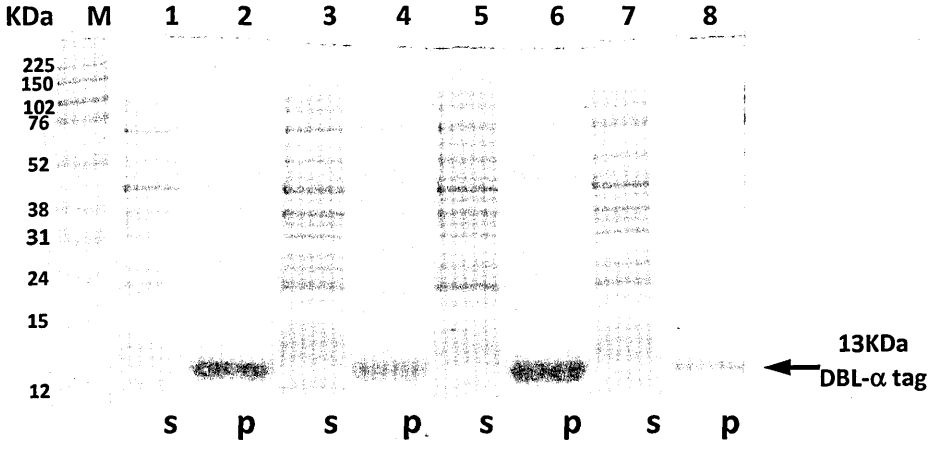

Fig 3.1 Comparison of the soluble (s) and the pellet/insoluble (p) fractions of recombinant DBL-α tag proteins expressed in: BL21 (DE3) pLysS lanes 1 and 2; BL21trxB(DE3)pLysS lanes 3 and 4; BL21 (DE3) CodonPlus-RIL lanes 5 and 6; origami(DE3)pLysS *E.coli* cells lanes 7 and 8. The proteins were analysed by 12% SDS PAGE and stained by coomassie blue dye.

*Pf*EMP1 proteins are particularly rich in Cysteine residues that are probably play a role in folding the proteins and maintaining their structure. I envisaged that the use of host strains optimized to enhance disulphide bond formation would enhance proper folding of the DBL-α tags hence improve their solubility. Expression in BL21trxB(DE3)pLysS and origami(DE3)pLysS *E.coli* strains resulted in no improvement as compared to the BL21(DE3) Fig 3.1 lanes 1-6.

While there was decreased yields obtained with the origami (DE3)pLysS *E.coli* cells, the quality of the expressed product was not improved in all the cells tested. The BL21 (DE3) CodonPlus-RIL *E. coli* strain is supplemented with extra copies of E. coli argU, ileY, and leuW

tRNAs that are overrepresented in AT rich genomes. This however did not enhance the solubility of the DBL-α tags tested (Fig 3.1, lanes 7 and 8).

3.2.2 Induction of protein expression at different time points

In order to establish whether late induction of protein expression would improve solubility of the expressed proteins, 50 ml of BL21 (DE3) pLysS *E. coli* cells transformed with recombinant pEXP5-NT/TOPO-DBLα plasmid were cultured at 37°C and induced with a final concentration of 1mM IPTG when OD_{600} was 0.4, 0.6, 0.8, 1.0, 1.4, 1.6, 1.9 and 2.1. The cultures were allowed to grow for 4 hours to allow for protein expression before they were harvested by centrifugation and processed as previously described.

By inducing expression in the latter stages of bacterial growth, Flick and colleagues observed an increase in the ratio of the amount of recombinant proteins in the soluble as compared to the insoluble fraction for each of the time points (Flick et al. 2004). While there was a gradual decrease in the amount of the proteins in the insoluble fraction with each delayed induction, it was not accompanied by a corresponding increase in the amount of soluble protein (Figs. 3.2 A and B). The decrease growth rates were thus not helpful in enhancing bacterial growth.

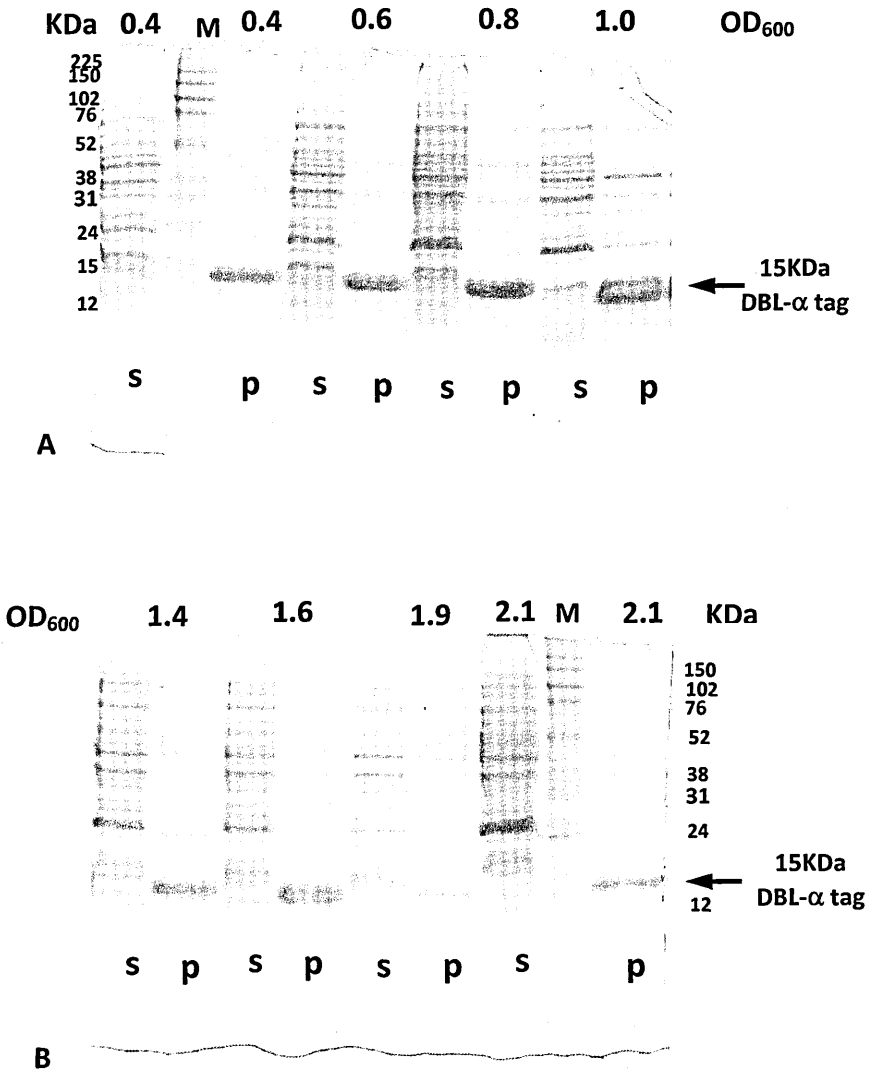

Fig 3.2 Comparison of the soluble (**s**) and the pellet/insoluble (**p**) fractions of recombinant DBL-α tag proteins expressed in BL21 (DE3) pLysS cells at OD_{600} of 0.4, 0.6, 0.8,1.0 (**A**) 1.4,1.6,1.9 and 2.1 (**B**). The proteins were analysed by 12% SDS PAGE and stained by coomassie blue dye.

3.2.3 Reduction in temperature at the time of induction

It has been reported that incubation of bacterial culture at low temperatures after induction greatly improves the solubility of the final product. To check for the effect of temperature on solubility, 50 ml of BL21 (DE3) pLysS *E.coli* cells transformed with recombinant pEXP5-NT/TOPO-DBL-α plasmid were cultured at 37°C and induced with a final concentration of 1mM IPTG when OD_{600} was 0.4 .The cultures were subsequently cultured at 20°C for 4 hours to allow for protein expression before they were harvested by centrifugation and processed as described earlier.

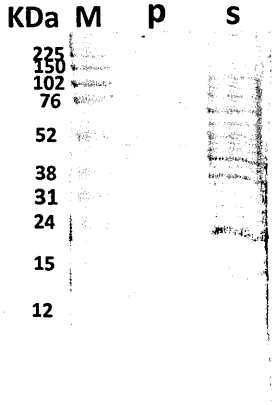

Fig 3.3 Impact of bacterial culture temperature on protein solubility of expressed protein. Comparison of the soluble (**s**) and the pellet/insoluble (**p**) fractions of recombinant DBL-α tag proteins expressed in BL21 (DE3) pLysS cells cultured at 20°C for four hours after induction.

Consistent with the results obtained by late induction, slowing bacterial growth by lowering culture conditions did not improve the solubility of the expressed product (Fig 3.3).

3.2.4 Protein refolding by dialysis

As it was not possible to express soluble protein through any of strategies listed above, I explored strategies to recover the protein from inclusion bodies. 50ml of bacterial culture was processed as described earlier to obtain the insoluble protein fraction. The insoluble fraction was washed in PBS and resuspended in Urea buffer (8M Urea, 200mM NaCl, 10mM Tris, pH 7.8) then mixed with 0.5ml Ni-TA agarose beads and purified as described in chapter 2. The proteins were eluted from the beads with low pH elution buffer (8M Urea, 200mM NaCl, 10mM Tris, pH 4.0). This was then subjected to four different dialysis strategies (table 3.1).

1). Direct dialysis. 1ml of the purified protein was placed in dialysis tube and dialyzed against 2L of refolding buffer (200mM NaCl, 10mM Tris, pH 7.4) in a beaker at $4^{o}C$ overnight.

2). Gradual dialysis with direct pH change. Similar to 1 but starting with the refolding buffer with denaturing conditions and at pH 7.4, (6M Urea, 200mM NaCl, 10mM Tris, pH 7.4). The urea in refolding buffer was diluted 1:2 using a diluent buffer, (200mM NaCl, 10mM Tris, pH 7.4) every two hours for 24 hours to a final concentration of 0M Urea as described in chapter 2.

3). Gradual dialysis + gradual pH change. Similar to 1 but starting with the refolding buffer with denaturing conditions and at **pH 4.5**, (6M Urea, 200mM NaCl, 10mM Tris, **pH 4.5**). The refolding buffer was diluted as in 2) allowing for gradual change in both urea concentration in the buffer as well as pH.

4). Similar to 3) but with addition of 10% glycerol to the refolding and diluent buffers.

10 DBLα tags were tested in each experiment and precipitates were removed from the solution by centrifugation at 13,000rpm for 10 mins. Quantity of the recombinant peptides was measured by the BCA assay as described in chapter 2 and is shown in table 3.2.

Table 3.1 Refolding proteins by dialysis

Experiment	**Recovery (No of proteins recovered)**
1. Direct dialysis	0/10
2. Gradual dialysis + direct pH change	4/10
3. Gradual dialysis + gradual pH change	8/10
4. Gradual dialysis + gradual pH change + 10 % glycerol	10/10

Table 3.2 Concentrations of proteins recovered after refolding by dialysis.

DBL-a tag	Molecular weight, Da	Isoelectric point	Concentration, µg/ml
6429	17137.24	9.32	300
6387	17908.98	8.32	348
6398	18259.24	7	216
6408	16789.76	8.87	279
6430	19342.1	6.55	326
6433	18572.89	8.83	255
6485	19240.14	8.29	213
6964	18316.28	7.7	212
7045	17674.57	6.22	180
7069	17180.08	8.5	190
7084	17796.69	7.14	531
7116	19028.13	8.61	212
7134	18321.29	7.08	213
7157	17687.69	9.14	199
7160	18306.16	6.75	123
7183	17468.4	5.95	216
7198	20152.38	7.76	270
7204	18303.29	7.73	263
7249	18651.71	8.86	456
7250	17700.44	6.23	115.1
7323	20068.31	6.66	266
7337	16884.95	6.75	169
7391	19118.29	8.27	180
7410	18446.52	6.5	267
7506	19480.38	6.16	244
7530	16724.49	6.59	311
7630	18779.96	8.72	324
7781	19277.33	8.6	236
7799	19150.16	8.97	409
7860	18537.55	7.12	244
7864	17581.67	7.83	378
8204	19035.11	6.54	243
8344	18547.79	7.16	235
8349	18498.42	6.3	193
8383	17130.28	9.06	195
8472	18578.53	7.74	347
8477	17056.11	9	245
8482	19184.06	7.04	360
8585	18451.35	6.7	178
8618	17955.87	8.64	240
8706	19453.21	8.2	279

3.3 Discussion

Characterization of the immunological or biochemical properties is best done on properly folded proteins. Soluble expression of a recombinant protein is typically a good indicator that it properly folded into its native structure. However, heterologous expression of eukaryotic proteins, particularly *P. falciparum*, results frequently in the formation of inclusion bodies (Vedadi et al. 2007; Mehlin et al. 2006). The process by which these inclusion bodies form is not known but is linked to over production of the heterologous target in the host (Carrió & Villaverde 2002). Almost invariably, expression of proteins in *E. coli* is targeted in producing as much of the protein as is possible. Overproduction of heterologous proteins is thought to overwhelm the protein translational machinery in *E. coli* resulting in truncated and/or misfolded forms of the protein that aggregate to form inclusion bodies. Successful strategies used to improve soluble expression of recombinant expression of plasmodial proteins in *E. coli* have either supplemented the *E. coli* translational machinery with the features it requires for expression or slowed the translation process so as not to overwhelm the translational machinery. These include co-expression with molecular chaperons and solubility enhancing fusion partners, codon harmonization, use of host strain supplemented with tRNAs that are abundant *P. falciparum,* use of weak promoters and lower bacteria culture temperatures (Flick et al. 2004; Stephens et al. 2011; Zhou et al. 2004; Yazdani et al. 2006).

The successes of these strategies vary from one recombinant protein to another. This study proposed to express different variants of the DBL-α tag in *E. coli* for antigenic characterisation. As expected, the expressed product formed inclusion bodies that

precluded further antigenic characterisation. In order to improve solubility, I tested several established strategies that have been proven effective for plasmodial proteins.

Use of plasmids that encode rare tRNAs found in *P. falciparum* has been shown to improve expression in *E.coli* (Zhou et al. 2004; Baca & Hol 2000). Four different strains of *E. coli* with differing genetic backgrounds were used to optimize expression: the BL21(DE3)pLysS strain; the BL21trxB(DE3)pLysS and origami(DE3)pLysS strain that enhance disulphide bond formation and the BL21 (DE3) CodonPlus-RIL strain that is supplemented with rare tRNAs to allow for expression of genes from AT rich genomes. In all the strains, the recombinant tag was expressed as an inclusion body.

Slowing down the synthesis of proteins is thought to allow the protein translational machinery ample time to fold newly synthesized protein into proper structures and thus improving solubility. Indeed, expression of plasmodial protein at the lag phase and growing bacteria at low temperatures where growth is slow have independently been shown to yields of soluble protein (Flick et al. 2004). Attempts to slow down bacterial growth by these methods did not improve the solubility of the expressed proteins.

Formation of inclusion bodies by bacteria is a reversible process (Villaverde & Carrió 2003; Carrió & Villaverde 2001). Soluble functional proteins can also be recovered from inclusion bodies via dialysis. Refolding by dialysis has been used to recover functional *P. falciparum* dihydrofolate reductase (Sirawaraporn et al. 1993) and falcipain-2 (Kumar et al. 2007) proteins from inclusion bodies. Protein refolding is a complicated procedure that requires extensive optimization to produce functional proteins (Vallejo & Rinas 2004). Different dialysis strategies of refolding DB-Lα tags were tested. A dialysis process that allowed for

both the gradual change in pH and the concentration of the urea allowed us to increase the number of proteins recovered from 4/10 to 8/10. Addition of 10% glycerol, allowed us to recover all the proteins that were tested. Glycerol reduces non-specific interactions between proteins.

For this study, a total of 39 recombinant DBL-α tags were expressed. All without exception formed inclusion bodies. However, it was possible to recover all the expressed proteins from inclusion bodies by refolding using dialysis. The strategy developed here, allows for efficient recovery of aggregated proteins of highly polymorphic nature from inclusion bodies. Refolding of plasmodial protein by dialysis, though under-utilized, provides an attractive option that offers the possibility of tremendously improving the recovery of plasmodial proteins and accelerate their characterization.

Chapter 4

Characterization of homologous and heterologous antibody responses to DBL-α tags isolated from clinical isolates

Humoral immune responses to the DBLα domain region have largely been studied using parasite material from adapted lab isolates. In most cases, this involves heterologous antigen-antibody pair measurements. In this chapter, I describe the pattern of acquisition of both homologous and heterologous immune responses to the DBL-α tags in the field. In addition, as a preamble to the next chapter that describes antigenic relationships, I wanted to explore the variability in the mean recognition of the antigens by the sera and the variability mean immunogenicity of the antigens. I report an increase in the homologous antibody response to the DBL-α tags that fits with the previously described "hole-in-the-repertoire" hypothesis in which individuals get infected by parasites to which they lack antibodies to.

4.1 Introduction

The surface of red blood cells infected with *P. falciparum* contains antigens of parasite origin that are highly immunogenic. Unlike other malaria antigens that require several rounds of exposure before generation of antibodies, a single infection is enough to generate appreciable amounts of antibody (Elliott et al. 2007). Acquisition of antibodies to these antigens on the erythrocyte surface has been associated with protection against malaria (Bull et al. 1998; Mackintosh et al. 2008b). There are several families of these surface proteins containing multiple copies in a family per haploid genome with extensive polymorphism between members, a possible indication that they are all under immune selection. The presence at the surface on the infected erythrocyte has been confirmed by surface staining for PfEMP1, RIFINs and STEVORs (Petter et al. 2007; Blythe et al. 2008). Similarly, recombinant antigens of PfEMP1, RIFINs and STEVORs are subject to recognition by naturally acquired antibodies (Abdel-Latif et al. 2002; Mackintosh et al. 2008a; Schreiber et al. 2008). However, current opinion and data support the view that most of this response is directed at *Pf*EMP1 molecules, though the role of non-*Pf*EMP1 antigens in natural immunity remains poorly defined. In a recent study Chan and colleagues developed genetically modified parasites that allowed them to silence the expression of PfEMP1 without affecting the expression of the other variant gene families (Chan et al. 2012). Using 2 different strains of *P. falciparum* they were able to demonstrate that a loss in *Pf*EMP1 expression was accompanied by a concomitant loss in recognition of the surface red blood cells infected by the mature forms of this parasite. While this supports the role of PfEMP1 as the dominant variant surface antigen, there is need for more extensive studies that include different variants of these proteins. A poorly immunogenic non-PfEMP1 variant antigen

paired with a highly reactive PfEMP1 antigen could potentially exaggerate the role of PfEMP1.

So far, antibody responses to *Pf*EMP-1 have been studied using red blood cells infected with trophozoites from lab isolates or field isolates as a target. The method measures the collective response to all variant antigens and is limited by the volume of the sample obtained when studying clinical isolates and by the inability to distinguish the target epitopes being recognised.

Cloning and expression of antigens as recombinant forms has been used extensively to generate a renewable source of purified proteins for immunological assays and, ultimately, development of vaccines. A number of laboratories have expressed recombinant domains from sequenced laboratory isolates and used those for the analysis of antibody responses to PfEMP1 by ELISA. In particular, several studies have used recombinant DBLα domains from the 3D7 *P. falciparum* isolate to show that it is a target of naturally acquired antibodies and that they are acquired at a rate that is determined by the degree of exposure (Cham et al., 2010; Joergensen et al., 2007; Mackintosh et al., 2008a). In two separate studies, it was observed that the order by which antibodies to the domains is acquired is non-random. Children acquire immunity to DBL domains isolated from group A or B/A PfEMP1 type antigens much earlier compared to group B and C *Pf*EMP1 (Cham et al. 2010; Cham et al. 2009). This is consistent with published reports that showed the association between the expression of group A or B/A PfEMP1 *Pf*EMP1 and severe disease in young children (Warimwe et al. 2009; Jensen et al. 2004). In a separate finding, Barry and colleagues showed that children acquire antibodies to group 2 DBL-α tags much earlier compared to the other Cys/PoLV groups (Barry et al. 2011). In their work, Joergensen and colleagues

observed limited cross-reactivity among DBL domains isolated from a single parasite genome but did not observe the ordered acquisition of antibodies with respect to the A, B/A, B, B/C and C types of *Pf*EMP1 (Joergensen et al. 2006).

The major drawback of these studies is that most of them are limited to analysing responses to DBLα region within a single sequenced genome. Extensive polymorphism among members of the *var* gene family has limited the expression of recombinant *Pf*EMP1 proteins from clinical isolates. A small tag region within the DBLα domain is accessible in most parasites and has been used to characterise the properties of these genes from clinical isolates.

4.1.1 The DBL-α tag

The N-terminal end of most sequenced *Pf*EMP1 members share a common N terminal head structure composed of the N-terminal sequence, DBLα and CIDR (NTS-DBLα-CIDRα) domains (Smith et al. 2000; Gardner et al. 2002). A recent study analyzing *Pf*EMP1 members from seven genomes found this domain structure present in up to 95% of all the *Pf*EMP1 analysed (n=311) (Rask et al. 2010). The DBLα domain is relatively conserved and has short islands of homology have allowed for the design of degenerate primers that allows this region to be sampled from most parasite genomes.

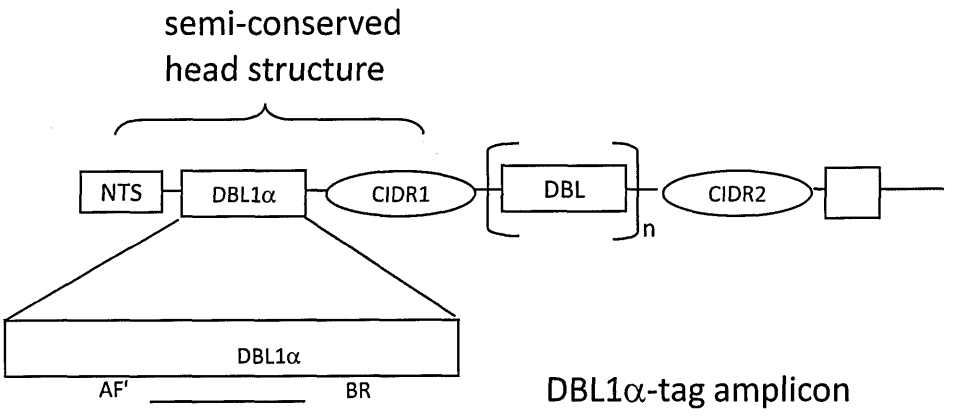

Fig 4.1 Domain structure of *Pf*EMP1. The extracellular end of PfEMP1 molecules is made up of variable numbers of Duffy biding like (DBL) and Cysteine Inter-domain Rich (CIDR) domains in differing permutations. The N-terminal end of most member has a semi-conserved head structure within with is a DBLa domain. The DBLα tag is a small region within this domain that is accessible by primers in most *Pf*EMP1 isoforms.

The region within the DBLα domain amplified by these primers is termed the DBL-α tag and is approximately 350bp long. It is due to this that this is the region of PfEMP1 that has been most studied from most clinical isolates. I isolated and expressed this region from 36 isolates and used them as a model antigen to measure immune responses to PfEMP1 isolated from sick children.

While *Pf*EMP1 plays a crucial role in host immune evasion, it is to date unclear why this *Pf*EMP1 repertoire is so big and what differences might exist in terms of cross-reactivity between the different *Pf*EMP1 proteins. In this work I wanted to test how recombinant expressed DBLα domains of *Pf*EMP1 from parasites of acutely ill children are recognized by their corresponding homologous sera and by heterologous sera obtained from children infected by other isolates within the same population. I hypothesize that the gains/losses of responses to heterologous antigens after infection is determined by the degree of antigen similarity between any two variant antigens.

To test my hypothesis I have chosen a sero-epidemiological approach and assessed antibody titres in plasma from 36 children admitted to hospital with acute malaria. Antibody titres were assessed against 36 different recombinant expressed DBL-α tags from *Pf*EMP1 derived from this same group of children. Recognition of the DBL-α tags was tested against plasma obtained at three time points; the time the child presented to hospital (Acute), 4 weeks post treatment (C2) and four months post treatment (C3).

Unlike influenza or respiratory syncitial viruses in which disease is caused by a single dominant antigenic variant that changes with seasonality, individuals living in malaria endemic areas are continuously exposed to multiple strains of *P. falciparum.* The number and type of variants that people are exposed to is expected to vary from individual to individual. This, coupled with the heterogeneity in the antigenicity of the variants, generates variability between serum donors in their total PfEMP1 specific IgG responses. By testing which DBL-α tags were recognized by these children at three different time points, I was able to study the variability of the individual mean antibody reactivity to the DBL-α tags and the variability in the individual mean antigenicity of the DBL-α tags and its dynamics through time.

4.2 Methods

4.2.1 Statistical analysis

Multiple linear regression was used to explore factors that influence variation in the responses measured against the tags. Multiple linear regression is a statistical tool that looks at linear relationships between one variable and other related variables. It measures how changes in one variable, the dependent variable, are affected when changes occur in other variables (independent variables) that share a relationship which is linear with the dependent variable. In the work described here, these models were used to describe factors that influence variability in the measure of antibody responses (O.D.) against recombinant DBLα tags.

The extent to which a change in the dependent variable is influenced by a change in any of the independent variables is given by the regression coefficient, β. It estimates the amount of change in the dependent variable when the independent variable changes by one unit. The larger the regression coefficient, the more a change in the independent variable influences the dependent variable. A p-value is attached to each regression coefficient, β that gives the probability of observing an influence of the independent variable on the dependent variable where none exists. Low p-values therefore suggest that the influence is real.

In most cases, a single independent variable explains only part of the variation in the dependent variable. To better describe the variation observed in a dependent variable it is necessary to include other variables in the model that also explain variation of the independent variable in the model. In a regression model with more than one variable, the

β coefficient describes the influence of changes in the independent variable on the dependent variable after correcting for the influence of all other independent variables in the model.

In the case at hand, there were repeated measures of immune responses taken over a short period of time for the same individual and this potentially violates the assumption that measures of the dependent variable are independent and uncorrelated. This was taken into account by fitting linear mixed effect models that included a random variable effect for each child.

The total amount of variation in the dependent variable that is explained by the independent variables in a regression model is quantified by the R^2 value. As explained above, when more independent variables are added to the regression model, more variation in the dependent variable is explained, i.e., adding more independent variables increases the R^2 value. Some of this increase could be due to chance: this is corrected by an adjusted R^2 value (R^2_{ADJ}) is computed that takes into account the number of independent variables in the model and the number of observations in the sample.

The models were built by stepwise addition of individual independent variables and assessment of their contribution to the variation explained. If adding the variable contributed significantly to the model then it was retained; otherwise it was dropped. This method ensured that the model ended up with the smallest possible set of independent variables included. The stepwise addition of independent variables in a model results in an additional increase of the variance being explained (R^2 change). At each step, an ANOVA was carried out to compare two models, Model 1(M1) and Model 2 (M2) by an F-test, where M1

is a nested model of M2 with the difference that M2 contains an additional independent variable whose effect on the overall model is being tested. The ANOVA test determines whether the increase in variance explained as a result of adding an independent variable is statistically significant.

4.2.1.1 Assumptions of the models

1. There is a linear relationship between the dependent variable and each of the independent variables.
2. The residuals follow a normal distribution
3. There is zero correlation between the dependent variables
4. There is homoscedasticity, i.e., the variance of the residuals remains approximately the same across levels of the independent variable in the regression.

To explore this variability, I built the following multiple linear regression models using antibody responses ($log_{10}OD$) as the dependent variable and various explanatory variables as described below.

Model 1, explanatory variable: Time of sampling

This is a simple linear regression model that has time as its only explanatory variable. In this analysis, I explored whether antibody responses to the DBL-α tags vary over time points.

Model 2, explanatory variables: time, antigens

In this model I explored the effect of antigenic differences on the antibody

responses having controlled for the effects of variation over time. I proposed that the 36 DBL-α tags I tested are antigenically different and therefore should show some level of differential recognition by human sera. For this and subsequent models, the categorical explanatory variable antigen was dummy coded for use in linear regression.

Model 3, explanatory variables: time, antibodies

In this model I explored the effect differences between individual sera having controlled for the effects of variation over time. Individuals are exposed to different variant antigens and as a result respond differently to the DBL-α tags. For this and subsequent models, the categorical explanatory variable antibody was dummy coded for use in linear regression.

Model 4, explanatory variables: time, antigens, antibodies

In this model I explored the effect of antibody differences on the antibody response having controlled for the effects of variation over time and antigenic differences. Similarly, we explore the effect of antigenic differences having controlled for variation over time and antibody differences.

Model 5, explanatory variables: time, antigens, antibodies, homologous-heterologous response

In this model I explored whether there are differences in homologous versus heterologous responses having controlled for variation over time, antigenic differences and antibody differences.

Model 6, explanatory variables: time, antigens, antibodies, interaction between antigens and antibodies

In this model I checked for interactions between antibody and antigens i.e. investigates whether there are particular antibody-antigen pair responses that are either high or low compared to the average for the antigen and antibody involved.

4.3 Results

In the case at hand, I employ linear regression models to explore variability in the antigenicity of the proteins as well as variability between serum donors in their total IgG directed at PfEMP1 and adjust for these in order to profile homologous-heterologous responses over time. Table 4.1 shows the amount of variance explained by each of the models (R^2_{Adj}) and the P values obtained from the ANOVA comparing nested models as described above. I built the model stepwise from individual independent variables and compared the contribution of the added variable to the overall fit of the model by carrying out ANOVA test comparing the model containing the independent variable to a nested model lacking the independent variable. This analysis tells us whether the additional variance explained by adding the additional independent variable is statistically significant i.e. whether the change in R^2_{Adj} is statistically significant.

Table 4.1. Overall IgG responses

Model	R_{adj}	ANOVA	P value
1	0.0114		
2	0.0975	Model 1-Model 2 (To test the effect of adding antigen to a model containing time)	0.004
3	0.2733	Model 1-Model 3 (To test the effect of adding antibody differences to a model containing time)	< 0.0001
4	0.3650	Model 4-Model 2 (To test the effect of adding antibody differences to a model containing antigen differences)	< 0.0001
		Model 4-Model 3 (To test the effect of adding antigen differences to a model containing antibody differences)	< 0.0001
5	0.3648	Model 5-Model 4 (To test for differences in homologous and heterologous responses)	0.4189
6	0.4579	Model 6-Model 5 (To test the effect of antibody antigen interactions)	<0.0001

From this analysis, there was significant variability between serum donors in their mean IgG directed at the DBL-α tags tested as well as variability in the mean antigenicity of the proteins indicating the heterogeneity of exposure and of the antigenic properties. After controlling for antigen and antibody differences, I analyzed the difference between the overall homologous and heterologous responses and observed that it was not statistically significant. However, there was a significant interaction between the two groups with time. At the time of infection, the heterologous response was high and declined significantly over the 16 week period while the homologous response was low at the acute time-point but gradually increased during the follow-up period (Fig 4.2).

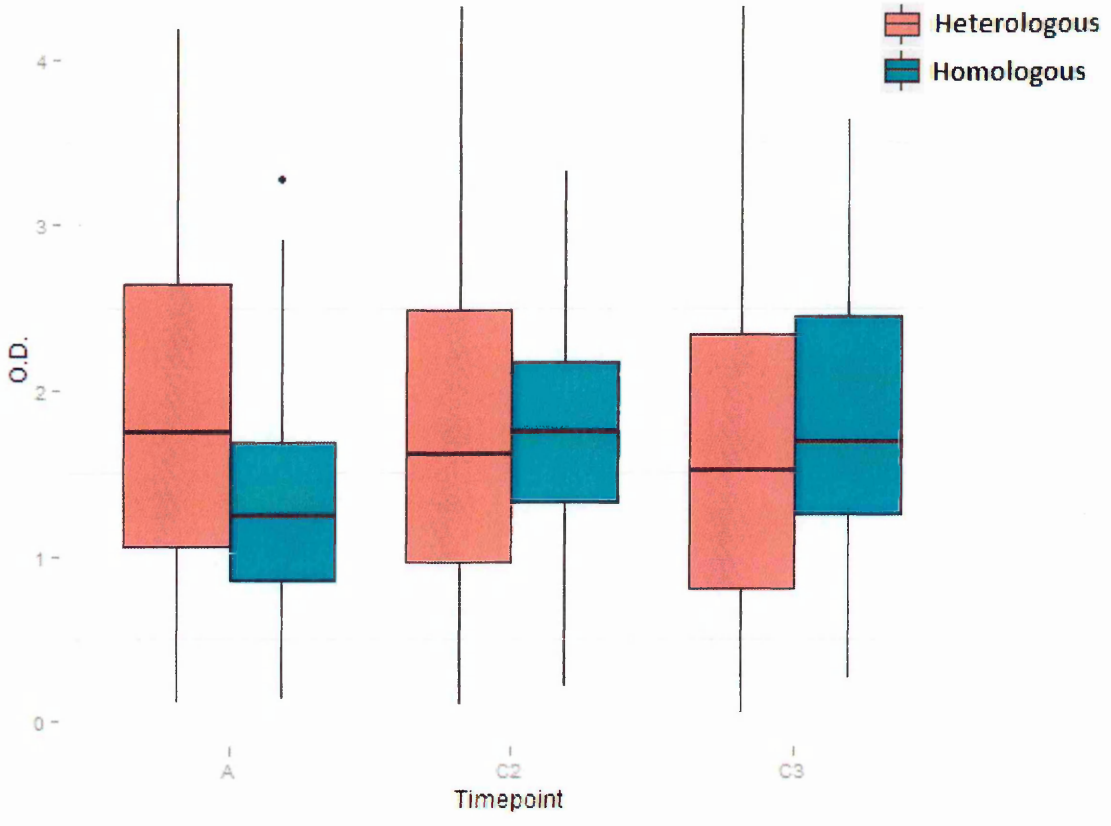

Fig 4.2 Acquisition of antibodies to 36 distinct DBLα-tag variants with time by 36 children. At the time of infection children had higher levels of antibodies to other circulating variants (Heterologous, red) as compared to the variant they were infected with (Homologous, blue). After infection, the children developed antibodies to their infecting variant.

I tested to see if there were interactions between the antigen and antibody using model 6. This allowed me to determine whether there are particular antibody-antigen pairs that have responses that are either high or low compared to the average response. From this analysis, I observed significant interactions between antigens and antibodies (Table 4.1). The dataset used in this analysis excluded immune responses directed at the homologous DBL-α tag and as such the antigen-antibody interactions observed involved heterologous antibody-antigen pairs. Such interactions signal gain or losses in heterologous IgG responses between specific antigen-antibody pairs after infection.

Many statistical tests assume that measurements or observations are independent. In the case at hand, linear regression models are built on the assumption that the OD measurements within and between individuals are independent or unrelated. In this study, repeated measures of OD were taken from the same individuals at 3 different time-points. Such repeated measures tend to be correlated. Linear regression treats data obtained from the 3 time points as independent, artificially increasing the sample size and decreasing the P value. This predisposes the analysis to type 1 error, i.e., observing effects as being significant when they are not. Analysing these data without accounting for the within person variability is analogous to using a 2 sample t-test where a paired t-test is required. In order to account for this dependency in the data set, I used linear mixed effects models in which the individuals were fitted as random variables. Even after correcting for within-individual correlations, the variations in mean DBLα specific antibodies in sera and the variability of the antigenicity remain significant. In the linear mixed effect models, the antigen-antibody interactions also remained significant (Table 4.2).

Table 4.2. Comparison of Linear mixed models

Linear mixed model ANOVA	P values corrected for repeated measures
Model 3-Model 4	<.0001
Model 4-Model 5	0.0366
Model 5-Model 6	<.0001

In addition, I carried out regression analysis of the antibody responses using datasets for each time point separately (Table 4.3 and 4.4). Although this reduces the sample size, it eliminates the dependency inherent in the dataset with all time points together. From this

analysis, there was a statistically significant variation in the mean reactivity of the sera against the 36 antigens tested at all the time points (Fig. 4.3) Similarly, I observed significant variations in the mean antigenicity of the antigens against the 36 sera tested (Fig. 4.4). This indicates that these individuals have exposures to different sets of antigens and that the DBL-α tags have different antigenic properties from one variant to another. After correcting for these sources of variation, I observed a significant difference between the mean homologous and heterologous IgG responses to the tags at acute and 4 week time-points but not at the 16 weeks. This is consistent with the observations seen with the combined analysis of all the time points in which the homologous response is low at the acute time point and increase to levels comparable to the heterologous response by the 16 week time-point. The distribution of the raw ELISA OD values for each of the antigens and antibodies at each of the acute, C2 and C3 time-points is shown presented in Figures 4.5, 4.6 and 4.7 respectively.

Table 4.3. Multiple linear regression models of immune responses by each time-point of serum collection.

Model	Explanatory Variables
Model 7	Antigens
Model 8	Antibodies
Model 9	Antigens, Antibodies
Model 10	Antigens, Antibodies, Homologous-Heterologous response

Table 4. 4. Multiple linear regression models of immune responses by time of serum collection.

	R_{adj}	ANOVA	P value
Acute			
Model 7	0.1441		
Model 8	0.1226		
Model 9	0.2858	Model 9- Model 7	<.0001
		Model 9- Model 8	<.0001
Model 10	0.3578	Model 10- Model 9	<.0001
4 weeks, C2			
Model 7	0.1023		
Model 8	0.4658		
Model 9	0.6087	Model 9- Model 7	<.0001
		Model 9- Model 8	<.0001
Model 10	0.6196	Model 10- Model 9	0.01090
16 weeks, C4			
Model 7	0.1087		
Model 8	0.4683		
Model 9	0.6182	Model 9- Model 7	<.0001
		Model 9- Model 8	<.0001
Model 10	0.6167	Model 10- Model 9	0.624

In order to exclude the effects of prior infections, I also analyzed the difference between the antibody measures at the acute sampling time and those from the two follow up periods (Table 4.5). There was significant variation in both the mean reactivity of the sera and the

mean antigenicity of the tags observed at 4 and 16 weeks after infection. This indicates heterogeneity in the parasites that infected these children even after correcting for past infections. However, there was a significant difference between the heterologous and homologous response at 4 weeks but not at 16 weeks.

Table 4.5. Multiple linear regression models of immune responses by the differences between the acute point of serum collection and subsequent follow up periods.

	R_{adj}	ANOVA	P value
4wks - Acute			
Model 7	0.119		
Model 8	0.3865		
Model 9	0.5417	Model 9- Model 7	<.0001
		Model 9- Model 8	<.0001
Model 10	0.5533	Model 10- Model 9	0.01444
16wks - Acute			
Model 7	0.1871		
Model 8	0.02171		
Model 9	0.2238	Model 9- Model 7	0.0482
		Model 9- Model 8	<.0001
Model 10	0.2939	Model 10- Model 9	<.0001

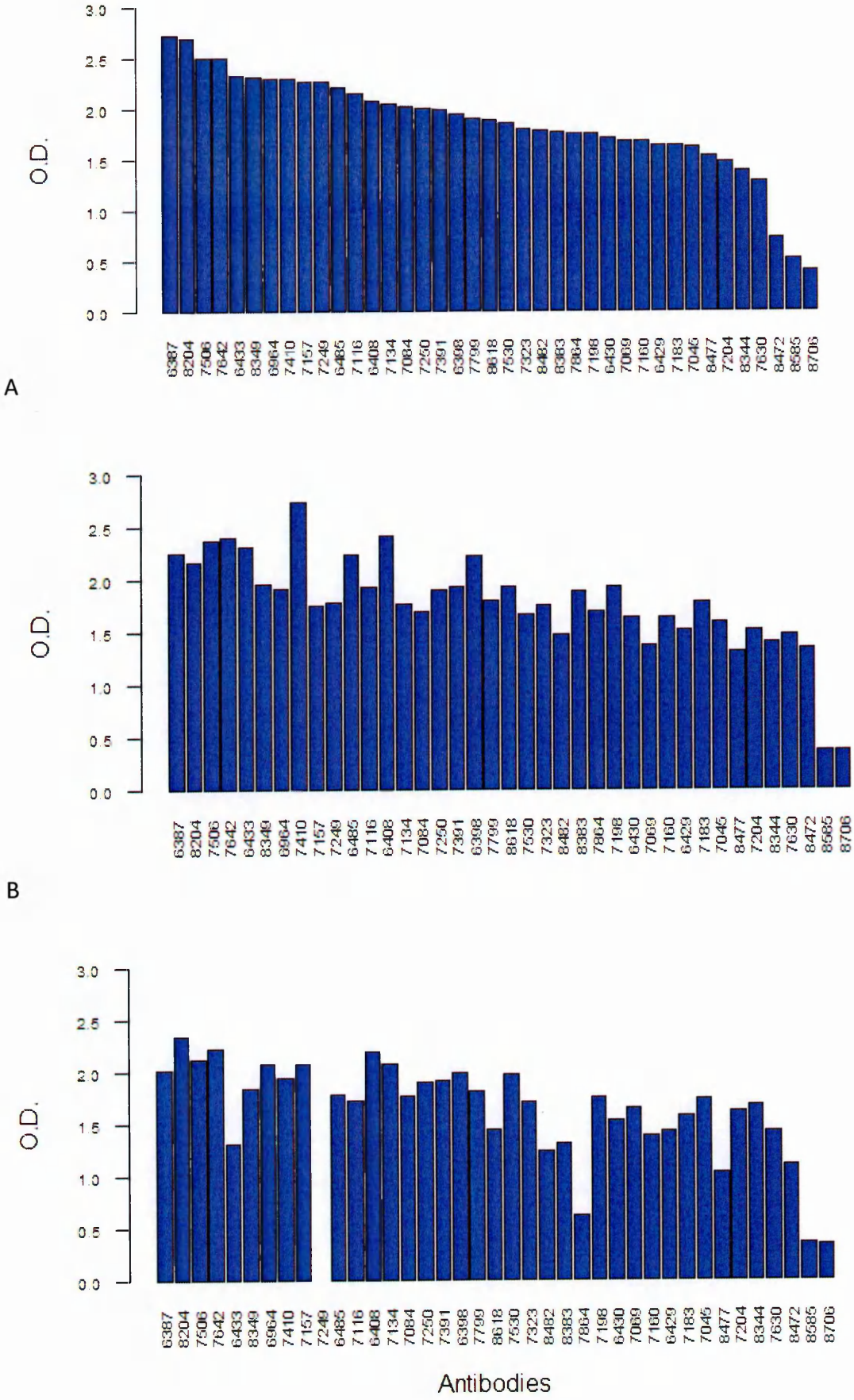

Figure 4.3 Variation in the mean reactivity of sera to antigens. The bar plot shows the mean response of the each child to the DBLα tag antigens at Acute (A), C2 (B) and C3 (C). 7249 serum volume was insufficient for C3 timepoint

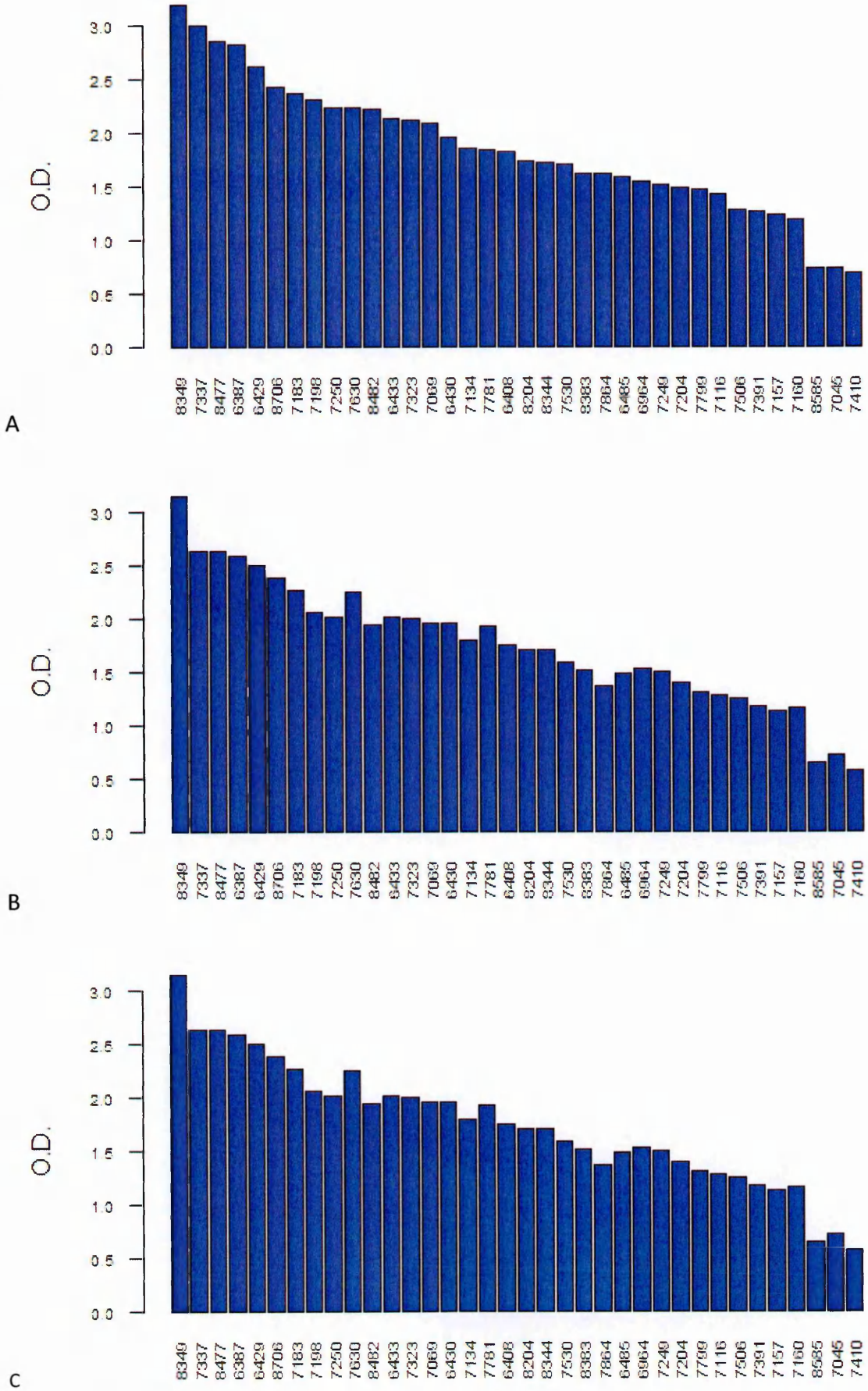

Figure 4.4 Variation in the mean immunogenicity of antigens. The immune response to each of the 36 DBLα tags measured against 36 sera was measured by ELISA. The bar plot shows the mean recognition of the each antigen at Acute (A), C2 (B) and C3 (C).

A

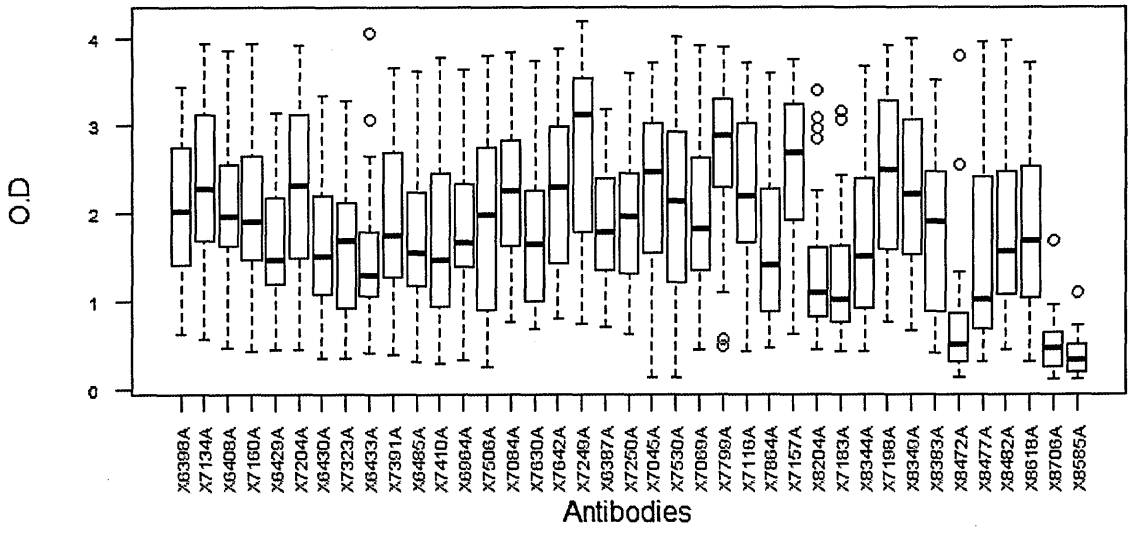

B

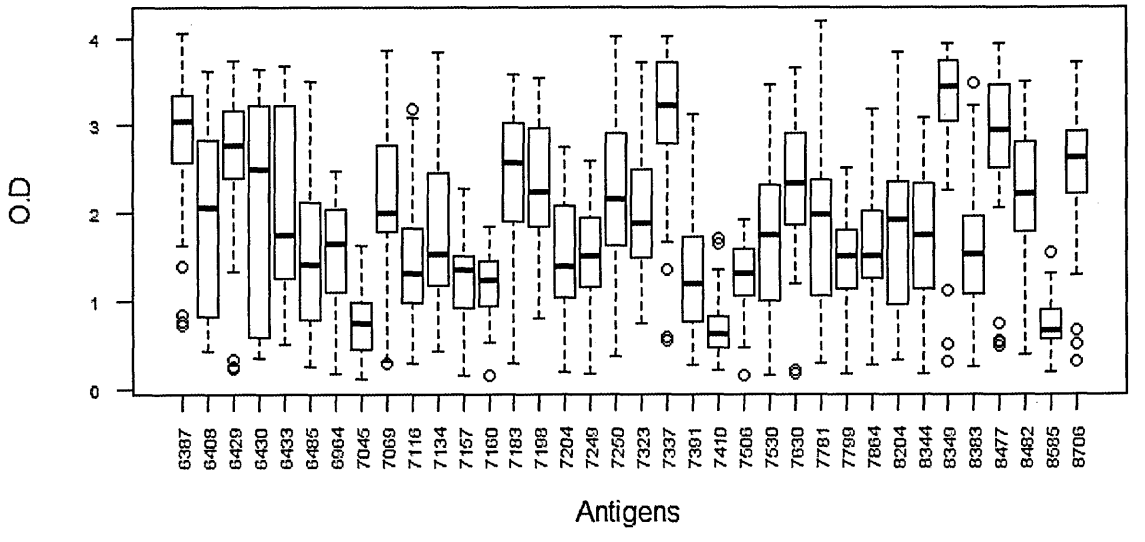

Figure 4.5 Distribution of the raw OD values for each of the serum antibodies tested against the 36 antigens (A) and for each of the antigens tested against the 36 sera (B) at the time the acute time-point.

A

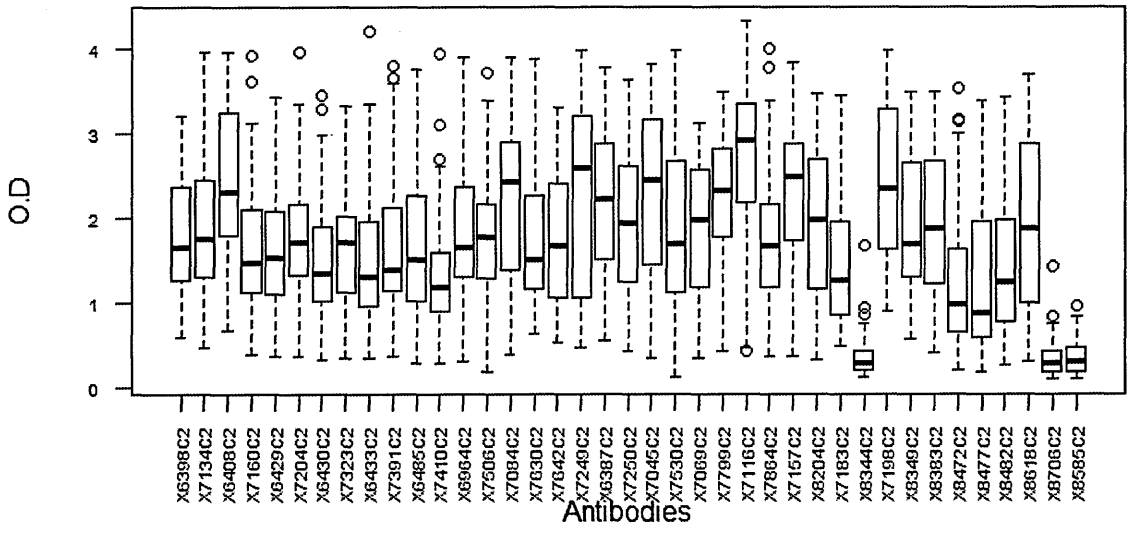

B

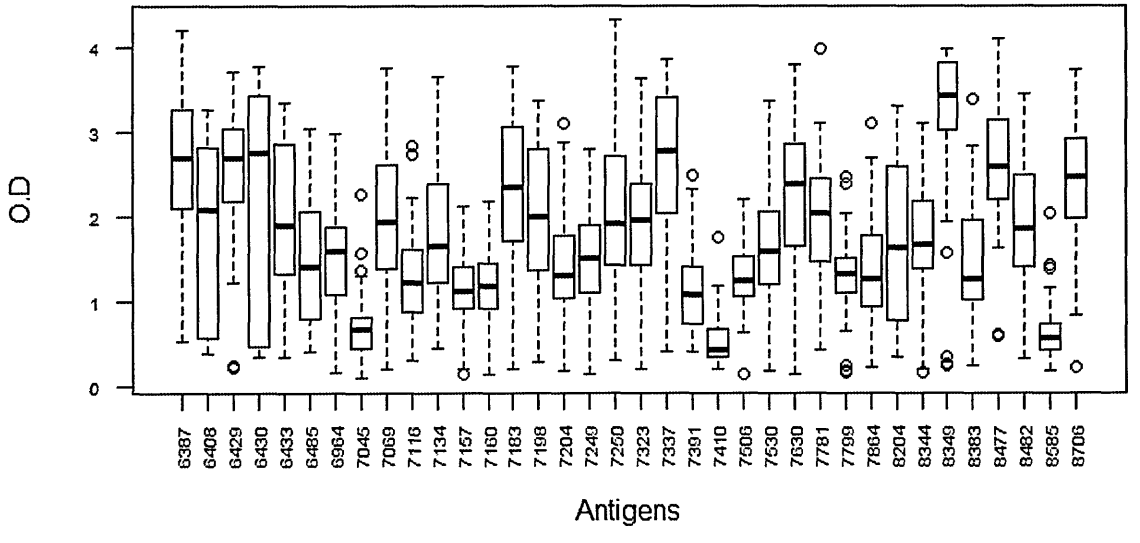

Figure 4.6 Distribution of the raw OD values for each of the serum antibodies tested against the 36 antigens (A) and for each of the antigens tested against the 36 sera (B) at the 2 week-convalescent time-point.

A

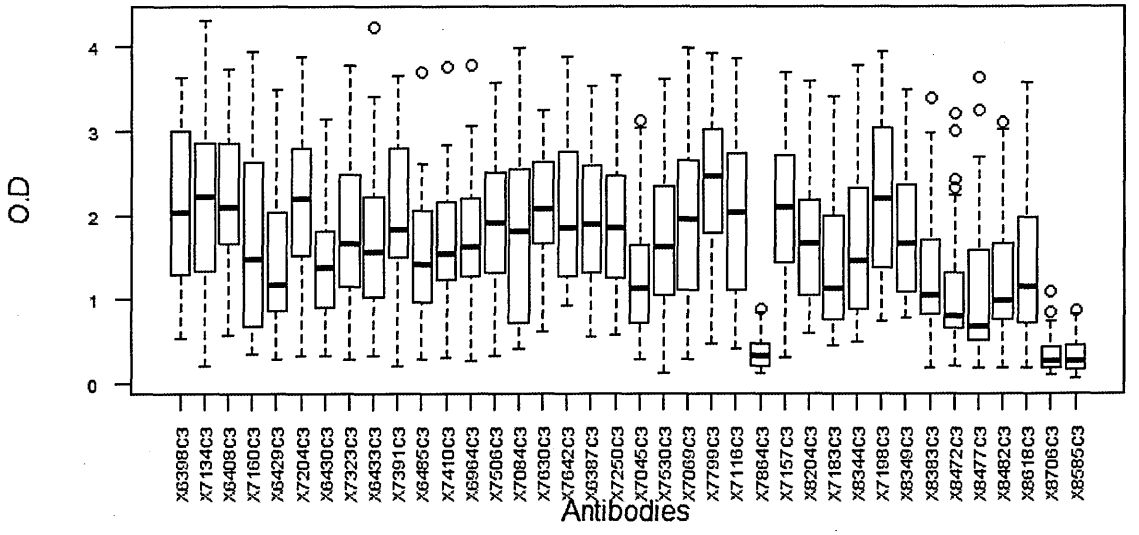

B

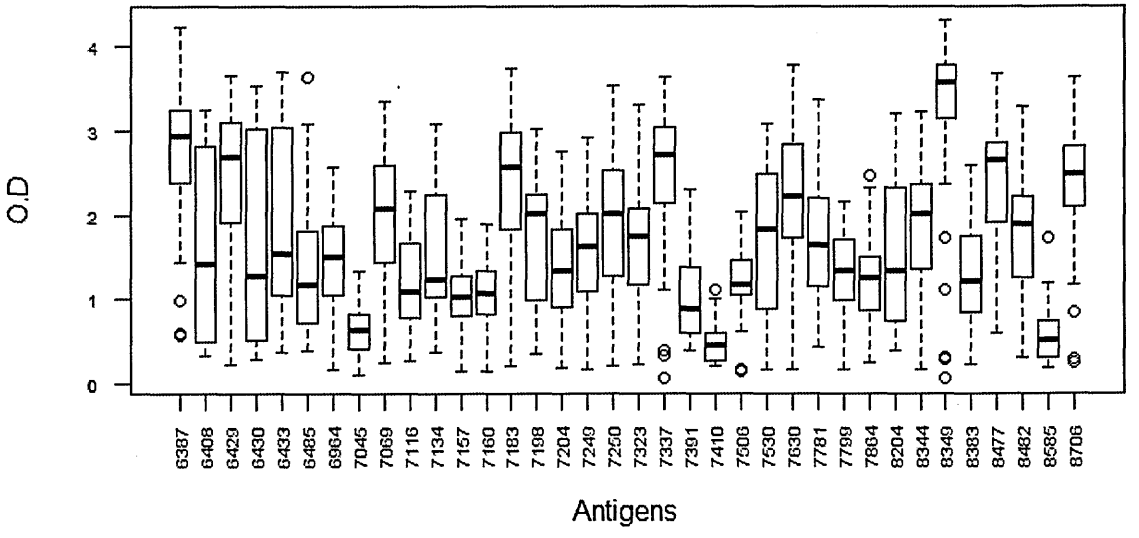

Figure 4.7 Distribution of the raw OD values for each of the serum antibodies tested against the 36 antigens (A) and for each of the antigens tested against the 36 sera (B) at the 4 month-convalescent time-point.

To test the assumptions of the models, a scatterplot of the residuals versus the fitted values was plotted. The distribution of the residuals remains fairly even for most of the fitted values in all the models. This indicates that the data meets the homoscedasticity assumption as shown for model 6 in figure 4.8. In addition, most of the residuals cluster around the zero line, indicating that the assumption of normality is justified. The histogram plot of the residuals shows normal distribution of the data (Figure 4.9). It is important to note that the dependent variable (O.D. values) were log transformed in all the models to achieve a normal distribution.

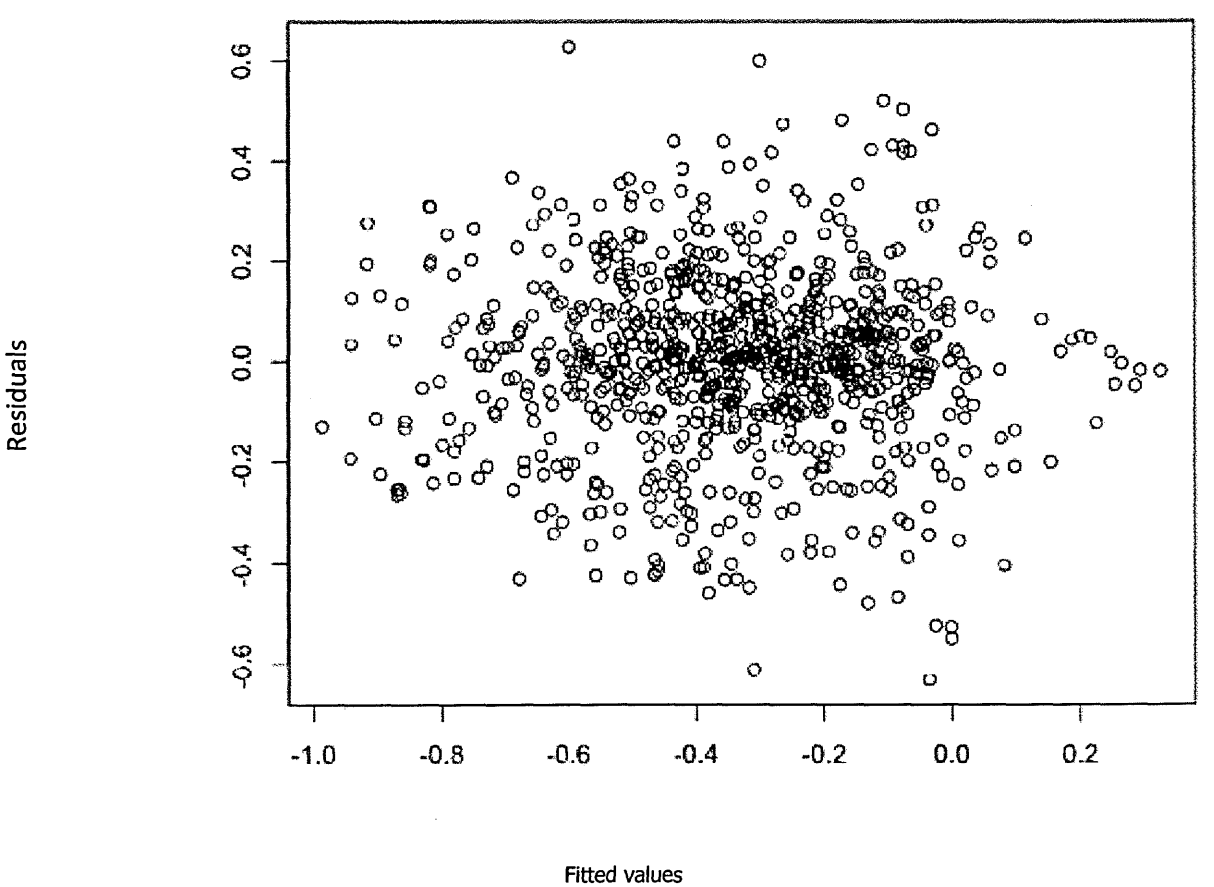

Figure 4.8 Scatter plot of residuals versus fitted values from model 6.

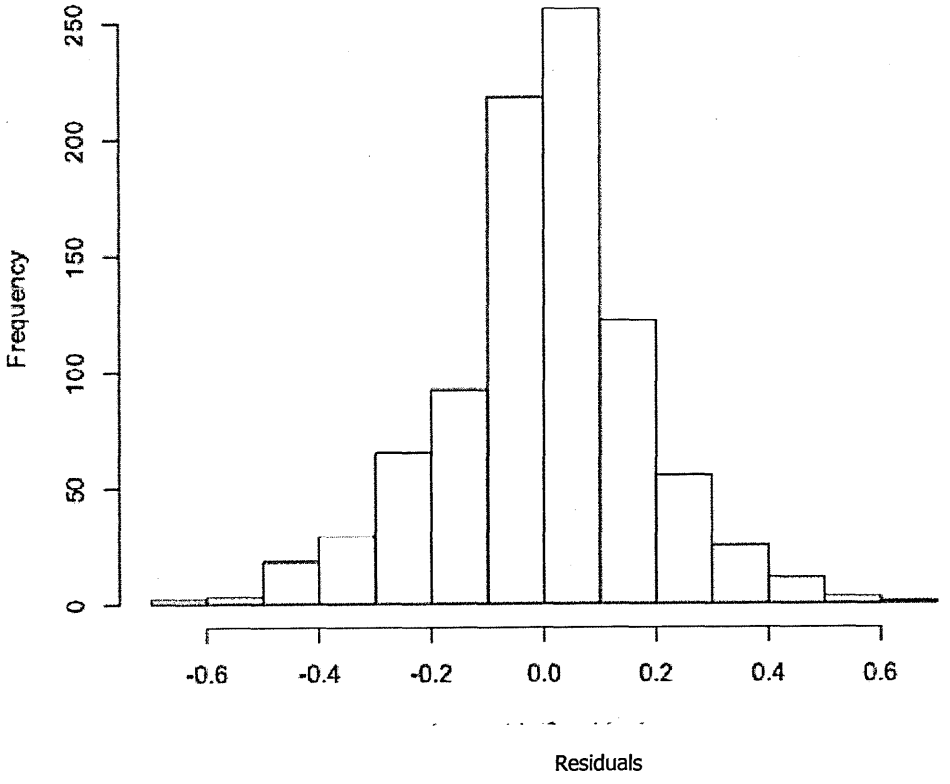

Figure 4.9 Histogram showing normal distribution of the residuals from the Model 6.

4.4 Discussion

In summary, I observed significant contribution to the variation of the immune response by both antigenic and antibody differences in all the models irrespective of whether the model was fitted to the collective responses at all time points (Table 4.1) or whether it was fitted to the immune reactivity measured at each time point separately (Tables 4.4) and this remained significant even after correcting for repeated measures (Table 4.2). This indicated that there is differential recognition of the DBL-α tags by IgG at all the time points.

In the model testing the interactions between homologous-heterologous responses with time, the levels of heterologous responses to the tags declined over time while the homologous responses increased over the follow up period in a pattern congruent with the "hole in the repertoire theory", i.e., a patient is infected by parasites expressing variants of the antigens to which the host has limited recognition as evidenced by the low recognition of the DBL-α tags at the time the child presented to hospital with the infection. The immunity to such variants is generated after infection as shown by the increased recognition of the DBL-α tags at subsequent follow up period. Bull and colleagues used a large prospective study to show that children falling ill with disease were more susceptible to infection with parasites to which they lack agglutinating antibodies than parasites to which they had antibodies (Bull et al. 1998). Taken from this perspective, the results presented here indicate that the DBL-α tag region could potentially be part of the epitopes targeted by the protective antibodies or has epitopes associated with the protective sites within the *Pf*EMP1 molecules. A recent case-control study analysing sex and age-matched children admitted to hospital with severe malaria and uncomplicated malaria found an association

between IgG responses to the DBLα and reduced parasite density. In the same study, severe malaria was associated with low IgG responses to DBLα (Rovira-Vallbona et al. 2012). In three separate studies using animal models, vaccine formulations based on the DBLα domain were effective in preventing infection with *P. falciparum*. Taken together, this points to a role for DBLα as a target of protective immune responses.

The immune responses to PfEMP1 are largely variant specific. However, I observed insignificant difference between homologous and heterologous responses (as measured by model 5) for the collective IgG responses (Table2) and this was true even after controlling for repeated measures (Table 3). When the analysis was run on the immune reactivity measured at each time point separately, significant differences were only observed between homologous and heterologous responses at 4 weeks post treatment, C2 (table 4.4). The increase in immune reactivity was more in the homologous responses indicating the responses were largely variant specific. Of interest is the increase in heterologous responses following a single episode of malaria. This point to the possible existence of a level of cross reactivity between different DBLα tags.

Most of the studies done on immune responses to recombinant DBLα are effectively measuring cross-reactive responses. In all these studies, the recombinant antigens are obtained from lab isolates to which the subjects from which the sera is obtained have probably not been exposed to (Joergensen et al. 2007; Joergensen et al. 2006; Mackintosh et al. 2008b; Cham et al. 2009; Rovira-Vallbona et al. 2012). The immune recognition observed in these studies points to the presence of strain transcending immunity. Immunisation with DBLα, has been shown to generate protective cross reactive immune

responses in an in vivo model of malaria (Moll et al. 2007; Ahuja et al. 2006).

Cross-reactive responses can only be generated by one antigen against another if they shared B cell epitopes and this would often be reflected at the genetic level by sequences similarity for linear or conformational epitopes and at the serological level by the pattern of responses. Two or more similar DBL-α tags will have a similar pattern of responses when tested against several immune sera. The heterologous antigen-antibody interactions is of particular interest and points at antigen-antibody specificity among heterologous pairs. This can be probed by further analysis of whether there are similarities /dissimilarities among the antigens with high/low heterologous interactions with the homologous antigen. This involves a combined analysis of the genetic and serologic properties of these DBL-α tags by antigenic cartography. Therefore, combining the genetic and serological data will allow us to refine the search for such epitopes.

Chapter 5

Antigenic Cartography: Quantifying antigenic relationships among variant recombinant antigens

Cross reactive responses against variant antigens of the same protein family within a parasite species provide empirical evidence of the presence of shared epitopes between variants. Analysis of such responses can yield important information about the antigenic structure of the parasite population. This information is important for vaccine design and immuno-surveillance in a post vaccine era. In influenza, for example, viruses are organized into distinct immunological clusters and vaccines are designed and continuously revised to be cluster specific. In this chapter, I utilized antigenic cartography - the tools used in the immunological analysis of cross reactive responses between influenza variants - to measure and visualize antigenic distances between variants of DBL-α tags from clinical isolates.

5.1 Introduction

The humoral immune system theoretically has the capacity to distinguish between an extremely large pool of antigens. In practice, it is common for different antigens to appear the same from the perspective of the immune system. In such cases, an antibody responses raised against one antigen fails to discriminate between the two different antigens. The ability of the antibodies to discriminate between antigens is a function of the antigenic similarity or differences between antigens.

There is no direct measure of antigenic similarity/differences between antigens. Antigenic distance is measured indirectly using common laboratory assays that include agglutination Inhibition (HI), microneutralization (MN), and Enzyme-linked immunosorbent assay (ELISA) (Smith et al. 2004). These assays rely on the ability of antibodies to distinguish between closely related molecules. Classical analysis presented immunological distance measurements from such assays in table format. In such a format, and especially for large antigen datasets, it is characteristic to have a lot of noise in the data and interpretation can be very challenging. Antigenic cartography is a recently developed computational tool that, similar to geographical cartography, draws maps based on the immunological distance measurements from assays that allows for visualization and quantification of distances between antigenic variants.

Antigenic cartography relies on the exquisite molecular specificity of antibodies for their ligands. The degree to which an antibody response specific to one antigen recognizes another antigen is dependent on the degree of similarity between the two antigens. Hence

two antigens that are both highly recognized by a particular antibody are antigenically similar and vice versa. A high assay reading on two antigens as measured by a particular antibody is therefore taken to indicate a close antigenic relationship.

The ability to distinguish between many closely related antigens is greatly enhanced when several antibodies with different specificities are tested against the antigens. In addition, it enhances the resolution of antigenic relationships and allows for a combined analysis of antigenic and genetic data where these are available.

When I analyzed antibody responses to the DBLα tag identified in clinical parasite isolates, significant gains and losses in heterologous antibody responses were observed as described in the previous chapter. The work discussed here describes the development of antigenic maps that explore these antigen-antibody interactions.

5.1.1 Immunological shape space concept

" Shape space" formalism was proposed by Perelson and Oster in 1979 as a theoretical concept in which antigen-antibody binding is represented in an abstract space of a given dimension (Perelson & Oster 1979). Antigens and antibodies are represented as points by coordinate vectors in this space and the distances between antigens and antibodies is related to their binding affinities. In their model, Perelson and Oster made the assumption that affinity measurements for the interactions between antibodies and antigens are related to the distances describing them in the shape space by a monotonic function. High experimental affinities are represented by small distances in shape space and vice versa. While they grossly estimated the "immunological space" to be of low dimensions, they had no means of deriving the actual coordinates of the antigens and antibodies in that space.

Given experimental data that measure the affinity between N antigens and M antibodies, the challenge is to derive the dimensions of the immunological space and the N+M coordinates describing the antigens and antibodies such that the distances between the antigens and antibodies in the shape space is monotonically related to the experimental data. Early approaches exploited techniques used in numerical taxonomy to represent antigenic relationships from an N×M panel in a multidimensional space whose dimensions were defined by M (Beyer & Masurel 1985; Dudman & Belbin 1988; Sneath & Sokal 1962). To illustrate this, take an N×M panel in which N antigens (in the rows) are tested against M sera (in the columns). Each row in this panel forms a vector that describes the coordinate of the respective antigen in an M dimensional space. Similarly, the columns contain vectors that describe the position of the antibodies in an N dimensional space. The antigen-antigen and antibody-antibody distances can then be deduced using the Euclidean method.

Table 5.1 Hypothetical antigen-antibody affinities.

		Antibodies	
		A	B
Antigens	X	0.5	2
	Y	1.5	2.5
	Z	2	1

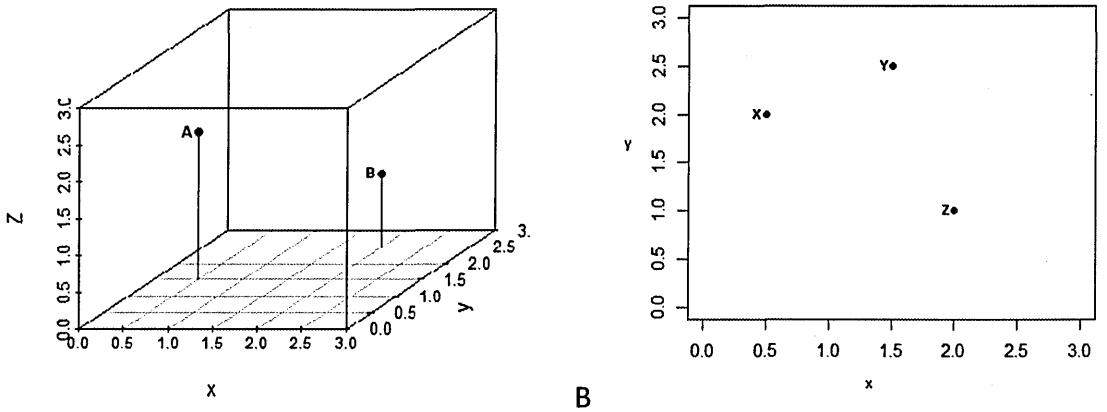

Fig 5.1. Relationships between antibodies (A) and antigens (B) as represented by numerical taxonomy. The co-ordinates for the antibodies are obtained directly from the experimental readings in the columns i.e. A (0.5, 1.5, 2) and B (2, 2.5, 1). Similarly, the co-ordinates describing the antigens are obtained from the rows i.e. X (0.5,2), Y (1.5,2.5) and Z (2, 1). Antigen-antibody affinities cannot be assessed because the antibodies are defined by a 3 dimensional space while antigens are defined by a 2 dimensional space.

5.1.2 Limitations of the numerical taxonomy method

In cases where antigens are tested against more than three antibodies, the configuration of the antigens is represented in hyperspace and is not immediately tractable to the human eye. In addition, the panel based approach defines coordinates either for the antigens (in M dimensional space) or for the antibodies (in N dimensional space) but not for both simultaneously (Fig 5.1). The antigens and antibodies cannot therefore be represented in the same space. Hence antigen-antibody distances cannot be deduced. Moreover, the distance obtained from this method is an aggregate of multiple measurements and does not correspond to the individual antibody-antigen distances in the experimental data. Lastly, Lapedes and Farber demonstrated that the dimensions defined by the width/length of the panel may not be the true underlying shape space that best describes the experimental data resulting in inaccurately projected similarities (Lapedes & Farber 2001).

Lapedes and Farber exploited ordinal multidimensional scaling (MDS), a technique developed in mathematical psychology that allowed them to define the true underlying dimensions of the shape space and position the antigens and antibodies in the same space such that antigen-antibody as well as antigen-antigen and antibody-antibody distances could be recovered. MDS are a set of algorithms that reconstruct the relative coordinates of points in shape space given only the experimental distances.

Serological Networks

Antigenic relationships between variant surface antigens have previously been described by a network approach (Buckee et al. 2009). This method adapts mathematical formulas used to describe relationships in human social networks to describe the population structure of the variant antigens by analyzing heterologous responses between *P. falciparum* parasite isolates obtained from clinical isolates as measured by an agglutination assay. In this method, the patient (antibody) and the parasite (antigen) are represented as one point/node in a space of pre-defined dimensions. The positioning of the points/nodes in this space is arbitrary and does not reflect any quantitative measure between the patient-antibody pairs. Instead, heterologous recognition between patient-parasite pairs are represented as a directed edge between the respective node pairs such that an edge directed away from a node represents recognition of the parasite while an edge pointing away from a node represents an agglutinating heterologous response from the patient. This method can help to easily identify which parasites or antigens are related, but cannot quantify the magnitude of these relationships. It reduces the quantitative data obtained from serological experiments into a binary measurement of whether or not parasite-patient (antigen-antibody) pairs have any sort of heterologous relations. Dichotomizing data in this way throws away data that would be helpful in distinguishing the degree of relationships among objects, parasites or antigens that share a relationship. The obvious advantage that antigenic cartography has over the network approach is that it provides a quantitative measure of the antibody-antigen, antigen-antigen and antibody-antibody relationships whereas the network approach is largely qualitative.

5.2 Method

5.2.1 Multidimensional Scaling

Antigenic cartography relies on multidimensional scaling which is an exploratory statistical technique that demonstrates relationship (distances or similarities) among objects by projecting the relationships in a low dimensional space such that there is a linear correlation between the measured/observed relationships among the objects and the relationships among the objects as projected in geometric space. Distance in the multidimensional space is summarized by the Minkowski distance model below

$$p_{ij} = \sqrt[1/r]{\left[\sum_{k=1}^{n} \left|x_{ik} - x_{jk}\right|^{r}\right]}$$

pij=measured distance between objects i and j

n= number of dimensions

x_{ik}=the position of point i on dimension k

x_{jk}= the position of point j on dimension k

r=user defined parameter that defines distance model; where

5. r=1, City-block distance model
6. r=2, Euclidean distance

Multidimensional scaling methods are used to project antigen-antibody relationships in geometric space such that distances between antigen-antibody pairs in that space match as

close as possible the antibody-antigen pair distances as measured by an immunological assay, e.g. the hemagglutination inhibition. In a typical experiment, multiple antigens are tested against multiple sera such that positions of the antigen and antibody points on the map are determined by multiple measurements. This improves the resolution and precision at which these data can be interpreted and minimizes noise and allows for the constructions of accurate maps even where some antigen-antibody pair readings are incomplete. In addition, by drawing the antigen-antibody positions in low dimensional space, it allows for the visualization and quantification of the antigen-antigen distances. In brief, the following steps are taken to generate an antigenic map.

i. Generate a matrix of pair wise antibody-antigen distances measurements from an immunological assay, (D_{ij} matrix), consisting of N number of rows (antigens) and M number of columns (antibodies).
ii. Choose an appropriate space of r dimensions.
iii. Draw an initial configuration in which points are allocated arbitrary coordinates in the r dimensional space
iv. The pair wise distances between antibody-antigen points are obtained from the initial projected configuration to make P_{ij} matrix using a Euclidean distance model.
v. Compare the D_{ij} matrix to the P_{ij} matrix by linear regression. The goodness of fit of the regression is computed by the least squares method in which the sum of square differences between the measured distances (D_{ij} matrix) and the projected distances (P_{ij} matrix). The goodness of fit measure is called the stress value and is calculated by the stress formula below.

$$Stress = \sqrt{\sum_{ij} |D_{ij} - P_{ij}|^2}$$

The stress value indicates the degree of correspondence between the measured values and the projected distances on the map

vi. Points in the projected configuration are then moved in the ordination space in a direction that minimizes stress the most. This is achieved with using multiple random starting points using the conjugate gradient optimization method (Ziegel et al. 1987).

vii. Steps iv-vi is repeated until the minimum stress value solution is obtained.

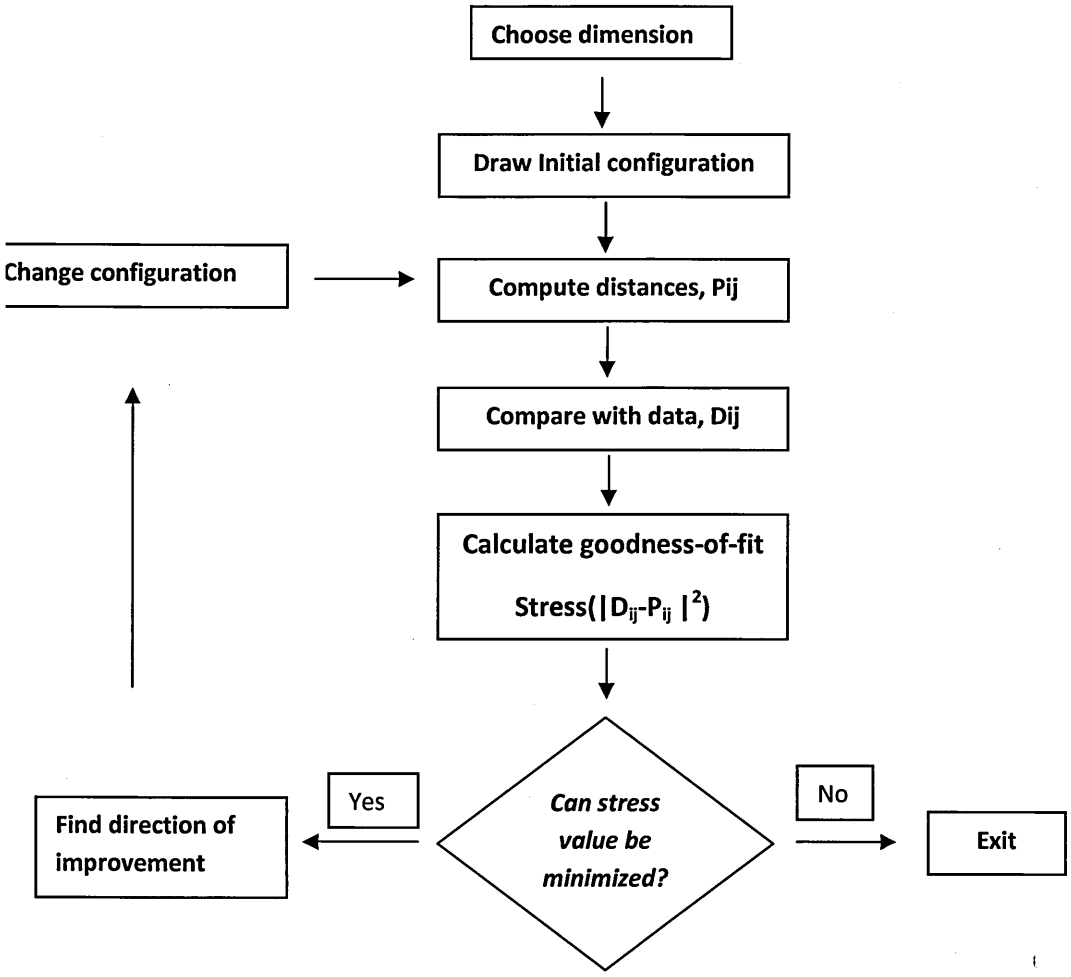

Fig 5.2 Schematic representation of the algorithm applied in developing antigenic maps.

5.2.2 Unfolding analysis

In a typical scenario, only the antigen-antibody distances are available from the experimental data. The antigen-antigen and antibody-antibody pair wise distances are only

unraveled after projecting the antigen-antibody distances in the same multidimensional space. This is referred to as the "unfolding problem" in MDS.

5.3 Results

5.3.1 Application to ELISA

Antigenic cartography has mainly been applied to study antigenic relationships among influenza viruses. Antibody reactivity in influenza is measured by the hemagglutinin inhibition assay using two-fold serial dilution with titre values ranging from <10 to >10,240 (Hirst 1943). A large inhibition of agglutination by sera induced by one strain against another strain indicates a small antigenic distance between them. In this work, antibody recognition was measured using ELISA, an immunological assay that measures the reactivity between a reference antibody and a test antigen by optical density (O.D.) measurements of a colorimetric reaction. Similarly, a high OD reading indicates that there is close similarity between the test antigen and the antigen against which the reference antibody was generated. Low OD values indicate distant relationships.

In order to apply the methods developed for influenza, the antigenic cartography maps were obtained by transforming the ELISA O.D. readings to equivalent titre dilution values suited to the hemagglutinin inhibition (HI) titres obtained from HI assay used by WHO and national influenza centers to quantify seroreactivity of influenza virus isolates (Ampofo et al. 2012; Smith et al. 2004). Briefly, the lowest OD reading was subtracted from the highest for each antigen tested to obtain the range which was subsequently divided by 11 to form categories of OD that correspond to the 11 HI titre dilution levels. The transformed OD readings were used develop antigenic maps through ACMACS-web program at

https://acmacs-web.antigenic-cartography.org/acmacs-web that employs metric multidimensional scaling in drawing its map. Metric multidimensional scaling is a parametric method that draws its maps in an Euclidean space.

In addition, an implementation of the ACMACS-web program in the R statistical software was also used. It included the modifications on metric multidimensional scaling described by Smith DJ and colleagues (Smith et al. 2004) in which the antigen-antibody pair wise immunological distances in the D_{ij} matrix are obtained transformed as below to normalize them.

a) The experimental distances (H_{ij}) were normalized to the maximum HI values

$$D_{ij} = b_j - log_2 (H_{ij})$$

b_j = the log_2 of the maximum transformed ELISA titre measurement for antibody j
H_{ij} = Transformed ELISA titre between antigen i and antibody j

5.3.2 Choice of Dimensions

The goodness of fit of an antigenic map to measured distances is greatly influenced by the number of dimensions in the ordination space. Ideally, the map should have no or low stress values in dimensional space that is tractable to the human eye (i.e. dimension ≤ 3). Maps that have acceptable stress values at dimensions higher than three cannot be visualized by the human eye and are difficult to interpret. On the other hand, maps projected on low dimensional space but with high stress values are highly distorted and are a misrepresentation of the original data.

In order to determine the choice of dimensions for the antigenic maps described here, I plotted a scree diagram (Fig 5.3) by projecting the stress as a percentage in different numbers of dimensions and choosing the dimension that has the best balance between the interpretability of the data and stress value. The stress value of the maps in a 2 dimensional space was 8.3 % which was acceptably low and comparable with published data.

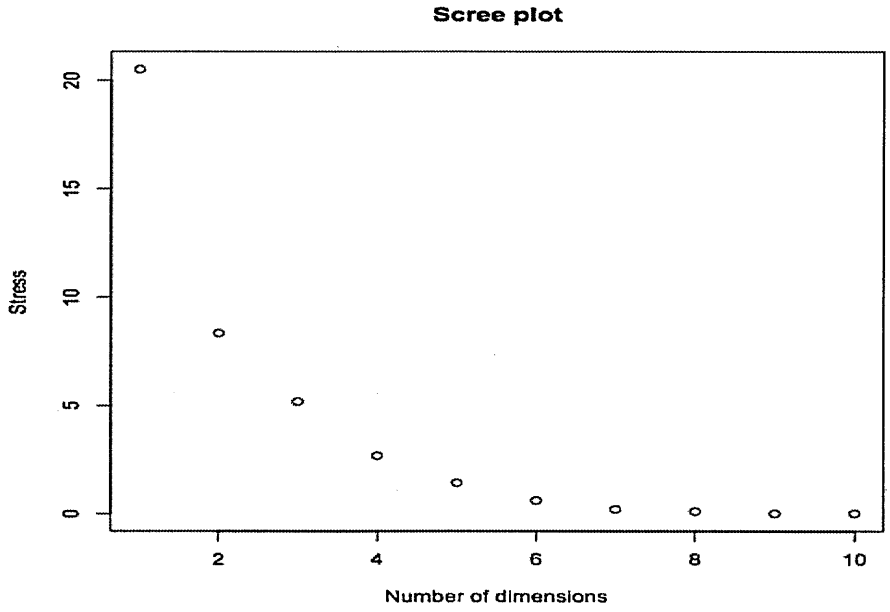

Fig 5.3 Percent stress values (x-axis) plotted against the corresponding number of dimension associated with it

From henceforth, therefore, all the maps were drawn in a 2 dimensional Euclidean space.

5.3.3 Selection of Informative Sera

Antigenic cartography relies on the ability of antibodies to discriminate between antigens. Sera that react highly or poorly with most antigens are poor molecular tools for discriminating antigens and have to be dropped from the analysis before drawing the antigenic maps. In addition, it is important to select sera with high diversity of reactivity

with the antigens in order to enhance the resolution of the maps. To address both these issues, only sera with a high standard deviation for recognition of antigens were included in the analysis. A standard deviation cut-off of 0.86 was used to select the sera (Table 5.3). This cut-off was selected based on the inspection of pattern of responses of individual sera (Fig 5.4). Dropping poorly discriminative sera from the construction of the map resulted in minimal movement of the positions of the antigens within the map (Fig.5.5 a,b,c). Despite this minimal change, subsequent maps were developed using informative sera.

To compare the changes in configuration of the points in the two maps, I used Procrustes analysis. This is a statistical tool that compares the geometry of two or more shapes in order to establish whether they are similar. It superimposes two configurations taking into account rotation, translation and reflection transformation to optimally align them to be as similar as possible.

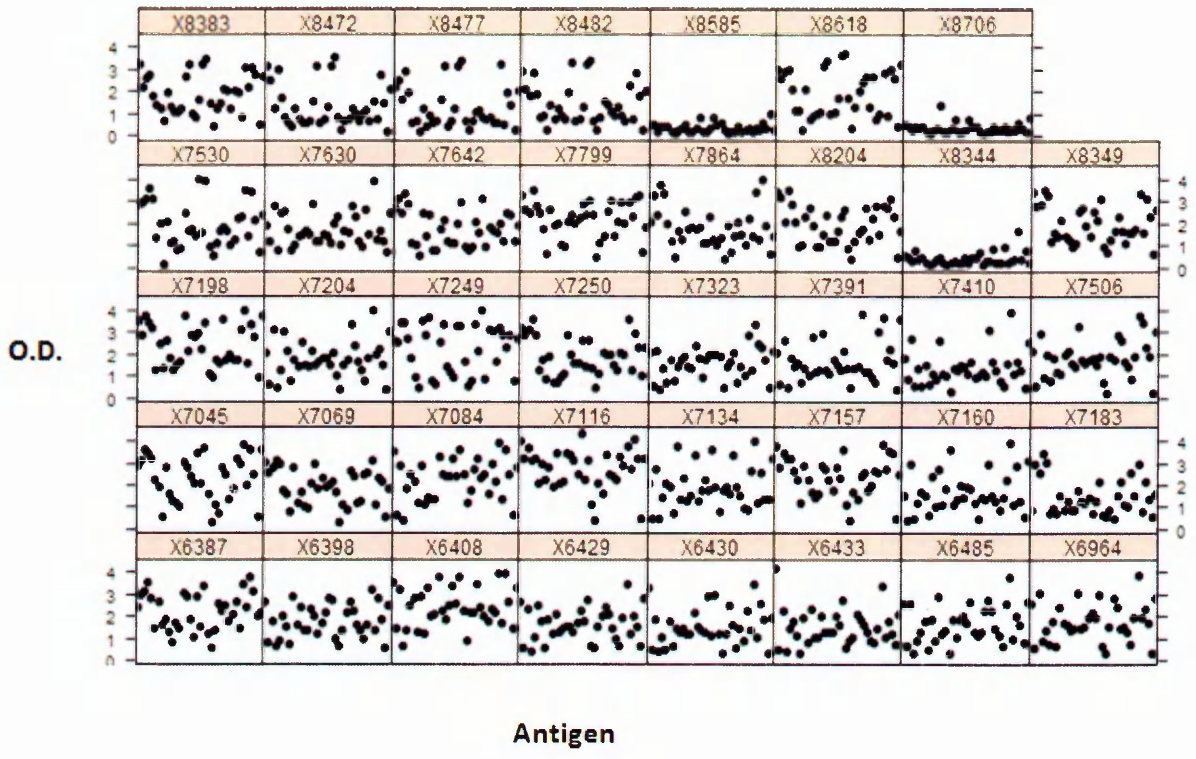

Fig 5.4 Multipanel plot showing the recognition profile of each serum to the 36 DBLα tags tested. Each panel shows the reactivity of one serum against 36 antigens. Recognition was measured as OD readings from ELISA (y-axis) and plotted against the 36 antigens (x-axis) for each serum.

Sera	8383	8472	8477	8482	8585	8618	8706	
SD	0.8806	0.9446	0.9587	0.9083	0.21203	1.0280	0.2591	
Sera	7530	7630	7642	7799	7864	8204	8344	8349
SD	1.00465	0.73189	0.77927	0.80174	0.89719	0.8487	0.3015	0.8347
Sera	7198	7204	7249	7250	7323	7391	7410	7506
SD	0.9285	0.83236	1.08394	0.8512	0.68680	0.90815	0.77654	0.84775
Sera	7045	7069	7084	7116	7134	7157	7160	7183
SD	1.02038	0.78614	0.90829	0.91362	0.92654	0.8791	0.88379	0.8134
Sera	6387	6398	6408	6429	6430	6433	6485	6964
SD	0.82722	0.74538	0.88393	0.73720	0.81898	0.81563	0.81730	0.86202

Table 5.2 Standard deviation of the recognition of each serum to the 36 antigen tested. An arbitrary cut off of 0.86 was set in order to select the most informative set of sera for antigenic cartography analysis. The sera that were dropped from this analysis are highlighted in yellow.

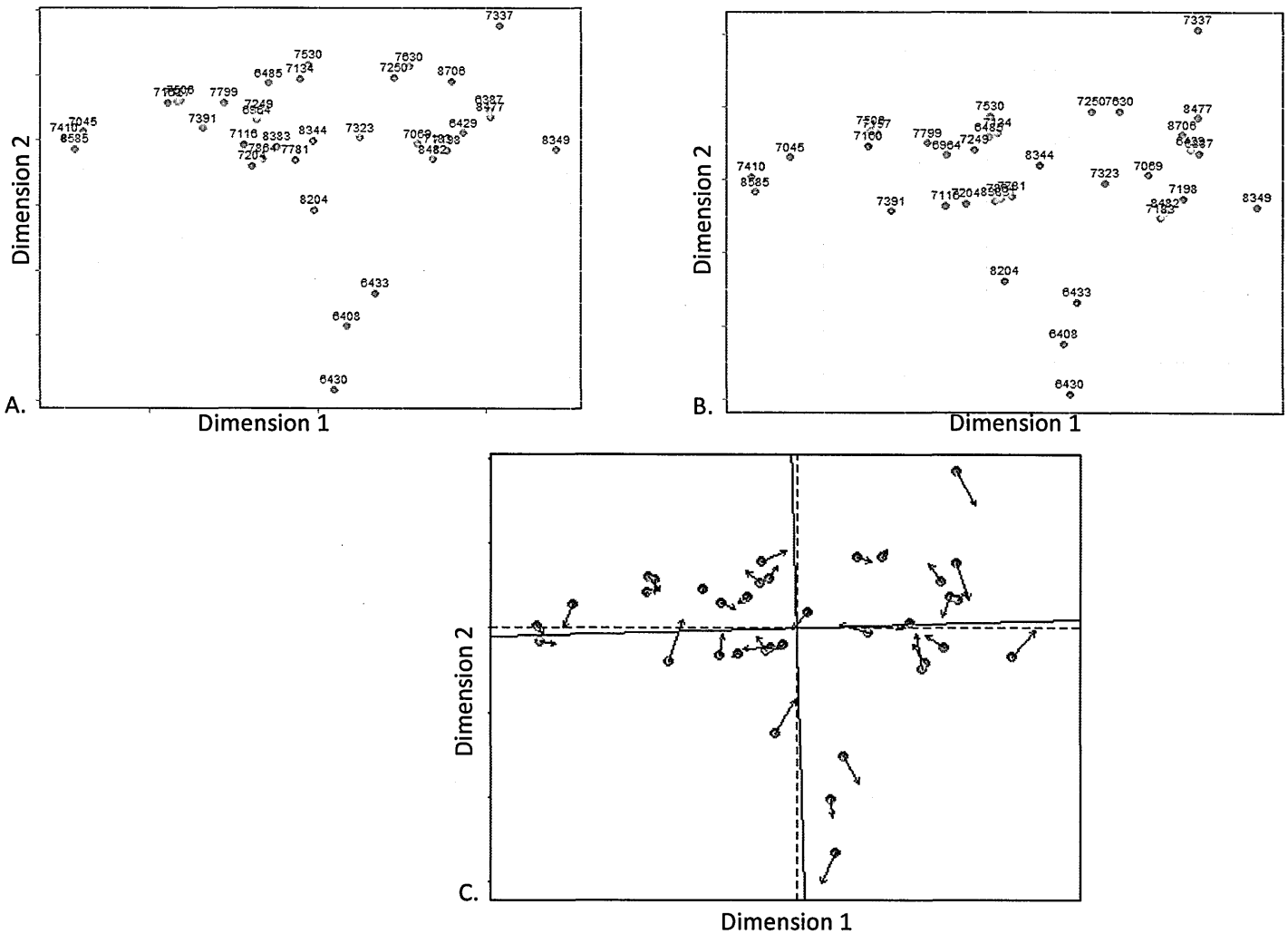

Figure 5.5 Antigenic map based on antisera at acute time-point for (A) all sera, (B) informative sera only. Procruste's analysis showing the difference between maps (A) and (B) is shown in (C). The points show the position of the map containing all sera and the arrows point to their respective point in the map containing informative sera. The dotted line shows the orientation of map with all sera and solid lines in the map indicate the degree of rotation of the map with informative sera taken to fit the two map

5.3.4 Adjusting for previous exposure

The sera used to discriminate the antigens were obtained from children living in a malaria endemic area. It is reasonable to presume that these children have had previous encounters with the parasite and will therefore contain in their sera antibody responses to variants of PfEMP1 from previous exposure(s). In such a scenario, it will be difficult to distinguish broad reactivity to multiple antigens observed as a result of the current infection in question from reactivity resulting from multiple antibody specificities to several antigens obtained past exposures. The ELISA OD readings at the acute time point give an indication of any long lived responses present in the sera from past exposure as well as early responses arising from the current infection. In order to filter out the effect of past exposure, the OD readings at acute time point were subtracted from those at the convalescent time points to obtain the immune responses that were as a result of the current infection under investigation. Antigenic maps were then developed maps on these values (Figs 5.6b and 5.7). This had the effect of shrinking the maps (Figs 5.6c and 5.8). This was because the average antibody titres had been reduced by subtracting previous titres. However, when this scaling effect was taken into account it was noted that some antigens moved to new positions resulting in a new pattern of orientation for the antigens. This shift of antigen positions was mostly among antigens defined by large antigenic distances whereas close antigenic relationships were maintained. As a result there was good correlation between inter point distances between antigens close to each other the two maps. For example, the antigenic relationship is maintained within the following 3 sets antigens in the two maps but not between them, i.e, (6964, 7157, 7506, 7160), (6430, 6433,

6408) and (7630, 7183, 8706). This analysis showed that responses from past exposure can confound the observed antigenic relationships especially between sets of antigens and it is important to exclude such responses before drawing antigenic maps.

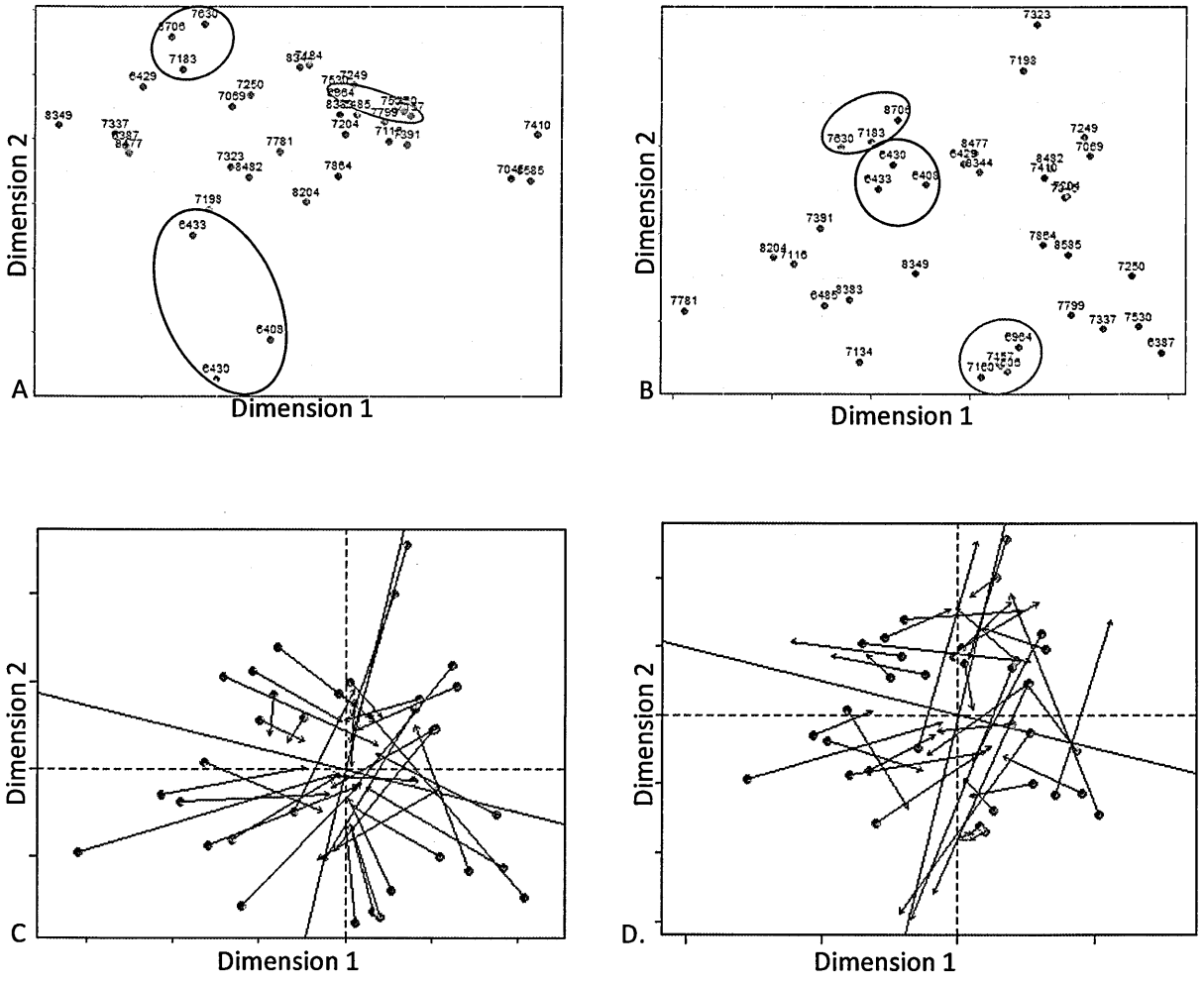

Fig 5.6 Antigenic map based on informative anti sera obtained 4 weeks after infection (A) before (B) after excluding responses from previous exposures. Procruste's analysis showing the difference between maps (A) and (B) is shown before (C) and after (D) adjusting for differences in scale between the maps. The points show the position of the map containing sera without previous exposure and the arrows point to their respective point in the map that includes responses due to previous exposure. The dotted lines indicated the orientation of the map drawn without previous exposure and solid lines in the map indicate the degree of rotation on the map with previous exposure taken to fit the two maps

5.3.5 Comparing the maps at 4 weeks versus 16 weeks

The apparent antigenic relationships between antigens change over time as the heterologous responses wane over time. There is a rearrangement of relative positions between points on the map at 16 weeks and as a result the overall pattern is altered when compared to the maps at 4 weeks. These movements included sets of antigens that shared close and distant relations. This is consistent with the temporal changes in heterologous response described in chapter 4. Due to this, the positions of the points in the immunological space are poorly constrained by the data at 16 weeks results and have alternative solutions that vary greatly from run to run.

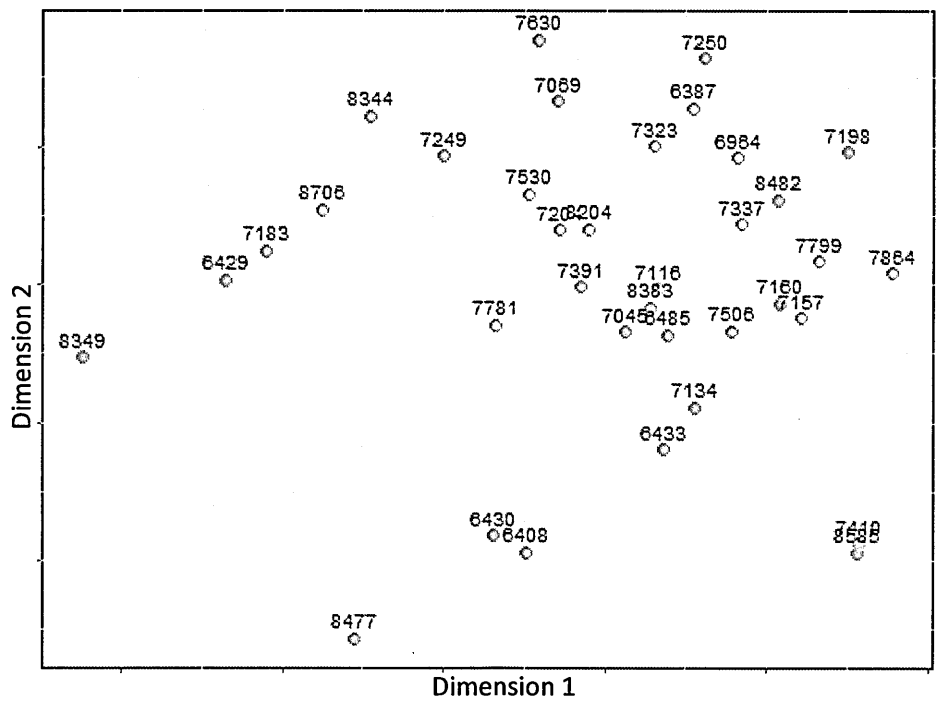

Fig 5.7 Antigenic map of the DBLα antigen tags at 16 weeks. In order to exclude the effects of previous exposure, the immune response at acute was deducted from that at week 16.

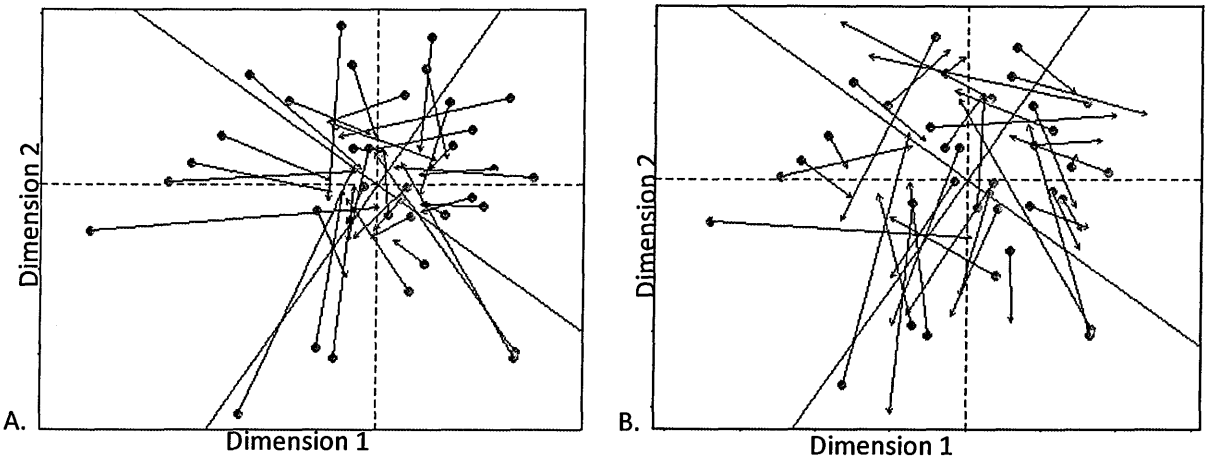

Figure 5.8 Procruste's analysis comparing the map drawn at 4 weeks to the map at 16 weeks before (A) and after (B) adjusting for differences in scale between the maps. The points show the position of the map at 4 weeks and the arrows point to their respective position at 16 weeks. The dotted line shows the orientation of the maps at 4 weeks and solid lines in the map indicate the degree of rotation on the maps at 16 weeks taken to fit the two maps.

5.3.6 Stability of the geometric solutions

The relative positions of the antigens and antibodies are constrained to specific coordinate positions within the immunological shape space depending on the amount of information contained within the sera. Highly informative sera restrict these positions to specific regions and result in a unique solution that varies only slightly from run to run. The only observed variations involve rotation, reflection or translation of the overall configuration while maintaining the relative distances between points. In contrast, solutions derived from low reactive sera are unstable. The positions of the antigens and antibodies are less constrained and vary greatly from run to run. To establish the rigidity of the antigenic configurations presented here, each data set was run though the antigenic cartography algorithm 10 times and the pair wise correlation between the points compared. For each dataset, the mean from the 20 pair-wise correlation permutations possible was computed. The average run to run correlation of the distances between points on the maps at 4 and 16 week convalescent time points was 0.95 and 0.80 respectively. Caution should be applied in interpreting maps that vary from run to run. Such variation could be restricted to a few egregious points or distributed evenly among all points.

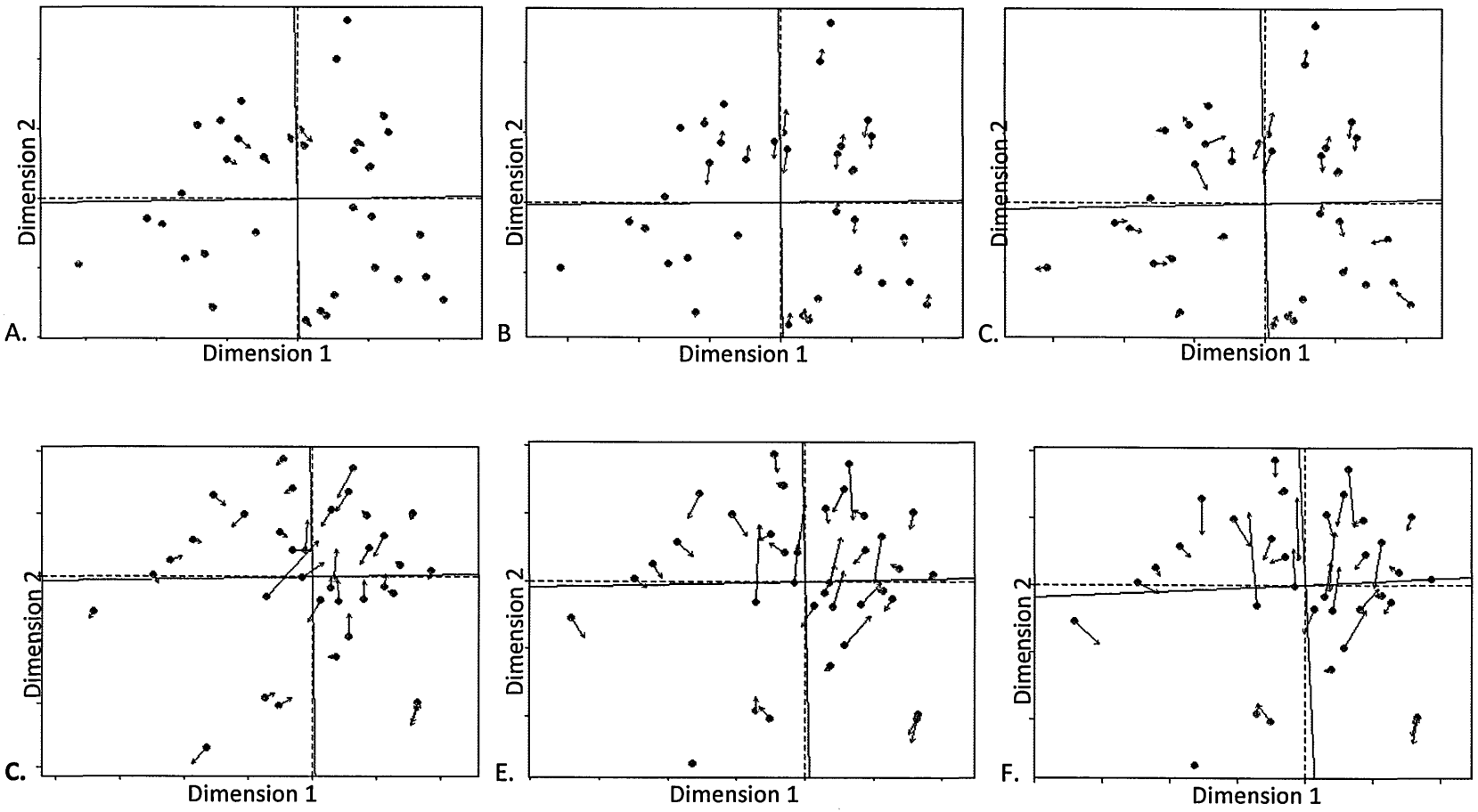

Figure 5.9 Procruste's analysis showing run to run variation of points for the antigenic map at 4 weeks (A, B, C) and at 16 weeks (C, E, F).

5.4 Discussion

The immunological shape space is a powerful concept that allows us to quantitatively project, *in silico*, how the humoral immune system processes information about antigens it encounters. In a naïve individual, this immunological space is devoid of immunological responses and hence there are no restrictions to antigens. Pathogens expressing any antigen variant can survive in this space. However, with each infection or vaccination, individuals develop immune responses that close the gaps occupied by antigens in this space. The degree to which an antibody is effective against an antigen is determined by their antigenic distance. By projecting antigens and antibodies in the same space, it is possible to determine the antibody-antigenic and antigenic-antigenic distances and determine the degree to which cross reactive responses are generated between antigens.

This method has been used to describe antigenic relationships in several antigenically variable viruses including human and animal influenza viruses, enteroviruses, lysaviruses and flavivirus (Smith et al. 2004; De Jong et al. 2007; Huang et al. 2009; Mansfield et al. 2011; Ducatez et al. 2011; Horton et al. 2010). The WHO relies on antigenic cartography to monitor antigenic changes in the circulating influenza viruses in order to decide on whether to update vaccines for the next season (Ampofo et al. 2012; Fouchier & Smith 2010). The malaria parasite lends itself to analysis by antigenic cartography; its immunological targets exhibit variation between and in some targets within parasite genomes. The shape-space of the malaria parasite and how the immune system covers it is probably complex. The parasite has several morphologically distinct developmental stages with multiple stage

specific antigens that exhibit great antigenic diversity. Defining the shape space parameters for individual antigens associated with protection provides a simpler alternative. The work presented in this chapter set out to determine the shape space characteristics of DBL*α* tag antigens.

Given experimental data, the computational task in antigenic cartography involves not only determining the coordinate points in shape space of antibodies and antigens that fit the data but also the dimensionality. Using qualitative arguments, Perelson and Oster estimated the dimensions of shape space describing antigen-antibody binding to be low, (N=5-10) (Perelson & Oster 1979). This was confirmed by Lapedes and Farber who exploited MDS to infer the dimension of shape space using a series of experimental HI data sets (Lapedes & Farber 2001). In determining the dimensionality of experimental data, maps are usually constructed in different numbers of dimension, say from 1 to 10, and the goodness of fit value analyzed for each dimension. The true underlying dimensions of the experimental data will be given by the minimum dimension in which coordinates of antigens and antibodies do not yield stress. For HI data, this was shown to between 4-5 dimensions (Lapedes & Farber 2001). For the work presented in this chapter, the zero stress solution was observed in 6 dimensions consistent with the estimations of Perelson and Oster. Such dimensions although low, are not tractable to the human eye; in most studies a compromise is made between the stress and the ease of interpretability. A certain amount of stress that does not distort the configuration too much is tolerable. There is no absolute cut off for acceptable stress levels. This is analyzed on case by case basis as stress increases

with increase in the size of the datasets even for the same underlying data structure and maybe evenly distributed across all points or restricted to a few egregious points. Kruskal and Clarke have proposed several "rules of thumb" to act as guidelines for evaluating stress (Kruskal J.B. 1964b; CLarke K. R. 1993).

Table 5.2 Guidelines on acceptable stress values proposed by Kruskal 1964b and Clarke 1993

% Stress	Kruskal's guidelines
2.5	Excellent
5	Good
10	Fair
20	Poor
	Clarke's guidelines
<5	An excellent representation with no prospect of misinterpretation.
5-10	A good ordination with no risk of drawing false inferences
10-20	Can still correspond to a usable picture, although values at the upper end suggest a potential mislead. Too much details should not be placed on details of the plot
>20	Likely to yield a plot that is relatively dangerous to interpret. By the time stress is 35-40 the samples are placed essentially at random, with little relational to the original distances

The antigenic map at 4 weeks yielded stress values of 0.21 for the one-dimensional solution, 0.08 for the two-dimensional solution and 0.05 for the three dimensional solution. The two dimensional solution was selected as the best solution for ease of interpretability.

This method relies on the information about the antigens that is contained within the antibody response/reactivity. Sera that have similar experimental reactivity to antigens they are tested against have little informational content about the differences between antigens. Sera that are highly reactive will have similar readings for all antigens and will end up close to each other on the shape space. Such sera offer little information that allows the determination of distances between antigens. On the other hand, maps drawn using sera with low OD or titre values to most of the antigens will fall into random positions every time the map is drawn. The position of the antigens in shape space is not constrained by the poorly reactive sera. In order to develop robust antigenic maps, I included only informative sera in my analysis. In this analysis, I used a cut off of 0.86 to exclude sera that reacted poorly with most antigens as well as sera that reacted highly with most antigens. The exclusion of these sera did not alter the geometric orientation of the maps consistent with the view that they contain little information. This also indicated that the sera used in the analysis contained enough information to constrain the location of the antigens and antibodies to specific coordinates in shape space.

Antigenic cartography has been used to study relationships between antigens in various pathogens. In all of these studies, the sera used to discriminate the antigens were raised in animals after a single infection (Smith et al. 2004; Horton et al. 2010). These are monospecific polyclonal sera i.e. it is a mixed population of antibodies that bind to different epitopes within a single antigen with varying binding affinities. Antigenic cartography represents the overall reactivity of these multiple specificities as a single point on the map.

This becomes challenging however for polyclonal polyspecific sera, i.e., sera that contains mixed population of antibodies that bind multiple antigens that have variable multiple epitopes within them. Antigenic cartography assumes that each antibody represents a single binding affinity to an antigen. Representing several sera with binding affinities to multiple antigens as a single point will inaccurately project the relationships between antigens. To illustrate this, consider sera obtained from individuals vaccinated with the leading malaria vaccine, RTS,S , a conjugate vaccine that contains both *P. falciparum* and hepatitis B virus antigens (Cohen et al. 2010). Such sera when experimentally tested will react strongly with the two organisms. When projected in shape space, this would show an erroneous antigenically relationship between *P. falciparum* and the hepatitis B virus. Similarly, the sera used in this study were obtained from children likely to contain antibody specificities to multiple antigens. The antigenic relationships observed maybe influenced by pre-existing antibody specificities acquired from exposure to previous infections. Exclusion of antibody responses acquired before the infection under investigation resulted in the movement of some antigens from specific regions of the shape space. These antigens appear to have been anchored at these positions by responses from past exposure or by responses generated very early in the immune responses. Within a single monoclonal infection, *P. falciparum* parasites can express more than one *Pf*EMP1 isoform resulting in sera with multiple specificities. For this study, antigens were expressed and sera obtained from individuals from whom we identified the dominant *Pf*EMP1 isoform. The degree to which a DBL-α tag was dominant varied widely among the parasite isolates (10-85%) (Gitau et al. 2012). A thorough investigation of the antigenic relationships between PfEMP1

antigens will require variant specific sera obtained from naive animals or individuals (i.e. first infection).

Chapter 4 describes temporal changes in the levels of homologous and heterologous responses over a 16 week period after infection. The decrease in heterologous response results in sera that have lower reactivity to the antigens at 16 weeks as compared to 4 weeks after infection. Such sera, because of low informational content, do not constrain the position of the antigens to specific coordinates within the immunological shape space. As a result, there was run to run variation in the relative position of the antigens in maps drawn using sera at 16 weeks. In contrast, the geometry of antigenic relationships of the maps 4 weeks after infection is resistant to such changes. My favored interpretation is that that the configuration of antigens observed at 4 weeks is maintained by short-lived cross reactive responses that are lost by 16 weeks. Recker and colleagues have developed mathematical models that implicate short lived cross reactive responses in maintaining chronic infection by orchestrating antigenic variation (Recker et al. 2004). In this hypothesis, short lived cross reactive responses to minor epitopes prevent the emergence of new *Pf*EMP1 variants while a dominant long lasting and variant specific response prevents the infecting variant from persisting for long. By combining antigenic cartography with sequence data, it may be possible to identify regions within the gene that underlie such cross reactive responses. Such regions, once identified, potentially form good components of a multi-epitope vaccine. This is investigated in more detail in chapter 6.

So far, I have assumed that the experimental data available are a measure of the distance between antigen-antibody pairs. The ordination method that assumes linear relationship between the experimental data and the distances projected in shape space is called metric MDS. It is possible however to recover an accurate reconstruction of the configuration of the points using only the rank order of the experimental data (Kruskal J.B. 1964b; Kruskal J.B. 1964a). The numerical values of the experimental data are only used to sort the values in rank order. Given enough data, the set of ordinal relations across and along the panel generates adequate variation on the distances between points in the space such that the solution from the derived simultaneous inequalities divides the immunological shape space into small regions to which the points are restricted. This form of ordination is called the ordinal or non-metric MDS.

Although ordinal MDS is non-parametric, it results in metric space from which accurate antigen-antibody, antigen-antigen and antibody-antibody distances can be obtained (Lapedes & Farber 2001). The advantage of this method is that no assumptions are made about the nature of the monotonic relationship between distances from the experimental data and the shape space distances. The nature of this relationship can be recovered using the ordinal MDS. When applied to hemagglutinin inhibition (HI) titres, the relationship between the experimental data and the shape space distances was found to be linear allowing Smith and colleagues to develop modify the algorithm originally described by Lapedes and Farber from ordinal to metric MDS which is computationally less intensive. This

becomes important especially where there is experimental data of low precision for which only ordinal relationship may have significance.

Chapter 6
Comparative quantitative analysis of antigenic and genetic relationships

The antigenic phenotype of any organism is largely determined by the genotype. In this chapter, I carried out an antigenic phenotype-genotype analysis in order to define regions in the genes encoding the DBL-α tags that best explain the serological patterns obtained by antigenic cartography. Genetic maps based on pair-wise distances obtained from sequence alignment of the DBL-α tags were compared to the antigenic map by a sliding window approach to identify regions in the genes that best fit the antigenic maps. The regions identified in this study exhibited considerable diversity even among members of a serologically distinct cluster indicating that they may be members of a conformational epitope. It also highlights the pitfall of inferring serological diversity from primary sequence data.

6.1 Introduction

In order to avoid clearance in the spleen, *P. falciparum* introduces antigens on the surface of the infected red cell that allows it to bind to the host's endothelial surfaces and sequester away from peripheral circulation in blood. While this may be an effective way to evade clearance in the spleen, it renders the parasite-infected red cells susceptible to humoral responses. To evade the latter, *P. falciparum* employs antigenic variation, a mechanism by which the parasite alters the antigens at the surface of the infected red blood cells. The metabolic cost of this to the parasite is expected to be high. The immune system is exposed to what appears to be an unlimited number of antigen/parasite variants and has to rise to the occasion by creating immune responses that recognise each and every variant. Given the extreme antigenic diversity within a parasite population that the immune system must experience in order to protect individuals from disease, how specific should the antibody responses be?

Although immunity to variant surface antigens is acquired mainly in a variant specific manner, it is accompanied by the generation of partly protective heterologous responses to parasites to which the host has not been exposed (Elliott et al. 2007). There are several lines of evidence to support this in both human and animal models: after a single episode of malaria in previously immunologically naive hosts, 5 out of 14 individuals, developed antibody responses that recognized variant surface antigens to which the host had not been exposed (Elliott et al. 2007). This has also been demonstrated in animal models: gibbons challenged with *P. falciparum* developed immune responses against heterologous parasites

(Cadigan & Chaicumpa 1969; Cadigan et al. 1969). Infection of *Aotus* monkeys previously exposed to a single variant of a homologous strain *P. falciparum* with antigenic distinct variants of the same strain yielded partial cross protection (Siddiqui et al. 1978). In humans, patients being treated for syphilis by infection with the malaria parasite developed immunity to malaria after relatively few infections (Reveiwed by Doolan et al. 2009). In the natural setting, the intuitive conclusion that anti disease immunity is acquired after relatively few infections compared to extreme diversity of variant surface antigens within a parasite population points to an accumulation of cross-reactive responses. Adult malaria-naive immigrants developed immune responses to malaria rapidly when exposed suddenly to malaria in an endemic zone (Baird et al. 1991; Baird et al. 1993). In a similar study, the threshold for acquiring anti-disease immunity was set at 4 infections within a two-year period (Baird et al. 2003). Collectively, these underscore the importance of cross-reactive responses.

The adaptive arm of the immune system has, in theory, receptors that can bind and discriminate between an extremely large repertoire of diverse antigens (Pancer & Cooper 2006). Naive B cells have broad specificity that allows them to bind closely related antigens. However, after affinity maturation, mature B cells arise that can discriminate between closely related antigens. Having bound their cognate antigens, receptors on naive B cells undergo a process of affinity maturation in which several rounds of somatic hyper-mutations followed by a selection of the best binders results in enhanced specificity of antibodies to their ligands. In theory, this should allow the immune system to generate

antibodies with high specificity for every antigen encountered. In practice, however, failure of the adaptive response to discriminate between different antigen/parasite variants is common. In that case, from the perspective of the immune system, two or more different but closely related antigens would appear the same. In such a scenario, just one infection would protect the host from parasite variants to which the host has not been exposed.

Generation of antibodies that recognize antigens on parasites strains (or species) that are different from the original strain that initiated the antibody response provides an accelerated and efficient way in which the immune system can cover extreme antigenic diversity. Such cross-reactive responses could arise as a result of a limitation imposed on the affinity maturation process such that the B cells have inadequate interaction with their cognate antigens to form specific high-affinity discriminatory antibodies during the first infection. Alternatively, the generation of cross-reactive responses could be driven by shared or similar antigens/epitopes between parasite strains or species.

Antibodies recognizing antigens other than those that initiated the first response are often observed in nature. The binding specificity of such antibodies is expected to be a function of the "antigenic distance" between any two antigens. There is no direct measure of antigenic similarity: these measurements are usually obtained indirectly using quantitative immunological assays that exploit the exquisite specificity of antibodies for their ligands, for example, the hemagglutination inhibition assay for the influenza virus (Hirst 1943). In this assay, the degree to which antiserum raised against one strain of influenza inhibits the agglutination of red blood cells by another influenza strain is taken as a measure of

antigenic similarity. A large inhibition infers small antigenic distance between the strains and vice versa. Antigens that are poorly discriminated by the humoral immune system will have very small distances between them. Representing such distances in low dimensional space allows for identification of antigenically related parasite strains/species and the development of cross-reactive antibody responses where these are generated as a result of antigenic similarity (Lapedes & Farber 2001; Smith et al. 2004). Furthermore, when combined with genetic similarity at the sequence level, the precise position of linear antibody epitopes driving such cross-reactive responses can, in principle, be found. In the work that follows I test the hypotheses that:

- antigenic distance and genetic distance are correlated.
- gain/loss in responses after infection is a function of the antigenic and/or genetic distance between variant antigens.

6.2 Structure of the antigenic map

For subsequent analysis, the antigenic map derived in chapter 5 from sera at 4 week convalescence period was used. This map was constructed using informative sera and removing effects of previous exposure by subtracting the ELISA OD readings at the acute time point from those at the 4 week convalescent time-point. From the immune system's point of view, antigens within a close cluster are perceived as being similar. In the antigenic map (Fig 6.1), it was observed that rather than being scattered across the antigenic space, there were small DBL-α tag antigenic clusters with some antigens pairs appearing almost antigenically identical, e.g. 7204 and 7045.

Antigens within a cluster are perceived to be similar by the immune system mainly because at the molecular level there are common epitopes shared between them. Such epitopes could either be linear and are much easier to decipher from sequence data and/or conformational that are much more difficult to decipher. Despite considerable sequence heterogeneity among PfEMP1 variants, the DBL-α domain is the most conserved domain within and between parasite isolates (Smith et al. 2000; Rask et al. 2010). It contains short stretches of conserved sequence that have been used to design universal primers with which DBL-α tags from both field and laboratory isolates can be sampled. Bull et al have exploited distinct sequence features within these tags to classify these DBL-α tag sequences into 6 groups (the Cys/PoLV grouping) (Bull et al. 2007; Bull et al. 2005). This classification is based on short blocks of sequences showing limited variability (PoLV) and the number of Cysteine residues (Cys).

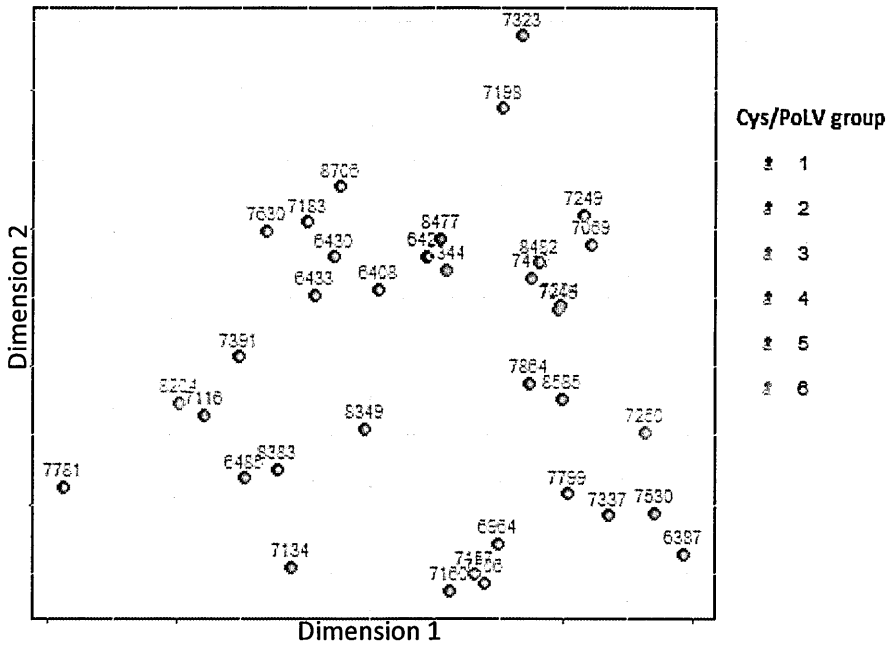

Fig 6.1 Antigenic map of the DBL-α tags colour coded according to the Cys/PolV grouping system. The map was derived from recognition of the antigens by a subset of the sera that showed great variability in recognizing the tags obtained from the convalescent children at week 4. In order to exclude the effects of previous exposure, the immune response at acute time point was deducted from that at week 4.

To investigate whether antigens cluster according to the Cys/PoLV grouping, the DBL-α tag sequences were classified as previously described and the map was color coded according to the genetic groupings. Comparison of the antigenic clusters to the Cys/PoLV grouping yielded no discernible clustering (Fig 6.1). To examine the degree of clustering in a more quantitative manner, the distances between all possible pairs of antigens were calculated and grouped according to whether the pair included antigens from the same versus different Cys/PoLV grouping (Fig 6.2). This showed that the antigenic distances within Cys/PoLV groups had a spread of values that were not different from the pair-wise distances between members of a particular Cys/PolV group or members of other different groups (Fig 6.2). It is thus apparent

that the antigenic similarity is poorly explained by the Cys/PolV groups and indicates that the epitope regions lie beyond the PoLV region.

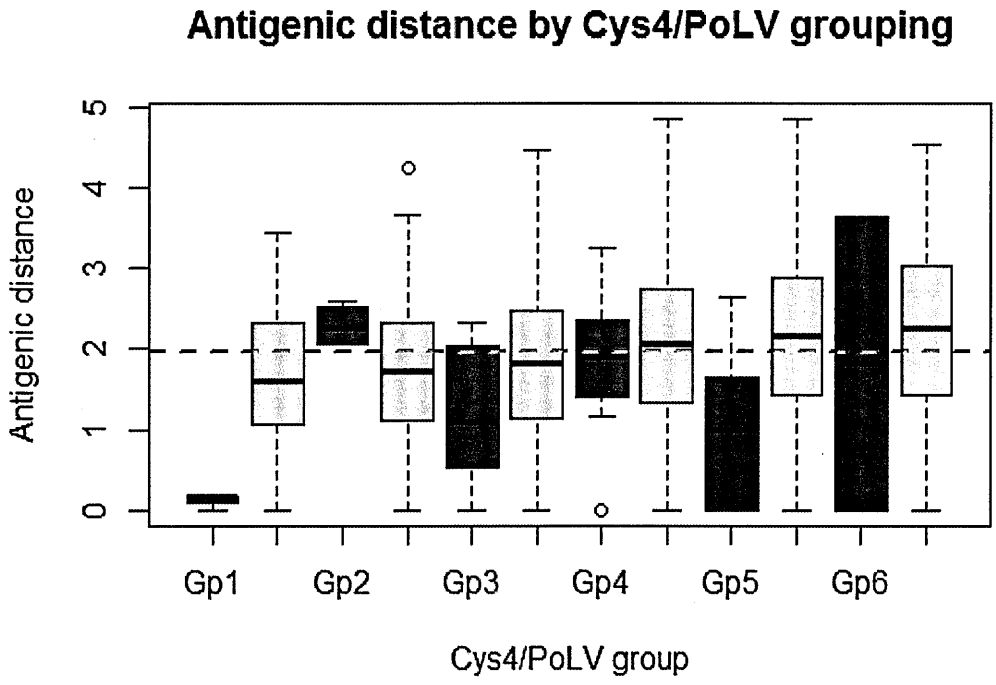

Fig 6.2 Antigenic distances between pairs of antigens in the same (blue boxes) versus different (green) Cys/PoLV groups. The interquartile range of the pair-wise antigenic distances is indicated by the length of the boxes while the median is shown by the vertical line through the box. The whiskers indicate the range of the distances excluding the outliers (indicated by points below and/or above the whiskers). The red dotted line indicates the mean antigenic distance for all tags.

To further examine clustering of antigenically similar DBLα-tags, unsupervised hierarchical cluster analysis of the pair-wise antigenic distance matrix from the antigenic map was carried out. This identified 6 main clusters at the antigen level as shown in the heat map in Fig 6.3. This result further indicates that the immune system recognises some groups of antigens as more similar than others and supports the clustering observed in the antigenic map (Fig 6.1).

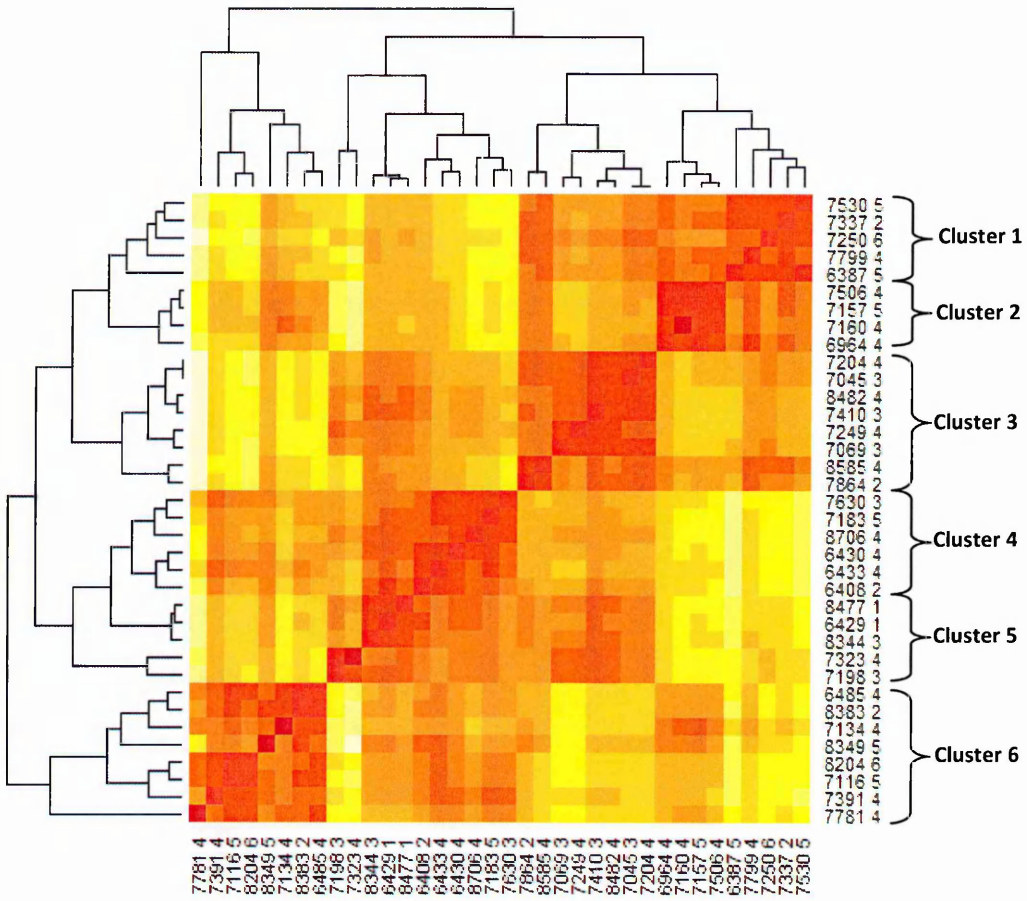

Fig 6.3 Antigenic clusters identified from unsupervised clustering of the pair-wise antigenic distances from the antigenic map. The rows/columns are labelled with the antigen name followed by the Cys/PoLV group type. The braces on the right vertical axis and the dendograms indicate the antigenic clusters identified.

6.3 Comparison of genetic map to antigenic map

In order to compare the relationship between the protein sequence and antigenic similarity of the DBL-α tags, genetic maps based on protein sequence alignment of the DBL-α tag sequences were constructed. To draw the genetic map, all the 36 sequences were aligned across the whole length of the DBL-α tag region (Fig 6.8) and the pair-wise identity scores between the

sequences were computed by the p-distance method. This method counts the number of amino acid differences at each site and expresses them as a proportion of all the sites analysed. Sites with missing data or alignment gaps were not included in this computation.

The genetic map was constructed using the same method and settings used for constructing the antigenic map. The resulting genetic map (Fig. 6.4) showed the DBL-α tags clustering according to the Cys/PoLV groups with more similarity within groups than between groups (Fig 6.5).

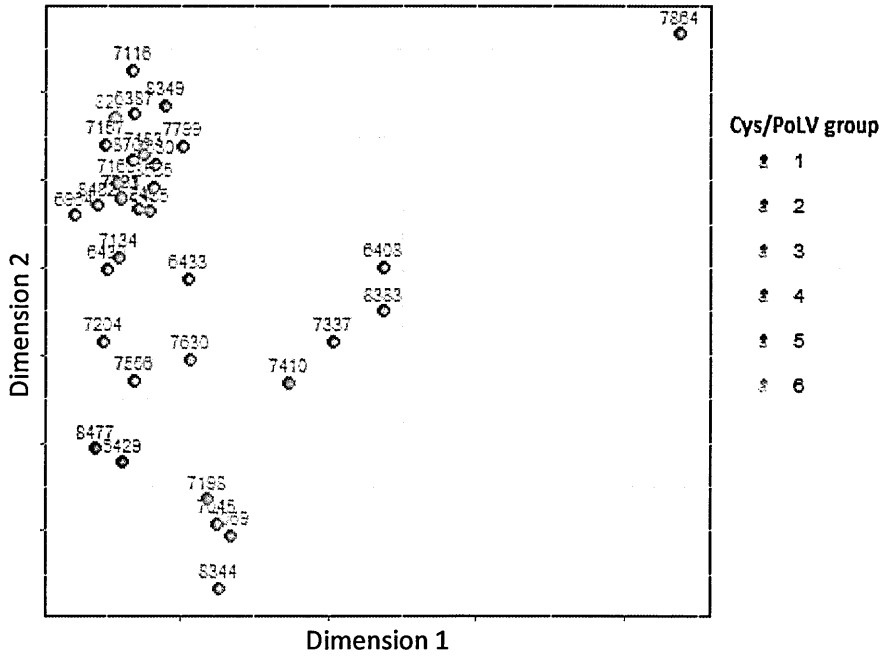

Fig 6.4 Genetic map of the DBL-α antigen tags colour coded according to the Cys/PolV grouping system. The map is a projection of the pair-wise identity scores of the DBL-α tag sequences.

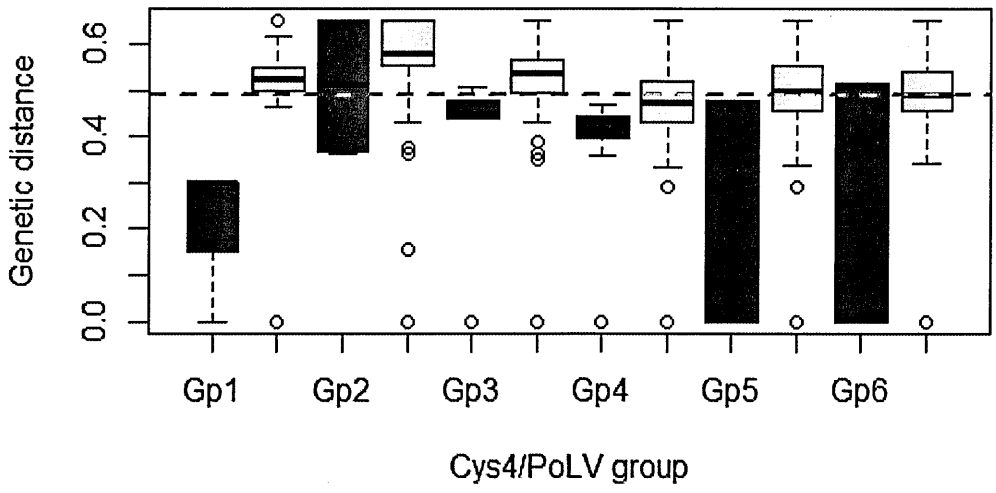

Fig 6.5 Genetic distances between pairs of antigens in the same (blue boxes) versus different (green) Cys/PoLV groups. The interquartile range of the pair-wise genetic distances is indicated by the length of the boxes while the median is shown by the vertical line through the box. The whiskers indicate the range of the distances excluding the outliers (indicated by points below and/or above the whiskers). The red dotted line indicates the mean antigenic distance for all tags.

As for the antigenic map, the genetic pair-wise distance matrix from the genetic map was used to construct a heat map. The heat map was ordered to follow the arrangement of antigens on the heat map that derived antigenic clusters by unsupervised cluster analysis (Fig 6.3). There was no correspondence between the clusters identified on the antigenic and the genetic map (Figs 6.6 A and B). However, as expected, the points in the genetic map clustered according to the Cys/PoLV grouping (Fig 6.6 C).

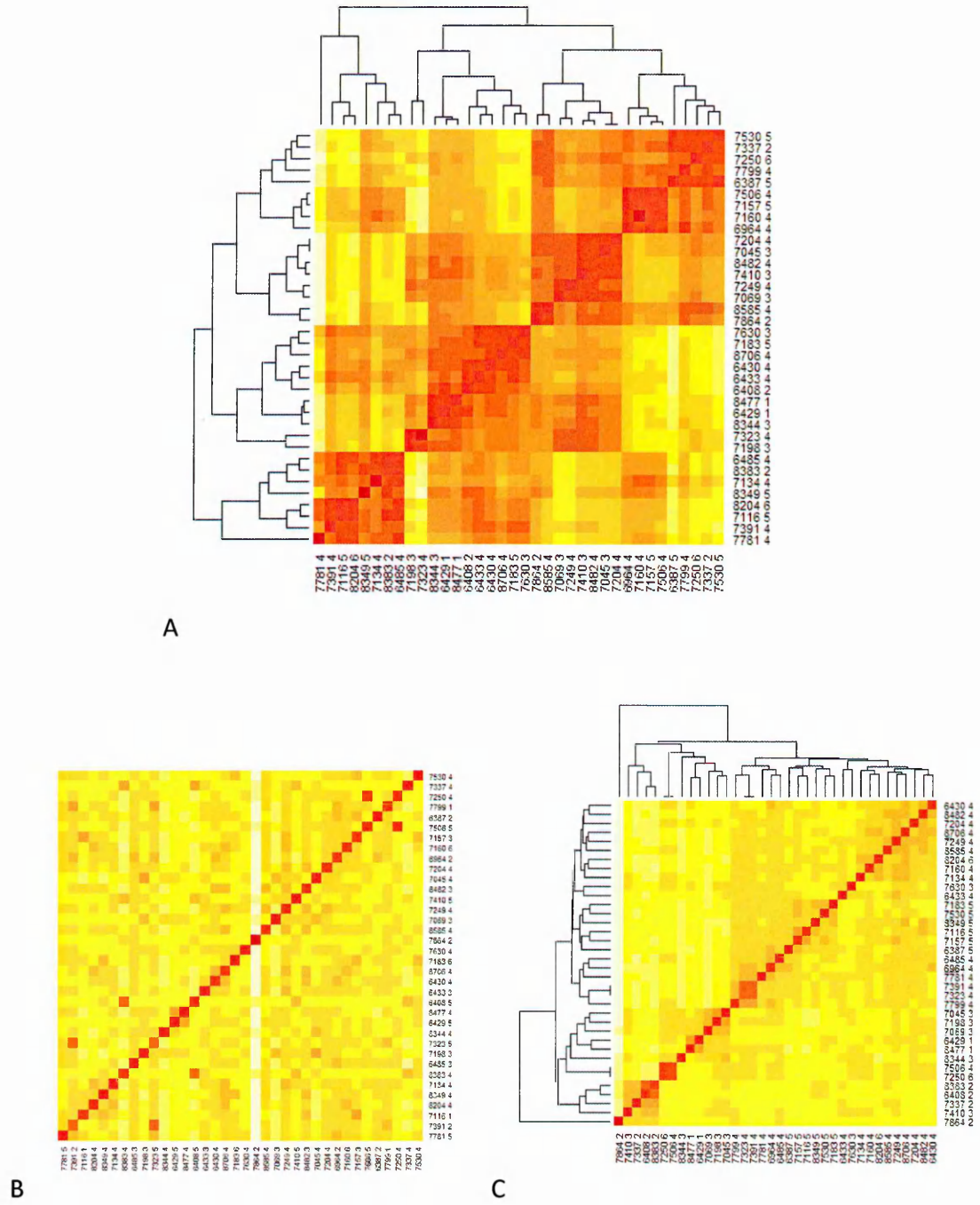

Fig 6.6 Heatmap of the matrix of the distances obtained from the antigenic map (A, same as Fig 6.3) and genetic maps (B and C). The Heatmap in (B) was arranged to have the same order of antigens as those in heatmap A, and for comparison, unsupervised ordering of antigens is shown in heatmap C.

To further compare the genetic map and antigenic maps, the pair-wise antigenic distances were obtained from the antigenic map (Fig 6.1) and regressed against the corresponding pair-wise genetic distances from (Fig 6.4). No overall relationship between the antigenic distance and the genetic distance was observed when analysed across all antigen and genetic groups

(Fig 6.7).

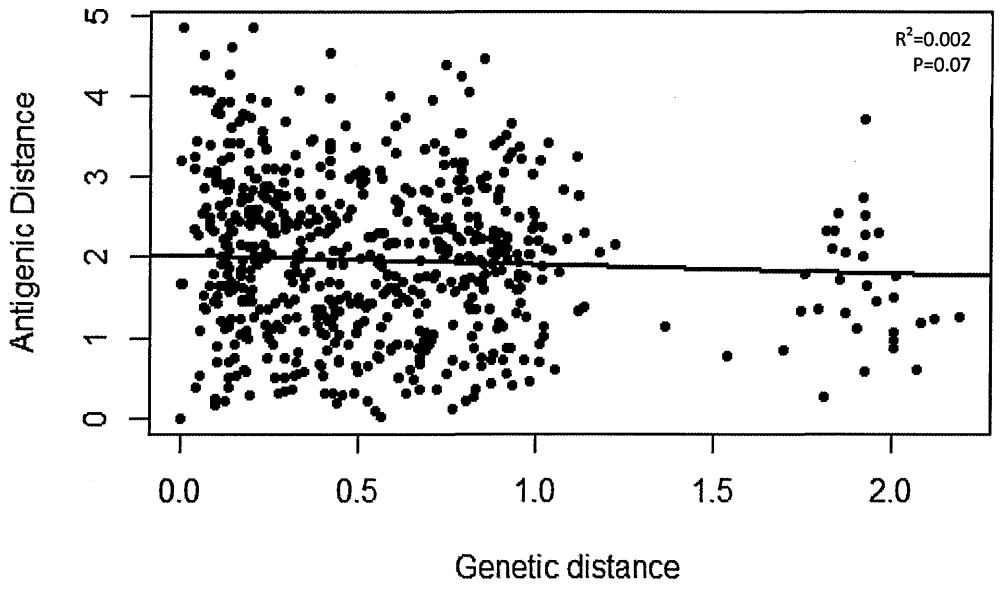

Fig. 6.7 Correlation between the antigenic and genetic distances between DBL-α tags obtained from the antigenic and genetic maps respectively. The line is the linear regression line for all pair-wise antigenic distances and genetic distances excluding homologous pairs.

Overall, the genetic clusters formed were different from the ones formed by the overall antigenic map and this was reflected in a poor correlation between distances on the overall genetic map and those on the antigenic map (Fig 6.7). This is not surprising because the pair-wise genetic distance between sequences used in this comparison contained both epitope and non-epitope regions. The inclusion of non-epitope regions in the analysis could dilute any potential correlation between genetic distance and antigenic similarity for a linear epitope for the antigenic clusters. In other words, that antigenic distance may be defined by just a small immunogenic region of the tag.

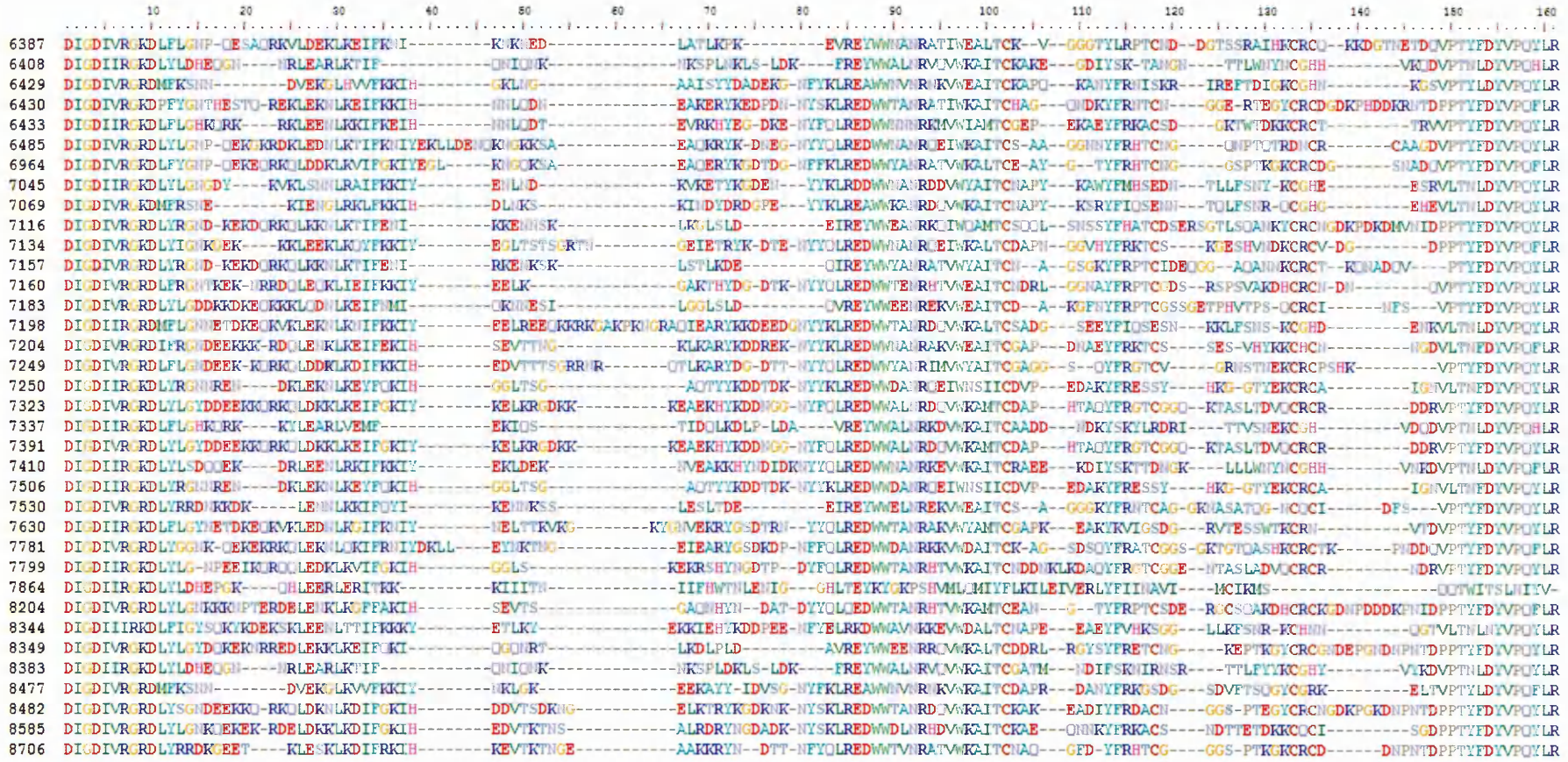

Fig. 6.8 Sequence alignment of the expressed 36 DBL-α tag antigens. The sequences were aligned by clustal in Bioedit using the default settings.

To determine whether there is a correlation between antigenic and genetic pair-wise distances driven by sub-regions of the DBL-α tag, a series of genetic maps based on small regions of the DBL-α tag were generated and compared to the antigenic map. Genetic maps were obtained from the alignment using a sliding window approach with a window length of 14 amino acids and an offset of 1 amino acid between each window. For each window, the distances from the genetic map were compared to those from the antigenic map and their correlation coefficient was plotted against the window location (Fig 6.9). It was found that there were correlation peaks adjacent to PoLV1 and between PoLV2 and PoLV3. This potentially identifies epitope regions.

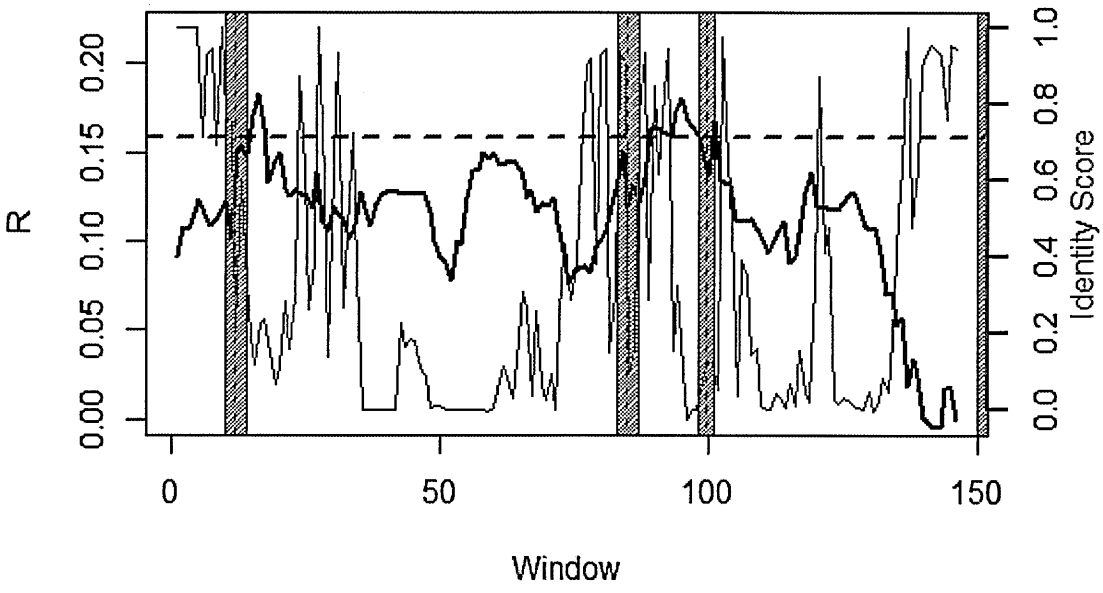

Fig. 6.9. Correlation between genetic distance and antigenic distances (black line, left y-axis) across the entire DBLα-tag region by sliding window analysis. The correlation based on the entire tag region is shown by the blue dotted line. The red plot indicates the amino acid identity score at each point (right, y-axis). The location of Positions of Limited Variability (PolVs) are in the alignment are indicated by the shaded blue bars.

The analysis showed that the regions with the highest correlations were located in protein regions with greater sequence variability (troughs in red line, Fig 6.9). This may indicate that such regions are undergoing diversifying immune selection. However, the sliding window analysis yielded little or no improvement on the correlation between genetic and antigenic distance using genetic windows compared with genetic distances based on the whole length of the DBLα-tag. By contrast, peaks with high correlation values could potentially identify epitope regions specific to each antigenic cluster. To determine this, the sliding window analysis was repeated on sub-groups of sequences falling within the antigenic clusters defined in Fig 6.4. This allowed for further refinement of potential regions within the sequences. For all the antigenic clusters, there was greater correlation between the genetic and antigenic distances at each window tested. As before, the regions with the highest correlation occurred within regions with high sequence variability. The high correlation observed at these regions signifies congruence between the relative positions of points of the antigens in the antigenic and genetic maps. That these regions show polymorphisms indicates that the relationships between the antigens are maintained in part by structural features that are similar within an antigenic cluster despite the considerable diversity at the sequence level. Such regions are likely to be components of conformational epitopes.

Smith and colleagues identified 10 hyper-variable blocks (I-X) of sequences that are interspersed between 10 homology blocks (A-J) among the DBL domains in PfEMP1 protein family (Smith et al. 2000). The DBL-α tag stretches from homology blocks D to H and

encompasses hyper-variable blocks V-VIII. In all the clusters, the regions with the highest peak in correlation were located towards the N terminal end of the DBL-α tag. For antigen clusters 2, 3, 4 and 6, this region occurred in homology block E (Fig 6.11. B, C, D, E) indicating that this region is potentially immunogenic across different clusters (Fig 6.10. B, C, D, E).

In the antigenic cluster 1 and 5 (Fig 6.10. A, F) the potential epitope region with the greatest correlation between the genetic and antigenic data occurs in homology block F (Fig 6.11 A, F). This region also exhibits high correlations in the antigenic clusters 2 and 6. This region is relatively conserved and contains two of the four conserved anchor points as well as PoLV2 that is used in the Cys/PoLV classification system (Bull et al. 2007). Due to relatively limited diversity in homology block F, the potential epitope regions identified from this region might be linear epitopes. Using synthetic peptides, Blomvqvist and colleagues have recently shown that this region of the DBL-α tag induces antibody responses that are cross-reactive and that recognize the surface of red blood cells infected with mature *P. falciparum* parasites (Blomqvist et al. 2013).

Cluster 5 exhibits high correlation coefficient across the entire region especially towards the N terminal end and is potentially immunogenic over larger areas than other clusters. In contrast, cluster 6 shows relatively lower correlation coefficients across the whole length and may be poorly immunogenic. This difference in the immunogenicity among variants of the surface antigens has been observed in field studies using whole parasites (Bull et al. 1999).

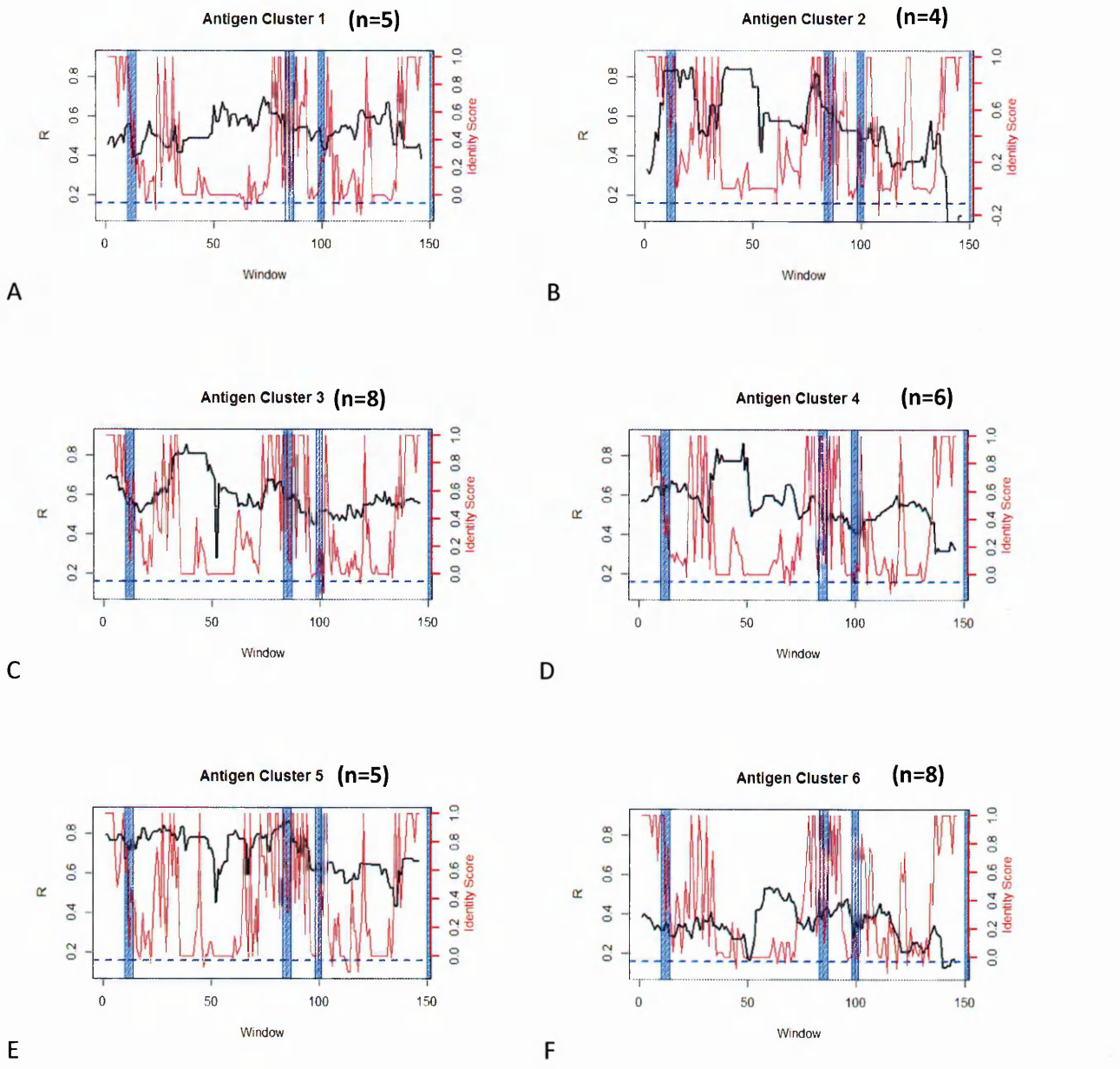

Fig 6.10 Correlation (y-axis) between genetic and the antigenic distances among an antigenic cluster (black line) by sliding window analysis for each antigenic cluster. Also shown is the correlation obtained between pair-wise distances between all the antigens and all the alignments of the complete DBLa tag sequence (blue plot). The red plot indicates the amino acid identity score at each point of the alignment. The location of Positions of Limited Variability (PolVs) are in the alignment are indicated by the shaded blue bars.

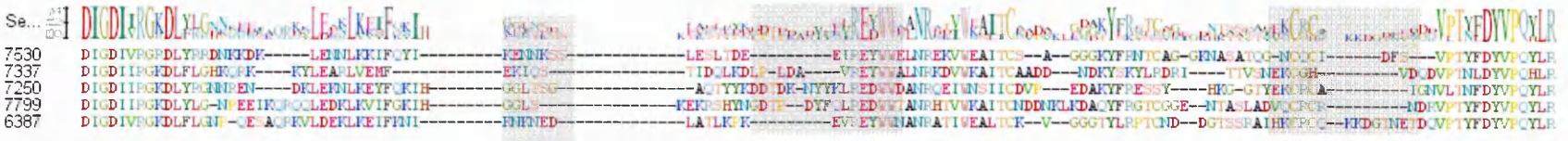

A. Cluster 1

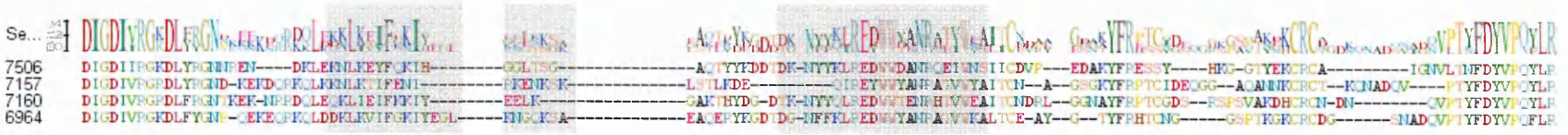

B. Cluster 2

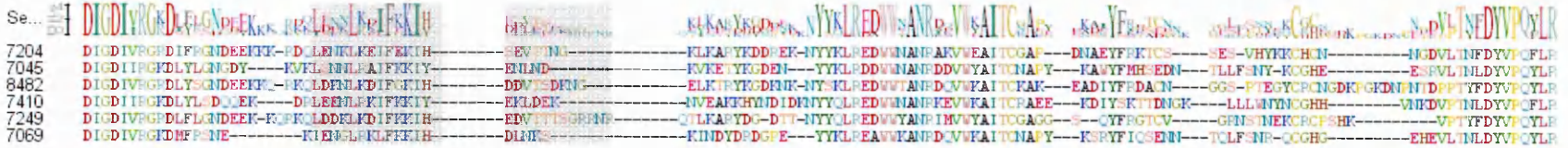

C. Cluster 3

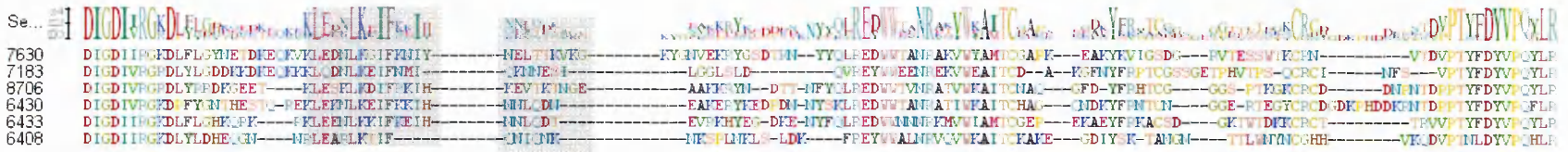

D. Cluster 4

E. Cluster 5

F. Cluster 6

Fig 6.11 Predicted epitope regions in clusters identified from the antigenic map. Multiple alignment of sequences from each antigen cluster showing regions with the highest correlation between the antigenic and genetic sequence (highlighted by the grey boxes).

6.4 Loss/gain in response versus antigenic/genetic differences

In order to determine whether the boost/loss in response was related to either the antigenic or genetic distances obtained from Fig 6.1 and Fig 6.4, a linear regression model was used. The boost in responses was defined as an increase in response between the acute time point and the 4 week convalescent time point. Individuals with high responses at both these time points may have little or no boosting which may be misinterpreted as a poor or no response. Therefore, the regression was done separately for individuals with high responses at the acute time point. The high responders were defined as those with responses above the median at the acute time point. There was a negative and significant relationship between boost in heterologous antibody response 4 weeks after infection and the antigenic distance between variants for both the high and low responders (Fig 6.12 A and B). This suggests that more closely related variants generate more cross-reactive responses. I observed no significant relationship between loss in response and antigenic distance (Fig 6.12 C and D). There was also no relationship observed between genetic distance and the boost (Fig. 6.13 A and B) for both the high and low responders respectively. However, there was a significant relationship between loss in response (Fig 6. 13 C and D) and the genetic distance for both the high and low responders. The highest loss in heterologous responses was observed in individuals infected by genetically distant variants. However, for both the genetic and antigenic distances, the R values describing their relationship with the changes in response after 4 weeks were low. This indicates that the changes in response after infection are largely explained by other factors.

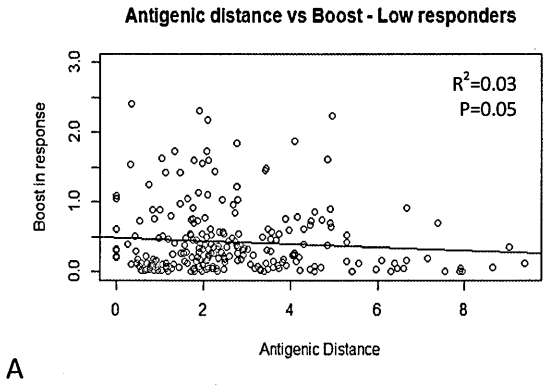

A

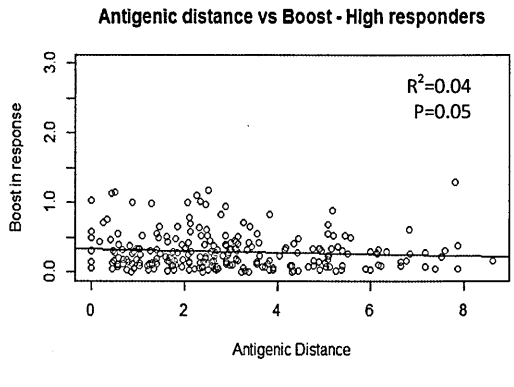

B

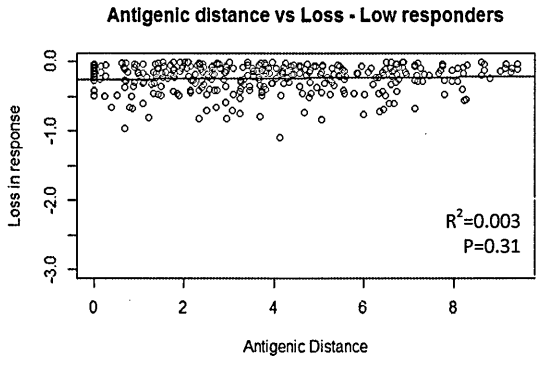

C.

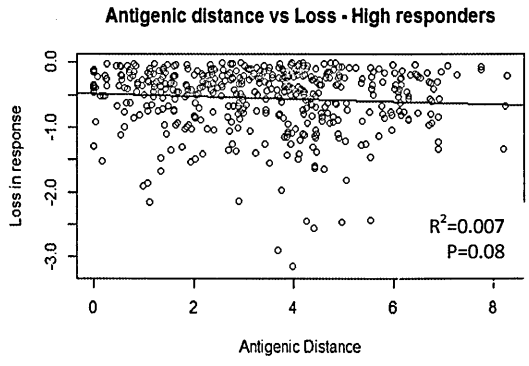

D

6.12 Boost/loss in IgG responses to other circulating variants of DBLα-tag the children had not been exposed to was measured 4 weeks after infection and regressed against the antigenic distance between the DBLα-tags as determined from antigenic cartography. The linear regression line was obtained for pair-wise antigenic distances excluding homologous data (black points). The red points on the graphs represent the heterologous data.

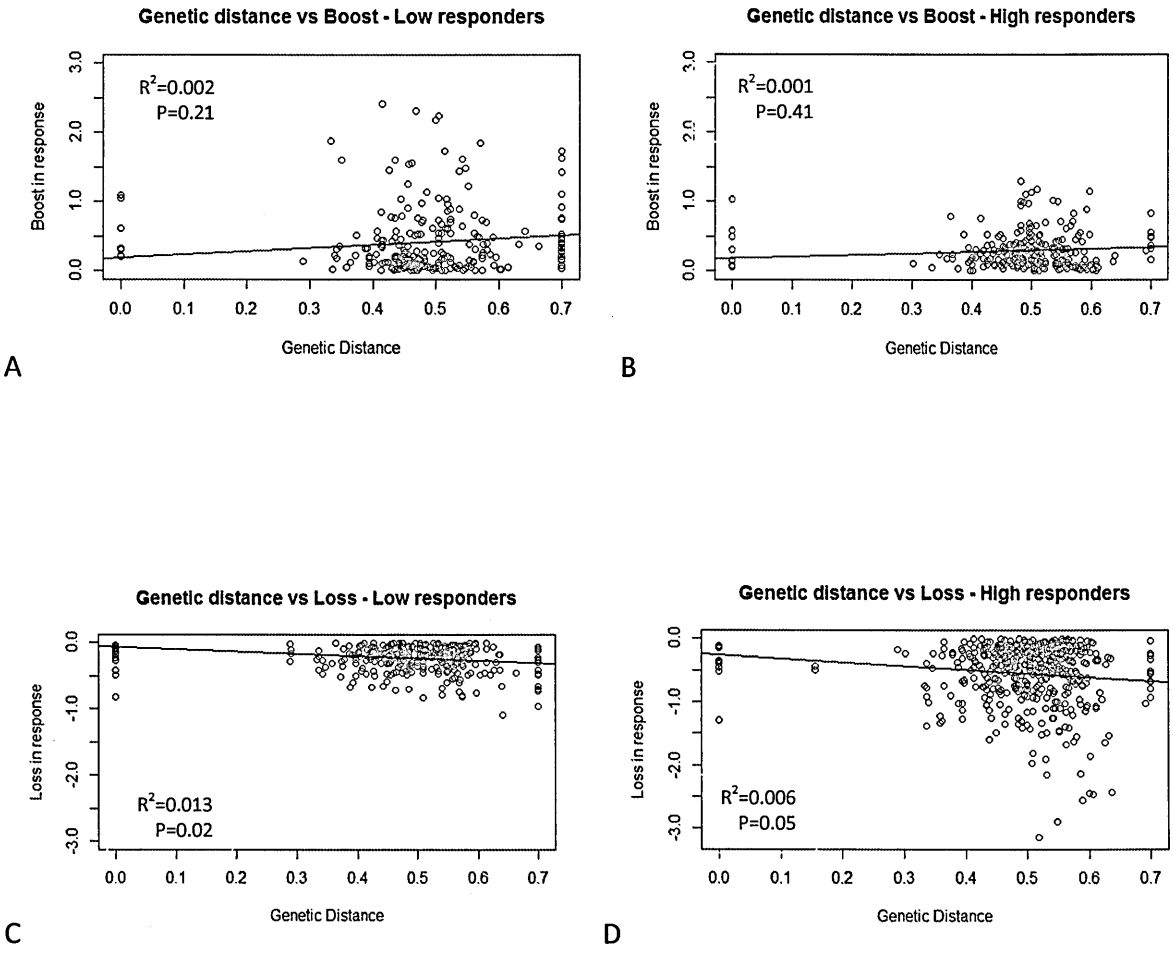

Fig 6.13 Boost/loss in IgG responses to other circulating variants of DBLα-tag the children had not been exposed to was measured 4 weeks after infection and regressed against the antigenic distance between the DBLα-tags as determined from antigenic cartography. The linear regression line was obtained for pair-wise genetic distances excluding homologous data (black points). The red points on the graphs represent the heterologous data.

6.4 Discussion

The adaptive arm of the immune system has, in theory, the capacity to recognize and mount a specific response to every antigen it encounters. B lymphocytes in particular, bind to their cognate antigen and undergo several rounds of somatic hyper-mutations at the antigen binding site of their receptor to create diverse receptors with different binding affinity to the antigen in the initial phase of an antibody response. These receptors are then selected for their ability to strongly bind the antigen resulting in highly specific receptors and thus secreted antibodies. This theoretical specificity is not always realized as antibodies that bind more than one antigen occur in nature. Using antigenic cartography, it was possible to quantitatively measure the antigenic distance between DBL-α tag variants to identify antigens that would cross-react with each other.

To gain perspective of how PfEMP1 proteins are organised in immunological space, I exploited antigenic cartography using recombinant DBL-α tag as a model antigen. It was possible to quantitatively measure the antigenic distance between DBL-α tag variants to identify antigens that would cross-react with each other. Immunity to PfEMP1 is thought to be largely variant specific. Based on this, it is expected that the immunological space describing PfEMP1 variants to be large and in which points are scattered and distant from each other. However, I observed both antigenically distinct and similar variants. The choice of variants could partly explain the different results obtained in earlier studies on agglutination that showed either a variant specific accumulation of antibodies or a strain-transcending pattern. It is conceivable that the global immunological PfEMP1 shape space is organised into distinct serological clusters that

show little or no cross reactivity between clusters. The members within specific clusters could be constrained by a common functional role e.g. binding to a particular receptor. The need to maintain functional/structural properties on one hand and the need to be polymorphic to evade humoral responses on the other could result in a balance where there are functional clusters that are immunologically distinct. Acquisition of effective cluster specific rather than variant specific responses would explain the rapid acquisition immune responses to PfEMP1. Such antigenic clusters are evident in other antigenically variable pathogens like Influenza, where viruses are organised into antigenic clusters in immunological space and vaccines are developed from a single strain that generates responses that protect people in a cluster specific rather than variant specific way (Smith et al. 2004; Smith 2003; Fouchier & Smith 2010).

To study this effectively in malaria, there is need for a more extensive study that will map out the global PfEMP1 immunological antigenic space and establish the number of clusters within it. More importantly, it is imperative to establish whether a cross-reactive response that is effective across a particular cluster can be identified. Using a prospective longitudinal study, it could be demonstrated whether there is decreased probability of infection with parasites expressing antigens mapping to areas covered by pre-existing antibodies in the immunological shape space. The circle of reactivity of such responses compared to the size and number of antigenic clusters can then be used to inform vaccine development. Wider circles of reactivity increase the antibody repertoire with fewer infections. I anticipate that the circle of reactivity of parasites that cause non-celebral severe malaria and placental malaria to be wide whereas

the corresponding parasites will form tight antigenic clusters in immunological shape space. This is because immunity to these syndromes is acquired rapidly after relatively few infections.

The boost in heterologous responses after infection was greatest among the antigenic similar variants indicating that the radius of effectiveness of this immunity is restricted to a certain area within immunological shape space. This makes biological sense because a wider circle of effectiveness would render the PfEMP1 repertoire immunologically redundant and the parasite would have no benefit in having multiple copies of this gene within its genome and at the population level. Joergensen and colleagues pointed this out in their work where they observed limited cross reactivity within members in a single genome (Joergensen et al. 2006).

Due to the transient nature of the cross reactive responses observed and their limited radius of recognition, it is plausible to argue that for them to effectively provide protection individuals must be infected by multiple parasites expressing different variants that elicit responses that completely cover the immunological space such that no new infections can be established. This is supported by epidemiological studies that show an increase in multiplicity of infection increases with age in areas with high exposure and this is associated with protection from disease (Beck et al., 1997; Färnert, Rooth, Svensson, Snounou, & Björkman, 1999; Henning et al., 2004; Smith, Felger, Tanner, & Beck, 1999; al-Yaman et al.). The product of multiplicity of infection and the antigenic diversity of the parasites allows older children and adults resident in endemic area to cover large areas of the immunological space while the chronic nature of this infection prolongs the transient nature of this protection. The inability of young children to maintain chronic asymptomatic parasitemia combined with the low levels of multiplicity in

infection could explain the susceptibility of children to malaria. Asymptomatic adults and older children in endemic areas may be protected partly by repeated exposure to low levels of a wide range of different *P. falciparum* strains.

Antigens are perceived by the immune system as similar possibly from sharing common epitopes or similar structural features. Regions within the DBL-α tags that best explain orientation of the antigens in the antigenic map were identified by comparing the genetic data to the antigenic map. Such regions form potential targets of antibody responses and, once verified by wet lab experiments, would be potential components of a multi epitope vaccine that would mimic naturally acquired immunity to malaria. The potential epitope regions identified were varied between antigen clusters and as pointed out earlier, more extensive work is required to define the number of such antigen clusters. The amino acid polymorphism identified at these potential antigenic sites suggests these polymorphisms are driven by immune selection pressures and could be part of conformational epitopes that are structurally similar within each antigen cluster. The antigenic sites identified in this study were located in regions that were different from those that define the Cys/PoLV grouping. This explains why there was little correspondence between the Cys/PoLV grouping and the antigenic clustering. Extending this analysis to other regions of the *Pf*EMP1 molecule will identify other antigenic regions.

The three-dimensional structures of DBL domains from the EBA-175 antigen from *P. falciparum* and the DBP in *P. Knowlesi* have been solved (Tolia et al. 2005; Singh et al. 2006). Despite limited sequence similarity, the two domains retain a remarkable similarity in their structure.

Using the solved EBA-175 as a template, Howell and colleagues exploited semi-conserved blocks defined by multiple alignments to develop a three-dimensional structure for the DBL-α domain from PfEMP1 (Howell et al. 2006). They observed that the DBL-α tag falls within the minimal region required for receptor binding for the DBL domain family (Ranjan & Chitnis 1999; Mayor et al. 2005). In a recent study, Juillerat and colleagues solved the crystal structure of the NTS-DBLα domain cassette from VarO, a rosette forming PfEMP1 isoform, and report that the secondary structure of the DBLa domain is similar to other known DBL structures (Juillerat et al. 2011). The region with the strongest affinity to the cognate ligand was traced by mutagenesis to two segments within the NTS region and a third region within the DBLα domain region. This third region occurred within the DBL-α tag region between PoLV1 and PoLV2. Lysine residues within the NTS-DBLα domain cassette have been shown to be important for the interaction between VarO and its ligand. It was interesting to note that, for antigen clusters 2, 3, 4 and 6, the potential epitope regions identified occurred between PolV1 and PoLV2 and that for clusters 2, 3, and 4 specifically, the predicted epitope region had a conspicuous Lysine residue. Taken together, this implies that epitopes identified within this region, whether linear or conformational, may be important for function. The use of antigenic cartography is not limited to antigen-antibody binding interactions but can be used to study any receptor-ligand binding interactions (Lapedes & Farber 2001). When applied to receptor-ligand binding interactions between *Pf*EMP1 and host receptor molecules, it may be possible to easily profile variants associated with binding to certain receptors. This, if combined with antigenic and genetic data

will allow us to identify potential immunogenic and functional regions within the proteins and determine whether these regions overlap.

In summary, the data presented here suggests that the immunity to malaria is made up of long-lasting, variant specific responses and short lived cross reactive responses generated against multiple parasites that share similar coordinates within immunological space. The effectiveness of such responses and their focus of reactivity remain to be determined. Such data will be instrumental in the selection of components to be included in a multi-component vaccine. In addition; it will assist in the temporal and spatial surveillance of the PfEMP1 repertoire at the population level for changes that move the parasites to unoccupied areas of the immunological space in a post vaccination era. If effective, there will be need to developed strategies of extending the half life of such responses before they can be considered for vaccine development.

Chapter 7

Summary of main points

Introduction

The immune system is tasked with defending the host from foreign agents that include infections. It must distinguish self molecules from non-self as well as one parasite from the next. This presents tremendous challenge when you take into account the immense diversity of pathogens to which the immune system could be exposed. Failure of the immune system to recognize pathogens usually results in infection and which may lead to disease. The underlying motivation for this thesis was to understand how the human host develops antibody responses against the variant antigen *Pf*EMP1 expresses by *P. falciparum*. As discussed in chapter 1, opinion is divided as to whether antibody responses to these antigens are acquired in a variant specific manner or whether the strain specific response is accompanied by variant specific responses. To explore this, I expressed the DBLα-tag region of *Pf*EMP1 from parasite isolated from children and used this region as a model antigen to study how the children developed antibody responses to their infecting parasite and to other parasites circulating in the community after the infection.

7.1 Main findings

1. The DBL-α tag region forms part of the epitopes targeted by the protective antibodies or has epitopes associated with the protective sites within the *Pf*EMP1 molecules. Children were infected by parasites that correspond to gaps in their antibody repertoire and this gap was sealed after recovery (Chapter 4). In a recent publication, Ravira-Vallbona and

colleagues found a negative association between IgG responses to the DBLα domain and parasite densities. In their work, they also report that severe malaria is associated with low IgG responses to DBLα (Rovira-Vallbona et al. 2012). Of practical importance is the work done in animal models indicating that immunization with DBLα constructs elicits humoral responses that protect from *P. falciparum* infection (Moll et al. 2007; Ahuja et al. 2006; Chen et al. 2004). Taken together, these data show that the DBL*α* is potentially an important target of natural immunity and should be given consideration for possible inclusion in a multi-component or multi-stage antigen sub-unit vaccine.

2. Children develop both variant and cross-reactive antibody responses to the DBL-α tag region of *Pf*EMP1 after infection. The influence of such cross reactive responses on the subsequent risk of infection, parasite density and clinical outcome remains unresolved. I postulate that this would be dependent of the antigenic relatedness between variants. Parasites bearing similar antigenicity to those present in a host's antibody repertoire would be excluded or controlled to a degree corresponding their antigenic relatedness. If cross-reactive responses play a dominant role then this might pave the way for vaccine development. This has been well studied for Influenza. The generation of cross reactive responses that recognize influenza variants is key to the success of influenza vaccination. By generating cross-reactive responses, a host is able to cover large antigenic space with relatively few exposures. Whether this is a deliberate strategy of the host to variant pathogens or an early phase transient state in the path to the

generation of antigen specific responses after affinity maturation remains to be determined.

3. The potential epitope regions identified from the DBL-α tag peptides are not conserved and are likely to be part of conformational epitopes that fold to form similar secondary structures between variants in an antigenic cluster. The conserved secondary structure could be due to functional constraints imposed of the *Pf*EMP1 molecule. Support for such a theory comes from recent work that traces the functional regions to the predicted potential epitope regions identified in this thesis (Juillerat et al. 2011). The polymorphisms observed at these sites could be due to a need to evade immune responses.

7.2 General Discussion

The description of the antigenic structure of variant antigens will be key deciding which variants to consider when designing vaccines that target polymorphic proteins such as *Pf*EMP1. From this work, I hypothesize that the *Pf*EMP1 antigenic repertoire is organized into discrete clusters that are serologically distinct. The acquisition of cluster-specific rather than variant-specific responses may present a plausible explanation to the relatively rapid acquisition of clinical immunity to malaria by adults and in children after a limited number of infection compared to the vast number of PfEMP1 variants in circulation in a given parasite population. Exploitation and manipulation of the cluster-specific properties of *Pf*EMP1 has the potential to assist in the development of an effective vaccine. The potential for such an approach may be particularly viable for parasites causing severe disease as such parasites appear to present and antigenically

distinct and limited number of variant surface antigens (Bull et al. 1999; Nielsen et al. 2002). Methods that quantitatively analyze antigenic variation therefore become important.

I used antigenic cartography to construct metric space in which the DBL-α tags are organized into serological clusters that elicit potentially cross-reactive responses within a cluster. A critical question that remains unanswered however is what role the cross-reactive responses play in protecting an individual from future infections from parasites expressing antigens within the same or different cluster. The answer to this question will require a longitudinal prospective study in which children presenting to hospital or in the community with disease, will be actively followed up and the subsequent antigens or parasites mapped onto the antigenic space. I hypothesize that antigens/parasites from secondary infections will map to new regions within the antigenic map. The distance between the antigens/parasites in the primary and secondary infections in the map will partly be determined by the time since infection because the heterologous response in this study declined over time. Therefore, the ability to maintain chronic parasitemia will be key in maintaining the heterologous responses which is consistent with increased antibody responses to a variety of malarial antigens in parasite-positive children (al-Yaman et al. 1995; Bull et al. 2002; Kinyanjui et al. 2004; Kinyanjui et al. 2009). In order to maintain antibody levels across the multiple serological cluster and hence broad protection, the host will have to asymptomatically maintain multiple parasite genotypes circulating in the bloodstream at any given point. The ability to maintain both chronic and multi-clonal infection will be key to reducing the risk of disease in this model.

In this work, I describe predicted epitope region within the DBL-α tags that exhibit considerable polymorphism within a defined serological cluster. Similar findings were observed in a study carried out by Gamain and colleagues (Gamain et al. 2001). In this study, the authors developed cross-reactive monoclonal antibodies against the CIDR region of *Pf*EMP1 in mice and used these to screen for epitopes within this region. The authors hypothesised that the cross-reactive monoclonal antibodies would be directed to the conserved regions within the CIDR domain. Contrary to their expectations, the monoclonal antibodies identified a genetically diverse region of CIDR as the epitopic region. In addition, the monoclonal antibodies identified in this study showed minimal reactivity to the conserved region. My favored interpretation of these observations and those presented in this study is that the parasite, under natural settings, diverts cross-reactive responses away from conserved regions in order not to make the antigenic repertoire redundant. As such immunogenic regions of PfEMP1 would mostly observed in polymorphic regions. However, some of these regions even though polymorphic, occur in functional areas and form tertiary structures that may be similar in structure and hence have comparable ligand-receptor interactions. It is conceivable that immune responses to such regions would be cross-reactive but limited within PfEMP1 proteins mediating a particular function. In this way, the parasite attains a balance in which the entire PfEMP1 repertoire is not exhausted.

Importantly, this also cautions against drawing conclusions about the serological diversity of antigens from *in silico* predictions of genetic data. The sequence diversity in this case appears to be exaggerating the serological diversity. A similar case has been observed for influenza

viruses (Smith et al. 2004). These viruses accumulate several silent mutations that do not change the serological properties of important immune targets. When projected in antigenic space, the authors observed viruses that had polymorphisms at the genotypic level falling within a single cluster. However, after accumulation of several mutations, the viruses are moved to a new antigenic space by one final mutation. It is therefore conceivable to have parasites with a diverse genotype but a relatively conserved phenotype. The conserved phenotype could be driven by the need to maintain a common function. The analysis of serological data together with functional binding data using multi-dimensional scaling techniques described here has the potential to elucidate serological clusters that are driven by common functional roles. A similar approach can be applied for the analysis of binding data to identify functional clusters.

7.3 Limitations of the study

Use of broad spectrum antibody serum

Antigenic cartography assumes that each antibody represents a single binding affinity to an antigen. In previous studies, serum raised in an appropriate animal model against one strain was used to measure antigen-antibody distances against other strains. Such sera will typically contain a mixed population of antibodies binding to different antigenic determinants of the strain with varying affinities. Despite this, the use of polyclonal sera against one variant has allowed for the construction high resolution maps with accurate antigenic relationships. The multiple antibody affinities are represented as a single point of action. However, this fails when

the sera contains antibodies against more than one variant. Representing several sera with binding affinities to multiple antigens as a single point will inaccurately project the relationships between antigens. The sera used in this study were obtained from children who may have been exposed to other variants of *Pf*EMP1 prior to the current infection. I tried to correct for this by excluding responses recorded by ELISA to previous infections. I however acknowledge the possibility that even within the period of a single infection, the parasite may have expressed more than one variant. This is compounded by a recent report showing the surface co-expression of two different *Pf*EMP1 antigens on a single plasmodium falciparum-infected red blood cell (Joergensen et al. 2010). The precision of the antigenic relationships between PfEMP1 antigens will be greatly improved using variant specific sera obtained from naive animals or first infection on individuals infected with parasites that have only expressed a single *Pf*EMP1 isogenic variant.

The surface of a red cell infected with mature stages of *P. falciparum* has PfEMP1 as one of several variant antigen families. In order to study specific immune responses to PfEMP1 it will be necessary to either express the antigens as recombinant antigens or carry out agglutination assays using variant specific sera raised in animals. Previous agglutination studies have measured an aggregate response to all the antigens families on the red blood cell.

Small antigenic region

The choice of the DBL-α tag as the region to study in this thesis was primarily driven by the previous observation that it is the only region of the *Pf*EMP1 ectodomain that is accessible to amplification by PCR in most parasites isolated from sick children. While the tag region is an

important target for the acquisition of both natural and vaccine-induced protection as out lined in section 4.1, it only represents a small region of the entire *Pf*EMP1 molecule. The *Pf*EMP1 molecules are large multi domain molecules with molecular weights of 200-300KDa. This is large compared to the DBL-α tag region which has molecular weights approximately ranging from 10-20KDa. In addition, several studies have demonstrated important functional and immunological properties of other non-DBLα domain regions of *Pf*EMP1. The functional and immunological findings described for the DBL-α tag region or domain can only form part of and cannot be taken to be representative of the whole PfEMP1 molecule. A comprehensive description of immune responses to *Pf*EMP1 molecules will require the ability to easily clone all domains of a given *Pf*EMP1 molecule and express them as recombinant antigens. The recent development of cloning vectors that allow for the rapid and efficient selection whole *var* genes repertoires from different *P. falciparum* strains (Louis et al. 2011) and the ability to recombinantly express full length *Pf*EMP1 molecules (Srivastava et al. 2013; Srivastava et al. 2010; Khunrae et al. 2010; Kraemer et al. 2003) make this possibility in the near future.

Sample size for cluster analysis

The work presented in this thesis describes an initial attempt at describing antigenic relationships in a small important region of the variant Plasmodium falciparum antigen *Pf*EMP1. I describe 6 serological clusters obtained by hierarchical cluster analysis analysis of the distances between 36 DBL-α tag antigens. This represents a small number. The repertoire of PfEMP1 variants in the population is much broader and there are potentially more serological clusters. There are no rules-of-thumb about the sample size necessary for cluster analysis. It is

anticipated however that the sample size required will be a factor of the extent of variability within the dataset. Variables with extensive variation are likely to form more clusters as compared to variables with limited variation and as a result, more data points may be required in order to adequately capture the number of clusters inherent in a variable with extensive variation. This makes the determination of sample size *a priori* difficult. This, however, can be inferred at the point where adding new data points to a variable do not yield new clusters. For PfEMP1 to be considered a viable vaccine candidate, extensive work should be carried out in order to include more variants in order to have a global understanding of the complex antigenic relationships of *Pf*EMP1 antigen family at the DBL-α tag region and other domains. If the antigenic space is finite, a point of saturation in the antigenic space will be attained beyond which addition of more samples will not yield new antigenic cluster. This will enable scientist to determine whether there are associations between particular clusters with certain clinical or phenotypic parasite features. In addition, there is a higher likelihood of forming random clusters with smaller sample sizes as compared to larger ones.

7.4 Concluding remarks

The methods described in this thesis, provide a powerful tool that can be used to inform whether vaccine development to variant surface antigens is a viable option. For this to occur, there is need to develop standardized methods and appropriate reference sera as discussed in section 7.2.1. The description of the antigenic clusters at the population level and comparisons of overlap between populations will be a key criterion in deciding whether a *Pf*EMP1 based vaccine is viable. In addition, antigenic cartography provides a powerful tool with which to

monitor the serological evolution of antigenically dynamic *Pf*EMP1 family of antigens for vaccine escape in a post-vaccine era.

References

Abdel-Latif, M.S. et al., 2002. Recognition of variant Rifin antigens by human antibodies induced during natural Plasmodium falciparum infections. *Infection and immunity*, 70(12), pp.7013–21.

Agarwal, A. et al., 2000. Hemoglobin C associated with protection from severe malaria in the Dogon of Mali, a West African population with a low prevalence of hemoglobin S. *Blood*, 96(7), pp.2358–63.

Aguiar, J.C. et al., 1992. Agglutination of Plasmodium falciparum-infected erythrocytes from east and west African isolates by human sera from distant geographic regions. *The American journal of tropical medicine and hygiene*, 47(5), pp.621–32.

Aguiar, J.C. et al., 2004. High-throughput generation of P. falciparum functional molecules by recombinational cloning. *Genome research*, 14(10B), pp.2076–82.

Ahuja, S. et al., 2006. Induction of cross-reactive immune responses to NTS-DBL-1alpha/x of PfEMP1 and in vivo protection on challenge with Plasmodium falciparum. *Vaccine*, 24(35-36), pp.6140–54.

ALLISON, A.C., 1954. Protection afforded by sickle-cell trait against subtertian malareal infection. *British medical journal*, 1(4857), pp.290–4.

ALLISON, A.C. & CLYDE, D.F., 1961. Malaria in African children with deficient erythrocyte glucose-6-phosphate dehydrogenase. *British medical journal*, 1(5236), pp.1346–9.

al-Yaman, F. et al., 1995. Humoral response to Plasmodium falciparum ring-infected erythrocyte surface antigen in a highly endemic area of Papua New Guinea. *The American journal of tropical medicine and hygiene*, 52(1), pp.66–71.

al-Yaman, F. et al., Reduced risk of clinical malaria in children infected with multiple clones of Plasmodium falciparum in a highly endemic area: a prospective community study. *Transactions of the Royal Society of Tropical Medicine and Hygiene*, 91(5), pp.602–5.

Ampofo, W.K. et al., 2012. Improving influenza vaccine virus selection: report of a WHO informal consultation held at WHO headquarters, Geneva, Switzerland, 14-16 June 2010. *Influenza and other respiratory viruses*, 6(2), pp.142–52, e1–5.

Angov, E. et al., 2008. Heterologous protein expression is enhanced by harmonizing the codon usage frequencies of the target gene with those of the expression host. *PloS one*, 3(5), p.e2189.

Baca, A.M. & Hol, W.G., 2000. Overcoming codon bias: a method for high-level overexpression of Plasmodium and other AT-rich parasite genes in Escherichia coli. *International journal for parasitology*, 30(2), pp.113–8.

Bach, O. et al., 2005. Falciparum malaria after splenectomy: a prospective controlled study of 33 previously splenectomized Malawian adults. *Transactions of the Royal Society of Tropical Medicine and Hygiene*, 99(11), pp.861–7.

Bachmann, A. et al., 2009. Absence of erythrocyte sequestration and lack of multicopy gene family expression in Plasmodium falciparum from a splenectomized malaria patient. *PloS one*, 4(10), p.e7459.

Baird, J.K. et al., 1991. Age-dependent acquired protection against Plasmodium falciparum in people having two years exposure to hyperendemic malaria. *The American journal of tropical medicine and hygiene*, 45(1), pp.65–76.

Baird, J.K., 1998. Age-dependent characteristics of protection v. susceptibility to Plasmodium falciparum. *Annals of tropical medicine and parasitology*, 92(4), pp.367–90.

Baird, J.K. et al., 1993. Age-specific prevalence of Plasmodium falciparum among six populations with limited histories of exposure to endemic malaria. *The American journal of tropical medicine and hygiene*, 49(6), pp.707–19.

Baird, J.K. et al., 2003. Onset of clinical immunity to Plasmodium falciparum among Javanese migrants to Indonesian Papua. *Annals of tropical medicine and parasitology*, 97(6), pp.557–64.

Barnwell, J.W. et al., 1983. Splenic requirement for antigenic variation and expression of the variant antigen on the erythrocyte membrane in cloned Plasmodium knowlesi malaria. *Infection and immunity*, 40(3), pp.985–94.

Barnwell, J.W., Howard, R.J. & Miller, L.H., 1982. Altered expression of Plasmodium knowlesi variant antigen on the erythrocyte membrane in splenectomized rhesus monkeys. *Journal of immunology (Baltimore, Md. : 1950)*, 128(1), pp.224–6.

Barry, A.E. et al., 2007. Population Genomics of the Immune Evasion (var) Genes of Plasmodium falciparum. *PLoS Pathogens*, 3(3), pp.1–9.

Barry, A.E. et al., 2011. The stability and complexity of antibody responses to the major surface antigen of Plasmodium falciparum are associated with age in a malaria endemic area. *Molecular & cellular proteomics : MCP*, 10(11), p.M111.008326.

Baruch, D.I. et al., 1995. Cloning the P. falciparum gene encoding PfEMP1, a malarial variant antigen and adherence receptor on the surface of parasitized human erythrocytes. *Cell*, 82(1), pp.77–87.

Baruch, D.I. et al., 1997. Identification of a region of PfEMP1 that mediates adherence of Plasmodium falciparum infected erythrocytes to CD36: conserved function with variant sequence. *Blood*, 90(9), pp.3766–75.

Beck, H.P. et al., 1997. Analysis of multiple Plasmodium falciparum infections in Tanzanian children during the phase III trial of the malaria vaccine SPf66. *The Journal of infectious diseases*, 175(4), pp.921–6.

Beeson, J.G. et al., 2000. Adhesion of Plasmodium falciparum-infected erythrocytes to hyaluronic acid in placental malaria. *Nature medicine*, 6(1), pp.86–90.

Berendt, A.R. et al., 1989. Intercellular adhesion molecule-1 is an endothelial cell adhesion receptor for Plasmodium falciparum. *Nature*, 341(6237), pp.57–9.

Beyer, W.E. & Masurel, N., 1985. Antigenic heterogeneity among influenza A(H3N2) field isolates during an outbreak in 1982/83, estimated by methods of numerical taxonomy. *The Journal of hygiene*, 94(1), pp.97–109.

Blomqvist, K. et al., 2013. A Sequence in Subdomain 2 of DBL1α of Plasmodium falciparum Erythrocyte Membrane Protein 1 Induces Strain Transcending Antibodies. I. Blader, ed. *PloS one*, 8(1), p.e52679.

Blythe, J.E. et al., 2008. Plasmodium falciparum STEVOR proteins are highly expressed in patient isolates and located in the surface membranes of infected red blood cells and the apical tips of merozoites. *Infection and immunity*, 76(7), pp.3329–36.

Brown, G. et al., 1979. The distribution of HLA on human lymphoid, bone marrow and peripheral blood cells. *European journal of immunology*, 9(4), pp.272–5.

Brown, K.N. & Brown, I.N., 1965. Immunity to malaria: antigenic variation in chronic infections of Plasmodium knowlesi. *Nature*, 208(5017), pp.1286–8.

Buckee, C.O., Bull, P.C. & Gupta, S., 2009. Inferring malaria parasite population structure from serological networks. *Proceedings. Biological sciences / The Royal Society*, 276(1656), pp.477–85.

Bull, P.C. et al., 2007. An approach to classifying sequence tags sampled from Plasmodium falciparum var genes. *Molecular and biochemical parasitology*, 154(1), pp.98–102.

Bull, P.C. et al., 1999. Antibody recognition of Plasmodium falciparum erythrocyte surface antigens in Kenya: evidence for rare and prevalent variants. *Infection and immunity*, 67(2), pp.733–9.

Bull, P.C. et al., 1998. Parasite antigens on the infected red cell surface are targets for naturally acquired immunity to malaria. *Nature medicine*, 4(3), pp.358–60.

Bull, P.C. et al., 2002. Plasmodium falciparum infections are associated with agglutinating antibodies to parasite-infected erythrocyte surface antigens among healthy Kenyan children. *The Journal of infectious diseases*, 185(11), pp.1688–91.

Bull, P.C. et al., 2005. Plasmodium falciparum variant surface antigen expression patterns during malaria. *PLoS pathogens*, 1(3), p.e26.

Bull, P.C. et al., 2000. Plasmodium falciparum-infected erythrocytes: agglutination by diverse Kenyan plasma is associated with severe disease and young host age. *The Journal of infectious diseases*, 182(1), pp.252–9.

Cadigan, F.C. & Chaicumpa, V., 1969. Plasmodium falciparum in the white-handed gibbon: protection afforded by previous infection with homologous and heterologous strains obtained in Thailand. *Military medicine*, 134(10), pp.1135–9.

Cadigan, F.C., Ward, R.A. & Chaicumpa, V., 1969. Further studies on the biology of human malarial parasites in gibbons from Thailand. *Military medicine*, 134(10), pp.757–66.

Carcy, B. et al., 1994. A large multigene family expressed during the erythrocytic schizogony of Plasmodium falciparum. *Molecular and biochemical parasitology*, 68(2), pp.221–33.

Carlson, J. et al., 1990. Human cerebral malaria: association with erythrocyte rosetting and lack of anti-rosetting antibodies. *Lancet*, 336(8729), pp.1457–60.

Carrió, M.M. & Villaverde, A., 2002. Construction and deconstruction of bacterial inclusion bodies. *Journal of biotechnology*, 96(1), pp.3–12.

Carrió, M.M. & Villaverde, A., 2001. Protein aggregation as bacterial inclusion bodies is reversible. *FEBS letters*, 489(1), pp.29–33.

Castelino, D. et al., 1981. Ovalocytosis in Papua New Guinea -- dominantly inherited resistance to malaria. *The Southeast Asian journal of tropical medicine and public health*, 12(4), pp.549–55.

Cham, G.K.K. et al., 2010. Hierarchical, domain type-specific acquisition of antibodies to Plasmodium falciparum erythrocyte membrane protein 1 in Tanzanian children. *Infection and immunity*, 78(11), pp.4653–9.

Cham, G.K.K. et al., 2009. Sequential, ordered acquisition of antibodies to Plasmodium falciparum erythrocyte membrane protein 1 domains. *Journal of immunology (Baltimore, Md. : 1950)*, 183(5), pp.3356–63.

Chan, J.-A. et al., 2012. Targets of antibodies against Plasmodium falciparum-infected erythrocytes in malaria immunity. *The Journal of clinical investigation*, 122(9), pp.3227–38.

Chattopadhyay, R. et al., 2003. Plasmodium falciparum infection elicits both variant-specific and cross-reactive antibodies against variant surface antigens. *Infection and immunity*, 71(2), pp.597–604.

Chen, Q., Fernandez, V., et al., 1998. Developmental selection of var gene expression in Plasmodium falciparum. *Nature*, 394(6691), pp.392–5.

Chen, Q., Barragan, A., et al., 1998. Identification of Plasmodium falciparum erythrocyte membrane protein 1 (PfEMP1) as the rosetting ligand of the malaria parasite P. falciparum. *The Journal of experimental medicine*, 187(1), pp.15–23.

Chen, Q. et al., 2004. Immunization with PfEMP1-DBL1alpha generates antibodies that disrupt rosettes and protect against the sequestration of Plasmodium falciparum-infected erythrocytes. *Vaccine*, 22(21-22), pp.2701–12.

Chen, Q. et al., 2000. The semiconserved head structure of Plasmodium falciparum erythrocyte membrane protein 1 mediates binding to multiple independent host receptors. *The Journal of experimental medicine*, 192(1), pp.1–10.

Clark, I.A. et al., 1981. Possible importance of macrophage-derived mediators in acute malaria. *Infection and immunity*, 32(3), pp.1058–66.

Clark, I.A. et al., 1987. Possible roles of tumor necrosis factor in the pathology of malaria. *The American journal of pathology*, 129(1), pp.192–9.

CLARKE K. R., 1993. Non-parametric multivariate analyses of changes in community structure. , 18(1), pp.117–143.

Cohen, J. et al., 2010. From the circumsporozoite protein to the RTS, S/AS candidate vaccine. *Human vaccines*, 6(1), pp.90–6.

COHEN, S., McGREGOR, I.A. & CARRINGTON, S., 1961. Gamma-globulin and acquired immunity to human malaria. *Nature*, 192, pp.733–7.

Demar, M. et al., 2004. Plasmodium falciparum malaria in splenectomized patients: two case reports in French Guiana and a literature review. *The American journal of tropical medicine and hygiene*, 71(3), pp.290–3.

Dodoo, D. et al., 2001. Antibodies to variant antigens on the surfaces of infected erythrocytes are associated with protection from malaria in Ghanaian children. *Infection and immunity*, 69(6), pp.3713–8.

Dondorp, A.M. et al., 2009. Artemisinin resistance in Plasmodium falciparum malaria. *The New England journal of medicine*, 361(5), pp.455–67.

Doolan, D.L., Dobaño, C. & Baird, J.K., 2009. Acquired immunity to malaria. *Clinical microbiology reviews*, 22(1), pp.13–36, Table of Contents.

Ducatez, M.F. et al., 2011. Extent of antigenic cross-reactivity among highly pathogenic H5N1 influenza viruses. *Journal of clinical microbiology*, 49(10), pp.3531–6.

Dudman, W.F. & Belbin, L., 1988. Numerical Taxonomic Analysis of Some Strains of Rhizobium spp. That Uses a Qualitative Coding of Immunodiffusion Reactions. *Applied and environmental microbiology*, 54(7), pp.1825–30.

Duraisingh, M.T. et al., 2005. Heterochromatin silencing and locus repositioning linked to regulation of virulence genes in Plasmodium falciparum. *Cell*, 121(1), pp.13–24.

Durand, P.M. & Coetzer, T.L., 2008. Pyruvate kinase deficiency protects against malaria in humans. *Haematologica*, 93(6), pp.939–40.

Eaton, M.D., 1938. THE AGGLUTINATION OF PLASMODIUM KNOWLESI BY IMMUNE SERUM. *The Journal of experimental medicine*, 67(6), pp.857–70.

Edozien, J.C., Gilles, H.M. & Udeozo, I.O.K., 1962. ADULT AND CORD-BLOOD GAMMA-GLOBULIN AND IMMUNITY TO MALARIA IN NIGERIANS. *The Lancet*, 280(7263), pp.951–955.

Elliott, S.R. et al., 2007. Antibody recognition of heterologous variant surface antigens after a single Plasmodium falciparum infection in previously naive adults. *The American journal of tropical medicine and hygiene*, 76(5), pp.860–4.

Färnert, A. et al., 1999. Complexity of Plasmodium falciparum infections is consistent over time and protects against clinical disease in Tanzanian children. *The Journal of infectious diseases*, 179(4), pp.989–95.

Fernandez-Reyes, D. et al., 1997. A high frequency African coding polymorphism in the N-terminal domain of ICAM-1 predisposing to cerebral malaria in Kenya. *Human molecular genetics*, 6(8), pp.1357–60.

Flatz, G., Pik, C. & Sringam, S., 1965. Haemoglobin E and beta-thalassaemia: their distribution in Thailand. *Annals of human genetics*, 29(2), pp.151–70.

Flick, K. et al., 2004. Optimized expression of Plasmodium falciparum erythrocyte membrane protein 1 domains in Escherichia coli. *Malaria journal*, 3, p.50.

Flint, J. et al., High frequencies of alpha-thalassaemia are the result of natural selection by malaria. *Nature*, 321(6072), pp.744–50.

Forsyth, K.P. et al., 1989. Diversity of antigens expressed on the surface of erythrocytes infected with mature Plasmodium falciparum parasites in Papua New Guinea. *The American journal of tropical medicine and hygiene*, 41(3), pp.259–65.

Fouchier, R.A.M. & Smith, D.J., 2010. Use of antigenic cartography in vaccine seed strain selection. *Avian diseases*, 54(1 Suppl), pp.220–3.

Fried, M. et al., 1998. Maternal antibodies block malaria. *Nature*, 395(6705), pp.851–2.

Fried, M. & Duffy, P.E., 1996. Adherence of Plasmodium falciparum to chondroitin sulfate A in the human placenta. *Science (New York, N.Y.)*, 272(5267), pp.1502–4.

Gamain, B., Miller, L.H. & Baruch, D.I., 2001. The surface variant antigens of Plasmodium falciparum contain cross-reactive epitopes. *Proceedings of the National Academy of Sciences of the United States of America*, 98(5), pp.2664–9.

Gardner, M.J. et al., 2002. Genome sequence of the human malaria parasite Plasmodium falciparum. *Nature*, 419(6906), pp.498–511.

Giha, H.A. et al., 2000. Antibodies to variable Plasmodium falciparum-infected erythrocyte surface antigens are associated with protection from novel malaria infections. *Immunology letters*, 71(2), pp.117–26.

Giha, H.A. et al., 1999. Nine-year longitudinal study of antibodies to variant antigens on the surface of Plasmodium falciparum-infected erythrocytes. *Infection and immunity*, 67(8), pp.4092–8.

Gitau, E.N. et al., 2012. T-cell responses to the DBLα-tag, a short semi-conserved region of the Plasmodium falciparum membrane erythrocyte protein 1. *PloS one*, 7(1), p.e30095.

Gräslund, S. et al., 2008. Protein production and purification. *Nature methods*, 5(2), pp.135–46.

Gupta, S. et al., 1999. Immunity to non-cerebral severe malaria is acquired after one or two infections. *Nature medicine*, 5(3), pp.340–3.

Handunnetti, S.M., Mendis, K.N. & David, P.H., 1987. Antigenic variation of cloned Plasmodium fragile in its natural host Macaca sinica. Sequential appearance of successive variant antigenic types. *The Journal of experimental medicine*, 165(5), pp.1269–83.

Hebert, C.J., Hall, C.M. & Odoms, L.N.J., 2012. Lessons learned and applied: what the 20th century vaccine experience can teach us about vaccines in the 21st century. *Human vaccines & immunotherapeutics*, 8(5), pp.560–8.

Henning, L. et al., 2004. A prospective study of Plasmodium falciparum multiplicity of infection and morbidity in Tanzanian children. *Transactions of the Royal Society of Tropical Medicine and Hygiene*, 98(12), pp.687–94.

Hirst, G.K., 1943. STUDIES OF ANTIGENIC DIFFERENCES AMONG STRAINS OF INFLUENZA A BY MEANS OF RED CELL AGGLUTINATION. *The Journal of experimental medicine*, 78(5), pp.407–23.

Hommel, M. et al., 1982. Expression of strain-specific surface antigens on Plasmodium falciparum-infected erythrocytes. *Parasite immunology*, 4(6), pp.409–19.

Horton, D.L. et al., 2010. Quantifying antigenic relationships among the lyssaviruses. *Journal of virology*, 84(22), pp.11841–8.

Howell, D.P.-G., Samudrala, R. & Smith, J.D., 2006. Disguising itself--insights into Plasmodium falciparum binding and immune evasion from the DBL crystal structure. *Molecular and biochemical parasitology*, 148(1), pp.1–9.

Huang, S.-W. et al., 2009. Reemergence of enterovirus 71 in 2008 in taiwan: dynamics of genetic and antigenic evolution from 1998 to 2008. *Journal of clinical microbiology*, 47(11), pp.3653–62.

Iqbal, J., Perlmann, P. & Berzins, K., Serological diversity of antigens expressed on the surface of erythrocytes infected with Plasmodium falciparum. *Transactions of the Royal Society of Tropical Medicine and Hygiene*, 87(5), pp.583–8.

Ishino, T. et al., 2004. Cell-passage activity is required for the malarial parasite to cross the liver sinusoidal cell layer. *PLoS biology*, 2(1), p.E4.

Jelinek, T. et al., 2002. Imported Falciparum malaria in Europe: sentinel surveillance data from the European network on surveillance of imported infectious diseases. *Clinical infectious diseases : an official publication of the Infectious Diseases Society of America*, 34(5), pp.572–6.

Jensen, A.T.R. et al., 2004. Plasmodium falciparum associated with severe childhood malaria preferentially expresses PfEMP1 encoded by group A var genes. *The Journal of experimental medicine*, 199(9), pp.1179–90.

Joergensen, L. et al., 2007. 3D7-Derived Plasmodium falciparum erythrocyte membrane protein 1 is a frequent target of naturally acquired antibodies recognizing protein domains in a particular pattern independent of malaria transmission intensity. *Journal of immunology (Baltimore, Md. : 1950)*, 178(1), pp.428–35.

Joergensen, L. et al., 2006. Limited cross-reactivity among domains of the Plasmodium falciparum clone 3D7 erythrocyte membrane protein 1 family. *Infection and immunity*, 74(12), pp.6778–84.

Joergensen, L. et al., 2010. Surface co-expression of two different PfEMP1 antigens on single plasmodium falciparum-infected erythrocytes facilitates binding to ICAM1 and PECAM1. *PLoS pathogens*, 6(9), p.e1001083.

John Rogers, M., 1996. Rare codon usage in Escherichia coli and the expression of potentially toxic genes. *Parasitology today (Personal ed.)*, 12(3), p.124; author reply 124–5.

Jong, J.C. De et al., 2007. Antigenic and Genetic Evolution of Swine Influenza A (H3N2) Viruses in Europe . *Society*, 81(8), pp.4315–4322.

Juillerat, A. et al., 2011. Structure of a Plasmodium falciparum PfEMP1 rosetting domain reveals a role for the N-terminal segment in heparin-mediated rosette inhibition. *Proceedings of the National Academy of Sciences of the United States of America*, 108(13), pp.5243–8.

Karunaweera, N.D. et al., 1992. Dynamics of fever and serum levels of tumor necrosis factor are closely associated during clinical paroxysms in Plasmodium vivax malaria. *Proceedings of the National Academy of Sciences of the United States of America*, 89(8), pp.3200–3.

Khunrae, P. et al., 2010. Full-length recombinant Plasmodium falciparum VAR2CSA binds specifically to CSPG and induces potent parasite adhesion-blocking antibodies. *Journal of molecular biology*, 397(3), pp.826–34.

Kinyanjui, S.M. et al., 2004. Protection against clinical malaria by heterologous immunoglobulin G antibodies against malaria-infected erythrocyte variant surface antigens requires interaction with asymptomatic infections. *The Journal of infectious diseases*, 190(9), pp.1527–33.

Kinyanjui, S.M. et al., 2009. What you see is not what you get: implications of the brevity of antibody responses to malaria antigens and transmission heterogeneity in longitudinal studies of malaria immunity. *Malaria journal*, 8, p.242.

Kraemer, S.M., Gupta, L. & Smith, J.D., 2003. New tools to identify var sequence tags and clone full-length genes using type-specific primers to Duffy binding-like domains. *Molecular and biochemical parasitology*, 129(1), pp.91–102.

Kruskal J.B., 1964a. Multidimensional scaling by optimizing goodness of fit to a nonmetric hypothesis. *Psychometrika*, 29, pp.1–27.

Kruskal J.B., 1964b. Nonmetric multidimensional scaling: a numerical method. *Psychometrika*, 29, pp.115–129.

Kumar, A. et al., 2007. Falcipain-1, a Plasmodium falciparum cysteine protease with vaccine potential. *Infection and immunity*, 75(4), pp.2026–34.

Kyes, S., Horrocks, P. & Newbold, C., 2001. A NTIGENIC V ARIATION AT THE I NFECTED R ED C ELL S URFACE IN M ALARIA. , pp.673–707.

Kyes, S., Pinches, R. & Newbold, C., 2000. A simple RNA analysis method shows var and rif multigene family expression patterns in Plasmodium falciparum. *Molecular and biochemical parasitology*, 105(2), pp.311–5.

Kyes, S.A. et al., 1999. Rifins: a second family of clonally variant proteins expressed on the surface of red cells infected with Plasmodium falciparum. *Proceedings of the National Academy of Sciences of the United States of America*, 96(16), pp.9333–8.

Kyriacou, H.M. et al., 2006. Differential var gene transcription in Plasmodium falciparum isolates from patients with cerebral malaria compared to hyperparasitaemia. *Molecular and biochemical parasitology*, 150(2), pp.211–8.

Lapedes, A. & Farber, R., 2001. The geometry of shape space: application to influenza. *Journal of theoretical biology*, 212(1), pp.57–69.

Leech, J.H. et al., 1984. Identification of a strain-specific malarial antigen exposed on the surface of Plasmodium falciparum-infected erythrocytes. *The Journal of experimental medicine*, 159(6), pp.1567–75.

Lengeler, C., 2004. Insecticide-treated bed nets and curtains for preventing malaria. *The Cochrane database of systematic reviews*, (2), p.CD000363.

Lindenthal, C., Kremsner, P.G. & Klinkert, M.-Q., 2003. Commonly recognised Plasmodium falciparum parasites cause cerebral malaria. *Parasitology research*, 91(5), pp.363–8.

Looareesuwan, S. et al., 1993. Malaria in splenectomized patients: report of four cases and review. *Clinical infectious diseases : an official publication of the Infectious Diseases Society of America*, 16(3), pp.361–6.

Louis, E.J. et al., 2011. Cloning of the Repertoire of Individual Plasmodium falciparum var Genes Using Transformation Associated Recombination (TAR). *Cloning*, 6(3).

Mackintosh, C.L. et al., 2008a. Acquisition of naturally occurring antibody responses to recombinant protein domains of Plasmodium falciparum erythrocyte membrane protein 1. *Malaria journal*, 7, p.155.

Mackintosh, C.L. et al., 2008b. Failure to respond to the surface of Plasmodium falciparum infected erythrocytes predicts susceptibility to clinical malaria amongst African children. *International journal for parasitology*, 38(12), pp.1445–54.

MacPherson, G.G. et al., 1985. Human cerebral malaria. A quantitative ultrastructural analysis of parasitized erythrocyte sequestration. *The American journal of pathology*, 119(3), pp.385–401.

Mansfield, K.L. et al., 2011. Flavivirus-induced antibody cross-reactivity. *The Journal of general virology*, 92(Pt 12), pp.2821–9.

Marsh, K. et al., Antibodies to blood stage antigens of Plasmodium falciparum in rural Gambians and their relation to protection against infection. *Transactions of the Royal Society of Tropical Medicine and Hygiene*, 83(3), pp.293–303.

Marsh, K. & Howard, R.J., 1986. Antigens induced on erythrocytes by P. falciparum: expression of diverse and conserved determinants. *Science (New York, N.Y.)*, 231(4734), pp.150–3.

Marsh, K. & Kinyanjui, S., Immune effector mechanisms in malaria. *Parasite immunology*, 28(1-2), pp.51–60.

Marsh, K., Sherwood, J.A. & Howard, R.J., 1986. Parasite-infected-cell-agglutination and indirect immunofluorescence assays for detection of human serum antibodies bound to antigens on Plasmodium falciparum-infected erythrocytes. *Journal of immunological methods*, 91(1), pp.107–15.

Matteelli, A. et al., 1999. Epidemiological features and case management practices of imported malaria in northern Italy 1991-1995. *Tropical medicine & international health : TM & IH*, 4(10), pp.653–7.

Mayor, A. et al., 2005. Receptor-binding residues lie in central regions of Duffy-binding-like domains involved in red cell invasion and cytoadherence by malaria parasites. *Blood*, 105(6), pp.2557–63.

McGregor, I.A., 1984. Epidemiology, malaria and pregnancy. *The American journal of tropical medicine and hygiene*, 33(4), pp.517–25.

Mehlin, C. et al., 2006. Heterologous expression of proteins from Plasmodium falciparum: results from 1000 genes. *Molecular and biochemical parasitology*, 148(2), pp.144–60.

Miller, L.H. et al., 1976. The resistance factor to Plasmodium vivax in blacks. The Duffy-blood-group genotype, FyFy. *The New England journal of medicine*, 295(6), pp.302–4.

Moll, K. et al., 2007. Generation of cross-protective antibodies against Plasmodium falciparum sequestration by immunization with an erythrocyte membrane protein 1-duffy binding-like 1 alpha domain. *Infection and immunity*, 75(1), pp.211–9.

Mouchet, J. et al., 1997. [The reconquest of the Madagascar highlands by malaria]. *Bulletin de la Société de pathologie exotique (1990)*, 90(3), pp.162–8.

Newbold, C. et al., 1997. Receptor-specific adhesion and clinical disease in Plasmodium falciparum. *The American journal of tropical medicine and hygiene*, 57(4), pp.389–98.

Newbold, C.I. et al., 1992. Plasmodium falciparum: the human agglutinating antibody response to the infected red cell surface is predominantly variant specific. *Experimental parasitology*, 75(3), pp.281–92.

Nielsen, M.A. et al., 2002. Plasmodium falciparum variant surface antigen expression varies between isolates causing severe and nonsevere malaria and is modified by acquired immunity. *Journal of immunology (Baltimore, Md. : 1950)*, 168(7), pp.3444–50.

Noedl, H. et al., 2008. Evidence of artemisinin-resistant malaria in western Cambodia. *The New England journal of medicine*, 359(24), pp.2619–20.

O'Meara, W.P. et al., 2008. Effect of a fall in malaria transmission on morbidity and mortality in Kilifi, Kenya. *Lancet*, 372(9649), pp.1555–62.

Ochola, L.B. et al., 2011. Specific receptor usage in Plasmodium falciparum cytoadherence is associated with disease outcome. *PloS one*, 6(3), p.e14741.

Pancer, Z. & Cooper, M.D., 2006. The evolution of adaptive immunity. *Annual review of immunology*, 24, pp.497–518.

Perelson, a S. & Oster, G.F., 1979. Theoretical studies of clonal selection: minimal antibody repertoire size and reliability of self-non-self discrimination. *Journal of theoretical biology*, 81(4), pp.645–70.

Petter, M. et al., 2007. Variant proteins of the Plasmodium falciparum RIFIN family show distinct subcellular localization and developmental expression patterns. *Molecular and biochemical parasitology*, 156(1), pp.51–61.

Ramasamy, R., Ramasamy, M. & Yasawardena, S., 2001. Antibodies and Plasmodium falciparum merozoites. *Trends in parasitology*, 17(4), pp.194–7.

Ranjan, A. & Chitnis, C.E., 1999. Mapping regions containing binding residues within functional domains of Plasmodium vivax and Plasmodium knowlesi erythrocyte-binding proteins. *Proceedings of the National Academy of Sciences of the United States of America*, 96(24), pp.14067–72.

Rask, T.S. et al., 2010. Plasmodium falciparum Erythrocyte Membrane Protein 1 Diversity in Seven Genomes – Divide and Conquer. *Seven*, 6(9).

Recker, M. et al., 2004. Transient cross-reactive immune responses can orchestrate antigenic variation in malaria. *Nature*, 429(JUNE).

Rogerson, S.J. et al., 1995. Chondroitin sulfate A is a cell surface receptor for Plasmodium falciparum-infected erythrocytes. *The Journal of experimental medicine*, 182(1), pp.15–20.

Rogerson, S.J. et al., 1999. Cytoadherence characteristics of Plasmodium falciparum-infected erythrocytes from Malawian children with severe and uncomplicated malaria. *The American journal of tropical medicine and hygiene*, 61(3), pp.467–72.

Romi, R. et al., 2002. Impact of the malaria control campaign (1993-1998) in the highlands of Madagascar: parasitological and entomological data. *The American journal of tropical medicine and hygiene*, 66(1), pp.2–6.

Rovira-Vallbona, E. et al., 2012. Low antibodies against Plasmodium falciparum and imbalanced pro-inflammatory cytokines are associated with severe malaria in Mozambican children: a case-control study. *Malaria journal*, 11, p.181.

Rowe, A. et al., 1995. Plasmodium falciparum rosetting is associated with malaria severity in Kenya. *Infection and immunity*, 63(6), pp.2323–6.

Rowe, J.A. et al., 1997. P. falciparum rosetting mediated by a parasite-variant erythrocyte membrane protein and complement-receptor 1. *Nature*, 388(6639), pp.292–5.

Sabchareon, A. et al., 1991. Parasitologic and clinical human response to immunoglobulin administration in falciparum malaria. *The American journal of tropical medicine and hygiene*, 45(3), pp.297–308.

Salanti, A. et al., 2003. Selective upregulation of a single distinctly structured var gene in chondroitin sulphate A-adhering Plasmodium falciparum involved in pregnancy-associated malaria. *Molecular microbiology*, 49(1), pp.179–91.

Saul, A. & Battistutta, D., 1988. Codon usage in Plasmodium falciparum. *Molecular and biochemical parasitology*, 27(1), pp.35–42.

Sayers, J.R. et al., 1995. AGA/AGG codon usage in parasites: implications for gene expression in Escherichia coli. *Parasitology today (Personal ed.)*, 11(9), pp.345–6.

Scherf, A. et al., 1998. Antigenic variation in malaria: in situ switching, relaxed and mutually exclusive transcription of var genes during intra-erythrocytic development in Plasmodium falciparum. *The EMBO journal*, 17(18), pp.5418–26.

Schneider, E.L., King, D.S. & Marletta, M.A., 2005. Amino acid substitution and modification resulting from Escherichia coli expression of recombinant Plasmodium falciparum histidine-rich protein II. *Biochemistry*, 44(3), pp.987–95.

Schreiber, N. et al., 2008. Expression of Plasmodium falciparum 3D7 STEVOR proteins for evaluation of antibody responses following malaria infections in naïve infants. *Parasitology*, 135(2), pp.155–67.

Sergent, E. & Parrot, L., 1935. L'immunite la premonition et la resitance innee. *Arch Inst Pasteur Algerie*, 13, pp.279–319.

Sherry, B.A. et al., 1995. Malaria-specific metabolite hemozoin mediates the release of several potent endogenous pyrogens (TNF, MIP-1 alpha, and MIP-1 beta) in vitro, and altered thermoregulation in vivo. *Journal of inflammation*, 45(2), pp.85–96.

Sherwood, J.A. et al., 1985. Antibody mediated strain-specific agglutination of Plasmodium falciparum--parasitized erythrocytes visualized by ethidium bromide staining. *Parasite immunology*, 7(6), pp.659–63.

Siddiqui, W.A. et al., 1978. Partial protection of Plasmodium falciparum-vaccinated Aotus trivirgatus against a challenge of a heterologous strain. *The American journal of tropical medicine and hygiene*, 27(6), pp.1277–8.

Singer, G.A. & Hickey, D.A., 2000. Nucleotide bias causes a genomewide bias in the amino acid composition of proteins. *Molecular biology and evolution*, 17(11), pp.1581–8.

Singh, S.K. et al., 2006. Structural basis for Duffy recognition by the malaria parasite Duffy-binding-like domain. *Nature*, 439(7077), pp.741–4.

Sinnis, P. & Coppi, A., 2007. A long and winding road: the Plasmodium sporozoite's journey in the mammalian host. *Parasitology international*, 56(3), pp.171–8.

Sirawaraporn, W. et al., 1993. The dihydrofolate reductase domain of Plasmodium falciparum thymidylate synthase-dihydrofolate reductase. Gene synthesis, expression, and anti-folate-resistant mutants. *The Journal of biological chemistry*, 268(29), pp.21637–44.

Smith, D., Lapedes, A. & Jong, J. de, 2004. Mapping the antigenic and genetic evolution of influenza virus. *Science*.

Smith, D.J., 2003. Applications of bioinformatics and computational biology to influenza surveillance and vaccine strain selection. *Journal of Theoretical Biology*, 21, pp.1758–1761.

Smith, J.D. et al., 2000. Classification of adhesive domains in the Plasmodium falciparum erythrocyte membrane protein 1 family. *Molecular and biochemical parasitology*, 110(2), pp.293–310.

Smith, J.D. et al., 1995. Switches in expression of Plasmodium falciparum var genes correlate with changes in antigenic and cytoadherent phenotypes of infected erythrocytes. *Cell*, 82(1), pp.101–10.

Smith, T. et al., 1999. Premunition in Plasmodium falciparum infection: insights from the epidemiology of multiple infections. *Transactions of the Royal Society of Tropical Medicine and Hygiene*, 93 Suppl 1, pp.59–64.

SNEATH, P.H. & SOKAL, R.R., 1962. Numerical taxonomy. *Nature*, 193, pp.855–60.

Snow, R.W. et al., Periodicity and space-time clustering of severe childhood malaria on the coast of Kenya. *Transactions of the Royal Society of Tropical Medicine and Hygiene*, 87(4), pp.386–90.

Snow, R.W. et al., 1997. Relation between severe malaria morbidity in children and level of Plasmodium falciparum transmission in Africa. *Lancet*, 349(9066), pp.1650–4.

Southwell, B.R. et al., Field applications of agglutination and cytoadherence assays with Plasmodium falciparum from Papua New Guinea. *Transactions of the Royal Society of Tropical Medicine and Hygiene*, 83(4), pp.464–9.

Srivastava, A. et al., 2010. Full-length extracellular region of the var2CSA variant of PfEMP1 is required for specific, high-affinity binding to CSA. *Proceedings of the National Academy of Sciences of the United States of America*, 107(11), pp.4884–9.

Srivastava, A., Durocher, Y. & Gamain, B., 2013. Expressing full-length functional PfEMP1 proteins in the HEK293 expression system. *Methods in molecular biology (Clifton, N.J.)*, 923, pp.307–19.

Staalsoe, T. et al., In vitro selection of Plasmodium falciparum 3D7 for expression of variant surface antigens associated with severe malaria in African children. *Parasite immunology*, 25(8-9), pp.421–7.

Stephens, L.L., Shonhai, A. & Blatch, G.L., 2011. Co-expression of the Plasmodium falciparum molecular chaperone, PfHsp70, improves the heterologous production of the antimalarial drug target GTP cyclohydrolase I, PfGCHI. *Protein expression and purification*, 77(2), pp.159–65.

Su, X.Z. et al., 1995. The large diverse gene family var encodes proteins involved in cytoadherence and antigenic variation of Plasmodium falciparum-infected erythrocytes. *Cell*, 82(1), pp.89–100.

Taylor, H.M. et al., 2000. A study of var gene transcription in vitro using universal var gene primers. *Molecular and biochemical parasitology*, 105(1), pp.13–23.

Tolia, N.H. et al., 2005. Structural basis for the EBA-175 erythrocyte invasion pathway of the malaria parasite Plasmodium falciparum. *Cell*, 122(2), pp.183–93.

Tonkin, C.J. et al., 2009. Sir2 paralogues cooperate to regulate virulence genes and antigenic variation in Plasmodium falciparum. *PLoS biology*, 7(4), p.e84.

Turner, G.D. et al., 1994. An immunohistochemical study of the pathology of fatal malaria. Evidence for widespread endothelial activation and a potential role for intercellular adhesion molecule-1 in cerebral sequestration. *The American journal of pathology*, 145(5), pp.1057–69.

Udeinya, I.J. et al., Plasmodium falciparum strain-specific antibody blocks binding of infected erythrocytes to amelanotic melanoma cells. *Nature*, 303(5916), pp.429–31.

Udomsangpetch, R. et al., 1989. Plasmodium falciparum-infected erythrocytes form spontaneous erythrocyte rosettes. *The Journal of experimental medicine*, 169(5), pp.1835–40.

Vallejo, L.F. & Rinas, U., 2004. Strategies for the recovery of active proteins through refolding of bacterial inclusion body proteins. *Microbial cell factories*, 3(1), p.11.

Vedadi, M. et al., 2007. Genome-scale protein expression and structural biology of Plasmodium falciparum and related Apicomplexan organisms. *Molecular and biochemical parasitology*, 151(1), pp.100–10.

Villaverde, A. & Carrió, M.M., 2003. Protein aggregation in recombinant bacteria: biological role of inclusion bodies. *Biotechnology letters*, 25(17), pp.1385–95.

Voss, T.S. et al., 2000. Genomic distribution and functional characterisation of two distinct and conserved Plasmodium falciparum var gene 5' flanking sequences. *Molecular and biochemical parasitology*, 107(1), pp.103–15.

Warimwe, G.M. et al., 2013. Plasmodium falciparum var Gene Expression Homogeneity as a Marker of the Host-Parasite Relationship under Different Levels of Naturally Acquired Immunity to Malaria. A. T. Jensen, ed. *PloS one*, 8(7), p.e70467.

Warimwe, G.M. et al., 2009. Plasmodium falciparum var gene expression is modified by host immunity. *Proceedings of the National Academy of Sciences of the United States of America*, 106(51), pp.21801–6.

Willcox, M. et al., 1983. A case-control study in northern Liberia of Plasmodium falciparum malaria in haemoglobin S and beta-thalassaemia traits. *Annals of tropical medicine and parasitology*, 77(3), pp.239–46.

Winter, G. et al., 2005. SURFIN is a polymorphic antigen expressed on Plasmodium falciparum merozoites and infected erythrocytes. *The Journal of experimental medicine*, 201(11), pp.1853–63.

Wongsrichanalai, C. & Meshnick, S.R., 2008. Declining artesunate-mefloquine efficacy against falciparum malaria on the Cambodia-Thailand border. *Emerging infectious diseases*, 14(5), pp.716–9.

Yadava, A. & Ockenhouse, C.F., 2003. Effect of codon optimization on expression levels of a functionally folded malaria vaccine candidate in prokaryotic and eukaryotic expression systems. *Infection and immunity*, 71(9), pp.4961–9.

Yamauchi, L.M. et al., 2007. Plasmodium sporozoites trickle out of the injection site. *Cellular microbiology*, 9(5), pp.1215–22.

Yazdani, S.S. et al., 2006. Improvement in yield and purity of a recombinant malaria vaccine candidate based on the receptor-binding domain of Plasmodium vivax Duffy binding protein by codon optimization. *Biotechnology letters*, 28(14), pp.1109–14.

Yenchitsomanus, P. et al., 1986. Alpha-thalassemia in Papua New Guinea. *Human genetics*, 74(4), pp.432–7.

Zhou, Z. et al., 2004. Enhanced expression of a recombinant malaria candidate vaccine in Escherichia coli by codon optimization. *Protein expression and purification*, 34(1), pp.87–94.

Ziegel, E. et al., 1987. *Numerical Recipes: The Art of Scientific Computing*,

Appendix

Table 8.1 A. Raw ELISA OD values from acute time-point

	6387A	6398A	6408A	6429A	6430A	6433A	6485A	6964A	7045A	7069A	7084A	7116A	7134A	7157A	7160A	7183A	7198A	7204A	7249A
6387	1.396	3.072	2.552	3.0955	3.049	4.044	2.4435	2.612	2.8	2.993	3.0715	2.994	3.2	3.6865	2.628	0.845	3.1325	3.6935	3.6125
6408	2.7685	1.0275	0.7375	0.878	0.618	0.872	1.1725	0.99	2.839	2.898	1.1965	3.1275	0.584	3.146	0.4375	2.073	2.5405	0.845	3.6185
6429	3.006	2.057	2.864	1.34	2.5155	2.2015	2.4505	2.576	3.696	3.729	2.7665	3.721	2.6255	3.4605	3.014	2.0885	3.7375	3.1315	3.5445
6430	3.0885	0.6325	0.6795	0.572	0.3615	0.587	0.594	1.082	3.1725	3.3535	0.7595	3.6005	0.564	3.436	0.4915	3.165	3.6355	0.546	3.5435
6433	2.903	0.6665	1.373	1.1945	1.0845	1.309	1.005	1.3595	2.866	3.1705	1.8005	3.475	1.1495	3.302	1.7385	3.075	3.2855	1.6655	3.4075
6485	1.2475	3.1825	2.5095	2.834	0.744	1.2555	1.1485	1.4095	1.9205	1.6195	2.5885	1.6865	3.31	2.1665	2.47	0.79	1.3565	3.5025	2.197
6964	1.845	2	2.105	1.603	1.579	1.2285	1.6075	1.684	2.068	1.4995	2.4795	1.8685	2.297	2.202	1.485	0.7665	2.332	2.1175	1.6845
7045	0.9815	0.745	0.636	0.4485	0.719	0.413	0.5435	0.51	0.137	0.605	0.886	1.369	0.884	1.2815	0.8515	0.423	1.2945	1.0405	1.2005
7069	2.195	2.8155	2.343	1.79	1.049	1.632	1.764	1.96	2.925	1.789	2.343	2.759	3.847	2.858	2.835	1.245	2.8365	2.7735	3.5875
7116	1.2705	1.968	1.298	1.0895	1.73	0.7385	1.376	1.9145	1.8065	1.4395	1.3845	1.1745	2.141	3.1765	1.3995	0.958	2.421	1.828	3.0915
7134	1.2555	2.542	3.0295	2.365	1.4785	1.524	3.2545	2.0735	1.1745	1.386	1.9545	3.2265	2.285	1.957	3.158	1.0565	1.5975	3.293	3.825
7157	1.4285	1.7105	1.724	1.4775	1.113	1.1395	1.285	1.453	1.499	1.1625	1.5555	1.6535	1.852	1.012	1.128	0.56	1.4825	1.5165	1.5925
7160	1.1115	1.852	1.732	1.432	1.0695	1.225	1.3735	1.5125	1.289	1.0995	1.5555	1.7585	1.7365	1.4415	1.17	0.6	1.4735	1.457	1.3235
7183	2.5625	2.6715	3.479	1.877	2.5815	2.1345	0.3165	3.0195	3.36	3.1695	3.5655	2.94	3.3975	3.0335	3.583	1.3135	3.5725	1.9305	2.9435
7198	2.308	2.4085	1.929	1.931	1.8335	1.4985	2.156	1.911	2.966	1.7	2.331	3.0605	2.651	3.086	1.877	1.131	3.272	2.894	3.5415
7204	1.617	1.4805	1.697	1.2195	1.2805	1.2115	1.5085	1.3915	2.5315	1.6885	2.1495	2.159	1.8925	2.4045	1.5145	0.961	2.7575	1.029	2.357
7249	1.3025	1.469	1.8385	1.4395	1.351	1.222	1.717	1.421	2.1075	2.2005	2.3165	1.9915	1.519	1.9475	1.916	0.985	2.6025	2.118	0.8505
7250	1.8935	2.5975	2.2595	2.111	2.634	1.8495	1.872	2.0955	3.0275	1.853	2.878	3.3245	2.88	2.9265	2.2745	0.741	3.1295	3.3385	1.4665
7323	1.711	3.222	2.446	1.733	1.1505	1.409	1.464	1.706	2.4255	2.103	1.7115	2.3895	3.719	2.4925	2.322	1.158	2.1945	2.4855	3.374
7337	2.9535	3.243	3.0675	2.878	3.1235	2.644	2.3335	3.0365	3.605	1.915	3.291	1.668	3.259	3.7545	3.2865	2.183	3.682	3.746	3.8705
7391	1.724	1.4105	1.8335	0.9695	1.9725	1.368	1.189	1.0965	1.2615	1.553	2.543	1.1695	0.824	1.15	1.724	0.6615	1.325	1.73	1.9845
7410	0.7145	0.876	0.4735	0.5675	0.404	0.5015	1.017	0.3425	0.4015	0.443	1.351	0.437	1.642	0.622	0.5485	0.839	0.766	0.452	0.741
7506	1.069	1.8465	1.932	1.468	1.0825	1.244	1.369	1.6135	1.3195	1.316	1.858	1.6765	1.8445	1.544	1.4755	0.682	1.5815	1.4675	1.6025
7530	2.194	2.4285	1.6265	2.255	2.0495	1.7445	2.1015	2.4995	1.151	0.933	2.086	0.943	2.5195	1.2535	2.4345	0.4925	1.5865	2.789	3.4615
7630	1.9885	3.052	3.0015	2.4795	2.199	2.077	2.8535	2.405	3.046	2.449	3.0775	2.3355	3.0465	2.5365	2.6725	1.272	3.659	3.181	2.676
7781	2.1725	2.445	2.0775	1.358	0.777	1.112	2.546	1.6035	2.3275	2.5065	2.285	2.198	2.9665	2.8445	2.31	1.797	2.0075	2.583	4.178
7799	1.6335	1.945	1.813	1.5725	1.557	1.355	1.8025	1.6525	1.6025	1.307	2.2425	2.0585	2.275	1.9025	1.6957	0.7695	1.836	2.4615	1.873
7864	1.5875	2.071	1.5035	1.47	1.127	1.0075	1.3815	1.4025	2.1445	1.264	1.4535	1.8785	1.9575	2.2225	1.6025	0.983	1.986	2.181	3.1465
8204	2.426	1.215	2.55	1.079	2.8895	0.881	1.18	1.2105	3.453	1.991	3.0935	2.784	0.9245	2.8165	1.9165	2.2705	1.9625	0.9455	3.3025
8344	1.7475	1.0145	1.998	1.3535	1.1665	1.379	1.8685	1.4745	2.7985	2.758	2.3405	2.2095	2.442	2.569	2.279	1.1445	3.0955	2.148	2.191
8349	3.1695	3.435	3.8105	3.1435	3.345	3.0665	3.614	3.6385	3.628	3.916	3.8435	3.7205	3.929	3.672	3.923	2.329	3.9175	3.9085	3.433
8383	1.6655	1.4215	1.65	1.2045	1.794	0.869	1.0815	2.2695	1.9275	1.474	1.848	1.459	1.7305	3.4855	1.5895	0.819	2.4385	2.6125	3.233
8477	3.1905	3.428	3.847	2.595	2.634	2.055	2.319	2.7975	3.4035	2.461	3.424	3.128	3.7415	3.7065	3.4015	2.428	3.7755	3.499	3.8005
8482	2.3865	2.5365	2.312	1.8865	1.826	1.29	1.7175	1.848	2.737	2.0785	2.1445	2.8385	2.21	3.4955	2.0445	1.3275	3.085	2.779	3.226
8585	1.2565	0.6795	0.573	0.839	0.4255	0.4885	0.9035	0.357	0.7225	0.658	0.767	0.642	1.3245	0.652	0.576	0.747	1.002	0.454	1.2205
8706	2.2285	2.843	3.142	2.4435	2.2055	2.135	2.8125	2.631	3.723	2.952	2.988	2.882	3.274	2.956	2.8885	1.447	3.5785	3.1295	3.04

Table 8.1 B. Raw ELISA OD values from acute time-point

	7250A	7323A	7391A	7410A	7506A	7530A	7630A	7642A	7799A	7864A	8204A	8344A	8349A	8383A	8472A	8477A	8482A	8585A	8618A	8706A
6387	3.4015	2.599	2.9955	3.1365	3.5	3.463	2.805	3.3675	3.71	2.318	3.093	1.6315	3.954	2.1165	2.548	3.1195	3.312	0.728	2.82	0.7675
6408	3.1185	0.7025	0.71	0.789	0.5715	2.986	0.971	3.0375	2.8375	2.726	2.8415	2.9975	3.23	2.379	0.871	2.325	2.283	0.5995	2.19	0.574
6429	3.0015	2.021	2.5655	2.779	2.789	3.349	2.5745	3.601	3.3185	2.5035	1.6465	3.1505	3.195	2.8695	0.343	2.4925	2.5755	0.2455	2.3615	0.2445
6430	3.589	0.354	0.4175	0.599	1.033	3.627	0.6785	3.155	3.534	3.277	2.9715	3.236	3.224	2.7835	1.126	2.5665	2.685	0.5745	2.5035	0.5645
6433	3.1735	0.798	1.7545	0.6415	1.7495	3.512	2.356	3.0625	3.6855	3.59	3.4095	3.506	3.3725	1.602	0.714	1.555	1.737	0.501	1.8145	0.5495
6485	1.2895	0.681	1.879	0.7375	0.262	1.771	0.9885	1.5455	3.2555	1.1725	0.656	0.4475	1.5315	1.9215	0.475	0.792	1.2345	0.4585	2.0825	0.564
6964	1.7165	1.704	1.3405	1.862	2.0025	2.3205	1.6515	1.2475	2.083	0.813	0.7965	0.9875	2.2735	0.491	0.8045	0.623	1.1425	0.182	1.0555	0.7975
7045	0.8315	0.583	0.826	1.004	1.2355	0.1465	0.983	0.8025	1.178	0.6765	0.7675	0.7865	1.627	0.475	0.133	0.3075	0.444	0.1185	0.306	0.111
7069	2.0825	1.828	1.7065	1.7445	2.1135	2.0055	2.3015	2.8705	2.8975	1.7785	1.78	2.3815	2.323	1.916	0.3625	1.8655	1.8775	0.3173	1.8667	0.2918
7116	0.851	1.8435	1.3235	0.996	0.535	1.2555	0.695	1.925	2.7385	0.704	1.296	1.0425	2.5065	1.3225	0.292	0.5385	1.076	0.3415	1.494	0.301
7134	1.2875	1.984	3.0695	1.479	0.43	1.0745	1.4495	3.489	2.769	2.156	0.811	0.907	1.5125	0.9385	0.893	0.847	1.1665	0.536	1.178	1.695
7157	1.0475	1.452	1.371	1.4745	1.884	0.9425	1.542	1.4315	2.275	0.888	0.7555	0.696	1.351	0.406	0.7485	0.597	1.061	0.1645	0.9195	0.652
7160	1.1155	1.4905	1.343	1.3395	1.673	0.9745	1.3845	1.0585	1.4505	0.787	0.6115	0.7545	1.2395	0.5235	0.8645	0.5955	1.0945	0.1625	0.9075	0.7315
7183	2.4985	2.2115	2.579	0.2985	2.6715	2.6835	2.756	2.3305	2.414	1.6655	1.1495	2.6425	1.6965	3.3085	0.5025	2.974	3.299	0.4	2.3105	0.332
7198	2.2145	2.067	1.9055	1.7585	2.9815	2.291	2.0385	2.9205	2.9555	2.247	1.4755	1.7155	3.0005	3.3115	0.9065	3.299	3.401	1.0995	3.3135	0.8035
7204	1.8095	0.7755	1.038	1.157	2.0625	2.2685	1.2565	1.357	2.3885	1.279	1.0905	2.1215	2.5375	0.812	0.2425	0.637	0.7905	0.1955	0.7895	0.2
7249	1.617	1.678	1.947	1.9365	1.9755	1.5	1.6335	1.169	2.5425	1.216	0.8555	2.0405	1.5215	1.04	0.497	1.0105	1.159	0.1775	0.8885	0.1705
7250	2.383	2.1705	3.148	3.2565	2.806	4.004	1.988	1.32	3.295	2.617	1.374	1.2285	3.6375	1.613	1.3265	1.458	1.6425	0.371	2.0375	0.5547
7323	1.4935	1.503	1.7605	1.6635	2.291	1.4975	1.8935	2.6465	2.845	1.3015	1.579	1.8865	2.153	3.5105	0.752	3.389	3.434	1.11	3.725	0.9245
7337	2.7345	2.8465	3.3665	3.1505	3.3545	4.003	3.162	3.7465	3.7235	1.3535	2.233	2.875	3.9835	3.2245	3.787	3.9445	3.9645	0.5905	3.705	0.5465
7391	1.373	1.816	0.6285	0.6225	0.279	1.1255	1.0035	1.44	3.127	0.7215	0.4605	0.424	1.259	2.1095	0.447	0.793	0.908	0.516	2.4515	0.463
7410	0.622	0.7505	0.477	0.8775	0.765	0.572	1.706	1.2435	0.493	0.467	0.806	1.0265	0.8275	0.643	0.2165	0.483	0.4865	0.217	0.8915	0.253
7506	1.194	1.496	1.3755	1.4405	1.6825	1.2105	1.6545	1.1605	1.592	0.886	0.724	0.849	1.239	0.475	0.8555	0.6115	1.206	0.1605	1.0335	0.9565
7530	2.2065	2.3095	1.97	2.3915	2.699	0.7055	2.347	2.8725	1.4545	0.717	1.0665	0.692	1.794	0.951	0.818	1.259	1.745	0.1635	1.309	0.213
7630	2.038	1.7355	3.131	2.9475	2.3345	2.04	1.762	2.2475	3.0475	1.4475	1.2005	2.233	2.745	2.122	0.219	1.585	2.2015	0.18	1.553	0.17
7781	2.0185	0.749	1.4325	1.2035	0.299	2.142	0.723	3.874	3.712	1.4245	0.9545	1.324	1.914	1.9925	0.4475	1.0155	0.7755	0.5395	2.896	0.486
7799	1.5155	1.4212	1.4775	1.4775	2.522	1.217	1.6475	1.5395	1.0945	0.935	0.987	0.942	1.4275	0.591	0.9725	0.7445	1.2975	0.1815	1.203	0.8795
7864	1.329	.408	1.2465	1.202	2.0815	1.366	1.584	2.359	2.873	1.393	1.1225	1.1885	2.1125	1.907	0.2695	1.5725	1.6245	0.282	3.18	0.2725
8204	2.299	2.272	0.678	0.4155	0.331	2.736	0.993	2.27	3.837	2.0235	1.081	1.397	1.926	2.1305	0.3605	0.739	1.2015	0.4585	1.4165	0.444
8344	1.927	1.153	2.82	2.5285	1.7385	2.525	1.6295	1.5375	2.339	1.585	1.0645	2.416	1.8185	0.9465	0.2505	0.7425	0.8285	0.203	0.874	0.1755
8349	3.5395	3.2885	3.6505	3.7835	3.6345	3.428	3.7365	2.794	3.893	3.0535	2.254	3.6675	2.9095	3.0985	1.117	3.0395	2.9505	0.515	2.5545	0.307
8383	1.624	1.0135	1.893	2.007	1.535	2.1275	0.8225	2.1295	3.1535	1.5415	1.083	0.829	2.8605	1.465	0.261	0.859	1.5295	0.2515	1.441	0.259
8477	3.084	2.4635	2.953	2.734	3.79	3.8635	2.8675	2.8475	3.6965	2.804	2.222	3.2185	3.934	2.559	0.547	0.7455	2.9545	0.4925	3.4285	0.5325
8482	2.33	1.7585	1.988	1.652	3.3265	2.8035	2.2205	3.3845	3.185	2.343	1.4015	1.875	3.1215	2.3525	0.3835	2.8015	1.6925	0.426	3.3305	0.4085
8585	1.1565	0.828	0.384	0.723	0.6	0.8575	0.959	1.5495	0.5745	0.603	0.893	1.181	0.6635	0.5855	0.2015	0.532	0.552	0.2165	0.8965	0.2085
8706	2.4065	2.24	3.2605	2.51	2.8085	2.855	1.954	2.6425	2.889	1.418	1.296	2.3765	2.566	2.8105	0.5025	2.263	2.388	0.3095	1.391	0.6585

	6387C2	6398C2	6408C2	6429C2	6430C2	6433C2	6485C2	6964C2	7045C2	7069C2	7084C2	7116C2	7134C2	7157C2	7160C2	7183C2	7198C2	7204C2	7249C2
6387	2.414	2.6845	3.552	2.6805	3.2855	4.2	2.5645	2.607	2.873	3.031	3.5205	4.0175	2.0885	3.7665	1.5075	0.8715	3.4775	2.099	2.6115
6408	3.001	0.8405	1.4675	0.585	0.473	0.5095	0.689	0.5355	3.153	2.557	0.6635	3.237	0.483	2.804	0.405	2.9555	2.839	0.6485	2.539
6429	3.1325	1.758	3.179	2.3165	1.8635	2.2755	2.536	3.018	3.627	2.808	2.9125	3.691	2.7075	3.4205	2.966	2.5935	3.707	3.072	3.4265
6430	3.501	0.639	0.6735	0.3715	0.4295	0.4265	0.3455	0.9155	3.435	3.095	0.402	3.14	0.4885	3.213	0.4555	3.4485	3.4255	0.4835	3.454
6433	2.809	0.8665	1.3455	1.027	1.0165	1.444	0.923	1.351	3.2195	2.948	1.828	3.1995	1.4615	3.1815	1.232	3.0735	3.1935	1.2915	2.705
6485	1.4565	2.0505	2.4615	2.4565	0.49	1.797	1.3215	0.7295	2.261	1.7425	2.463	2.073	2.0525	2.632	1.6995	0.7235	1.23	3.0385	1.8215
6964	2.6305	1.5275	2.811	1.7815	1.793	1.1365	1.734	1.735	1.902	1.565	2.1535	2.9715	1.953	2.2355	1.5325	0.9545	2.4275	2.164	0.9565
7045	1.5815	0.713	1.2565	0.5985	0.6795	0.3615	0.5105	0.625	0.585	0.806	1.2325	2.276	0.6795	1.1595	0.6745	0.72	1.3205	0.7695	0.476
7069	1.827	2.9025	2.903	1.8605	1.425	1.9475	1.883	2.413	2.8105	2.777	2.863	2.7825	3.7485	2.8855	2.3775	1.5085	2.6245	1.7465	3.4675
7116	1.2625	1.638	1.2265	1.1785	1.3185	0.7845	0.917	1.7185	1.6	1.1675	1.124	1.945	1.3565	2.216	1.0615	0.899	1.7985	1.4425	2.8315
7134	0.8145	2.403	3.3175	2.102	1.492	2.33	2.901	1.614	1.283	1.6555	1.4155	3.4325	2.2995	1.6935	2.734	1.2845	1.292	2.5255	3.658
7157	1.66	1.394	2.0355	1.305	1.2155	1.0505	1.179	1.3605	1.1865	1.0405	1.3855	2.117	1.2825	1.414	1.1225	0.906	1.5325	1.5325	0.753
7160	1.456	1.3645	2.065	1.4355	1.184	1.0135	1.3825	1.4305	1.021	0.944	1.3715	2.183	1.4995	1.561	1.8232	0.905	1.6515	1.39	0.6225
7183	3.053	2.352	3.7435	1.5195	2.1705	2.034	0.291	3.0915	3.0505	2.0675	3.259	3.4615	3.382	2.8845	3.601	1.755	3.763	2.1725	2.577
7198	2.862	2.0245	2.264	1.5335	1.5545	1.3325	1.822	1.425	2.82	2.9975	2.4865	3.369	1.2485	2.7555	1.1465	1.258	2.126	1.5175	3.328
7204	1.859	1.1865	1.83	1.317	1.3655	1.2605	1.0545	1.5725	2.3895	1.874	2.4365	3.1015	1.742	2.2095	1.3875	1.163	2.866	1.699	1.4215
7249	1.091	1.683	2.4835	1.68	1.2985	1.258	1.8375	1.9305	2.051	2.3475	2.399	2.519	2.2235	1.782	2.0045	1.467	2.789	1.856	1.1415
7250	2.892	2.1965	3.395	2.2665	2.92	1.99	1.992	2.211	3.425	1.928	3.2165	4.309	1.7755	2.8265	1.463	0.7205	2.9165	1.852	0.9765
7323	1.5615	2.8015	2.547	1.762	1.143	1.6255	1.668	1.963	2.078	2.0155	2.4005	2.2705	3.5665	2.3205	1.9115	1.267	2.2605	1.463	3.28
7337	3.3795	2.7285	3.778	2.742	2.9815	2.7645	2.6675	3.0055	3.7005	2.1935	3.635	3.1475	1.9565	3.5645	1.866	2.1975	3.4225	2.097	3.2485
7391	1.199	0.933	2.265	0.658	1.2155	0.5505	1.2805	0.63	1.59	1.6945	2.4935	1.097	0.761	1.1215	1.1935	0.6355	1.1015	1.0535	1.6415
7410	0.5525	0.6255	0.853	0.6075	0.354	0.8955	1.1715	0.3055	0.347	0.347	1.196	0.427	1.7555	0.384	0.4875	0.5385	0.9065	0.3685	0.5435
7506	1.341	1.3605	2.2125	1.503	1.247	1.068	1.305	1.5545	1.146	1.1375	1.7555	2.082	1.8935	1.656	1.447	0.8645	1.7605	1.503	0.778
7530	2.586	2.2035	2.174	2.05	2.488	2.075	2.264	2.81	0.725	0.904	2.6965	1.5595	1.5905	1.326	1.3215	0.501	1.604	1.7425	3.3615
7630	2.278	2.681	3.4395	2.3795	1.611	1.876	2.767	2.4075	2.828	2.618	3.176	3.3675	3.3755	2.3825	2.938	1.5115	3.6085	3.3385	2.1635
7781	2.478	2.274	2.421	2.0545	0.6005	1.596	2.268	1.4385	2.516	2.4135	2.321	2.4985	1.9115	2.593	1.519	2.191	1.78	2.3905	3.964
7799	1.7655	1.6055	2.047	1.4525	1.46	1.2965	1.4325	1.4985	1.3225	1.228	2.4615	2.382	1.4905	1.7645	1.267	1.116	2.0055	1.6825	0.8325
7864	2.1175	1.383	1.7745	0.98	0.9005	0.916	1.128	1.276	1.805	1.303	1.613	2.205	0.932	1.9775	0.8765	1.0535	1.711	1.2465	3.1025
8204	2.678	0.9865	2.3545	0.684	2.229	0.775	0.671	0.7365	3.179	2.5155	2.9215	3.3015	0.8915	2.676	1.4715	2.586	1.77	0.7875	3.062
8344	1.478	1.5815	2.1415	1.97	1.351	1.431	2.5785	1.951	2.9655	2.5825	2.1385	2.8595	2.606	2.5345	2.2075	1.493	3.097	1.862	1.6795
8349	3.459	3.207	3.909	3.422	3.442	3.351	3.753	3.8855	3.807	3.1255	3.898	3.791	3.962	3.832	3.913	2.99	3.979	3.948	3.1615
8383	2.3895	1.374	1.7205	1.243	1.037	1.0245	0.9805	1.9445	1.9755	1.1515	1.3745	2.6815	1.2305	2.7125	1.126	0.8055	1.613	1.9435	2.838
8477	3.7735	2.8035	3.956	2.0145	2.538	1.805	1.992	2.3375	3.5715	2.3395	3.6235	4.103	2.5835	3.501	2.849	2.186	3.366	2.236	2.2815
8482	3.1445	1.858	2.6915	1.5515	1.827	1.2385	1.58	1.702	2.512	2.1875	2.45	3.2405	1.3425	3.4465	1.3005	1.3435	2.7915	1.512	2.834
8585	2.0505	0.605	1.43	0.6815	0.3385	0.719	0.7755	0.316	0.5755	0.5195	0.617	0.484	1.3935	0.4585	0.582	0.5365	0.968	0.3935	0.7595
8706	2.175	2.506	3.322	2.8255	1.9425	2.0885	2.6215	2.8095	3.5905	1.802	2.7915	3.202	3.224	2.4525	3.1245	1.6185	3.7225	3.0395	2.715

Table 8.2 B. Raw ELISA OD values from 2 week convalescent (C2) time-point

	7250C2	7323C2	7391C2	7410C2	7506C2	7530C2	7630C2	7642C2	7799C2	7864C2	8204C2	8344C2	8349C2	8383C2	8472C2	8477C2	8482C2	8585C2	8618C2	8706C2
6387	3.198	2.0305	2.1	1.853	2.153	2.8595	1.8785	2.685	3.2775	2.085	3.4185	0.531	3.4345	3.262	3.168	2.1805	2.936	0.5285	3.007	0.546
6408	2.84	0.57	0.595	0.844	0.5355	2.925	1.1695	3.0875	2.5915	3.2575	3.14	0.44	2.789	2.166	2.479	2.4825	2.089	0.507	2.601	0.4485
6429	3.071	2.107	2.6115	2.6985	2.906	3.1105	2.8025	2.4355	2.487	2.4015	2.04	0.254	2.818	2.624	1.2275	1.6125	1.8235	0.226	2.922	0.2345
6430	3.5645	0.355	0.469	0.5185	0.9495	3.563	0.792	3.311	3.4775	3.763	3.4645	0.7635	3.493	2.762	3.0005	2.9465	2.863	0.45	3.004	0.46
6433	2.838	1.323	1.823	1.376	1.9745	3.0965	2.4315	2.821	2.7345	3.351	2.867	0.3545	3.2225	1.809	1.6905	1.974	1.89	0.4635	2.0815	0.387
6485	1.2225	0.733	1.4175	0.574	0.8095	1.3425	2.5325	1.052	2.4405	1.941	2.085	0.406	1.171	1.422	0.8475	0.613	0.8075	0.41	1.1855	0.4185
6964	1.734	1.7445	1.5875	1.5175	1.8385	1.965	1.714	1.043	1.737	1.131	0.9515	0.1845	1.533	1.245	0.5545	0.668	0.8835	0.166	1.1755	0.168
7045	0.834	0.801	0.7325	0.5815	1.1575	0.13	0.7535	0.53	0.6175	0.448	1.0445	0.1245	1.37	0.634	0.393	0.197	0.2775	0.105	0.306	0.108
7069	1.9055	1.454	1.3615	1.0725	1.067	2.0125	0.9875	2.438	2.5935	1.636	2.2635	0.22	2.0925	1.9735	1.253	1.2467	1.367	0.2667	2.101	0.2695
7116	0.671	1.7145	1.053	0.8875	1.9935	1.1035	1.419	1.391	1.8555	1.227	2.7275	0.3825	1.3875	1.297	0.7295	0.3965	0.7295	0.3155	0.778	0.313
7134	0.689	1.869	2.772	2.6155	2.157	1.1405	1.493	2.3565	1.996	2.509	1.914	0.4575	1.2175	1.058	0.5695	0.8925	1.222	0.4915	0.897	1.4225
7157	0.9325	1.4385	1.2015	1.062	1.5835	0.7825	1.657	0.7595	1.042	1.7325	0.9605	0.217	0.9365	1.049	0.628	0.6015	0.917	0.149	1.0025	0.155
7160	1.1195	1.3365	1.2515	1.0505	1.452	0.8695	1.4955	0.7735	0.961	1.823	0.9425	0.1485	1.064	1.226	0.6625	0.6705	0.7865	0.1515	1.0915	0.1505
7183	2.8285	2.345	2.946	0.2965	3.258	2.4795	2.8585	1.7105	2.02	1.7425	1.4795	0.2045	2.529	2.6875	1.546	1.6295	1.951	0.32	3.1425	0.3235
7198	2.01	1.821	1.234	1.318	1.7195	1.668	1.188	2.1375	2.393	1.7915	2.3875	0.301	2.6895	3.2665	3.1435	3.1845	3.303	0.8215	3.3615	0.7495
7204	1.616	0.944	1.112	1.2525	1.5985	1.734	1.1285	1.15	1.982	1.0485	1.163	0.2145	1.8645	0.9555	0.57	0.4545	0.6505	0.1945	0.958	0.2055
7249	1.618	1.7265	1.763	1.473	1.722	1.4395	1.515	1.1175	2.1885	1.114	1.1755	0.173	1.426	0.8555	0.715	0.6365	0.7415	0.149	1.0875	0.16
7250	2.6015	1.984	1.513	1.4335	1.8025	3.9725	1.4185	1.0755	2.8755	2.3015	1.6385	0.434	2.55	1.6525	1.3355	1.2375	1.2875	0.36	1.7225	0.3065
7323	1.4185	1.958	1.2755	1.0775	1.4865	1.569	1.0535	1.944	2.3865	1.2655	2.3255	0.2095	2.109	3.2085	3.1615	3.1605	3.2315	0.851	3.6185	0.7715
7337	2.612	1.9975	2.158	1.683	1.87	3.8505	1.987	2.9055	3.004	1.038	2.6	0.4185	3.0775	3.4925	3.5345	3.3765	3.418	0.483	3.6965	0.4415
7391	1.316	1.8625	1.339	0.922	0.738	0.9285	2.2545	0.9325	2.3355	1.294	0.869	0.431	0.937	1.479	0.8335	0.6375	0.6615	0.577	1.686	0.4225
7410	0.4455	0.474	0.443	1.013	0.2165	0.4845	0.9725	0.804	0.4355	0.3715	0.332	0.672	0.7045	0.421	0.282	0.2615	0.2745	0.237	0.3155	0.218
7506	1.0735	1.3985	1.324	1.1595	1.942	1.109	1.6855	0.958	1.1185	1.854	1.1325	0.157	1.2315	1.216	0.693	0.6475	0.8015	0.143	1.311	0.144
7530	2.096	1.6325	1.4535	1.058	1.7715	1.642	1.593	2.0635	1.408	0.664	1.5265	0.2845	1.6295	1.488	0.725	1.09	1.579	0.223	2.045	0.1845
7630	1.971	2.078	3.793	3.0995	2.863	1.8145	2.792	1.606	2.509	1.399	1.6935	0.2615	2.2575	2.101	1.256	1.1575	1.3815	0.1565	2.4135	0.162
7781	2.0085	0.7	1.187	1.637	2.6085	1.6375	2.284	3.1005	2.984	2.039	2.678	0.8735	1.6175	2.019	0.9595	0.8225	1.062	0.445	2.6935	0.463
7799	1.508	1.3825	1.173	1.2855	1.659	0.978	1.1585	0.9305	1.416	1.512	1.263	0.1835	1.097	1.2645	0.659	0.7435	0.917	0.1715	1.3455	0.2515
7864	1.258	0.992	0.972	0.7845	1.404	1.268	0.917	1.7945	2.083	1.014	2.208	0.229	1.594	2.068	1.0275	0.863	1.3235	0.2755	2.6955	0.273
8204	2.068	2.828	0.7235	0.5725	0.8765	2.1785	2.5975	1.639	2.937	2.224	2.766	0.939	1.5975	1.934	1.124	0.6055	0.933	0.3495	0.7795	0.397
8344	2.013	1.2575	3.0465	1.569	1.869	2.2845	1.472	1.556	1.933	1.4345	1.512	0.216	1.757	0.8455	0.634	0.568	0.6725	0.1635	1.027	0.167
8349	3.624	3.3135	3.6405	3.9265	3.719	3.462	3.8695	1.9435	2.928	3.3875	2.8065	0.2785	3.318	3.0505	1.5805	3.2695	2.2995	0.3465	2.8205	0.253
8383	1.2735	2.452	1.704	1.123	3.3855	1.3755	1.2145	1.1685	2.302	1.248	2.7135	0.346	1.5725	2.181	0.752	0.538	0.7855	0.254	0.9465	0.248
8477	2.933	2.3325	2.2445	1.631	2.2995	3.4035	1.6615	2.4245	3.1935	3.9885	3.0535	1.6685	3.0685	3.0605	2.724	1.949	2.844	0.6245	3.026	0.607
8482	2.3015	1.729	1.608	1.23	1.898	2.1575	1.1985	2.373	3.2315	1.8885	2.318	0.3355	2.2605	2.783	1.4325	1.409	1.7775	0.368	2.5905	0.369
8585	0.9975	0.461	0.3765	0.4495	0.198	0.6915	0.6445	1.1745	0.6525	0.6005	0.4285	0.7665	0.581	0.4945	0.2215	0.3005	0.3	0.965	0.454	0.1925
8706	2.294	2.1595	3.581	2.5115	2.9885	2.3535	2.4735	1.857	1.831	1.3865	1.6795	0.2385	2.626	2.643	2.103	2.035	2.0235	0.228	3.2595	0.847

Table 8.3 A. Raw ELISA OD values from 4 month convalescent (C) time-point

	6398C3	7134C3	6408C3	7160C3	6429C3	7204C3	6430C3	7323C3	6433C3	7391C3	6485C3	7410C3	6964C3	7506C3	7084C3	7630C3	7642C3	6387C3	7250C3
6387	3.1145	3.2535	3.4835	2.3905	2.5035	3.2945	3.112	2.9515	4.237	3.0205	2.5485	2.6465	2.6005	3.103	2.9165	3.1595	3.883	3.517	3.268
6408	0.676	0.5125	1.4925	0.345	0.3825	0.444	0.3355	0.4695	0.536	0.6935	0.5805	0.8815	0.4675	0.44	0.535	1.077	2.9185	2.8155	3.0855
6429	1.8165	2.7125	2.8355	2.927	2.321	2.8955	1.8215	2.5915	2.3205	2.5915	2.132	2.483	2.8715	2.2935	3.1085	2.6895	2.939	3.2075	3.002
6430	0.5395	0.5205	0.6885	0.4215	0.3595	0.387	0.596	0.2925	0.45	0.4115	0.381	0.5745	0.897	0.6575	0.424	0.659	3.546	3.533	2.858
6433	0.8855	1.1345	1.482	0.995	0.571	0.8675	0.934	1.051	1.545	2.2635	1.058	1.1155	1.322	1.4325	1.524	2.5125	2.758	2.993	3.2555
6485	3.631	2.998	1.976	0.8335	2.499	3.0775	0.6525	0.6765	1.5055	1.8015	1.9106	0.848	0.766	0.8035	0.727	2.6105	1.256	0.7995	1.2385
6964	1.5785	2.3125	2.5675	1.4475	1.382	2.205	1.379	1.596	1.149	1.8755	1.48	1.889	1.807	1.831	1.6135	2.072	1.3145	2.333	1.7415
7045	0.6245	0.63	0.818	0.636	0.451	0.562	0.5395	0.7855	0.4685	0.661	0.4495	0.683	0.3955	0.5805	0.644	1.039	0.927	1.336	0.779
7069	3.35	2.2485	2.605	2.648	1.6835	2.5895	1.7015	2.004	2.2575	2.0545	1.8575	1.884	2.38	2.22	2.8475	2.6115	2.2215	1.6725	1.9055
7116	2.289	1.5455	1.1875	0.509	0.775	1.743	1.37	1.744	0.959	1.5135	0.981	1.3365	1.8095	1.669	0.466	1.59	1.563	0.5575	0.802
7134	2.2535	2.394	3.0055	1.028	1.858	2.305	1.4605	1.5275	2.333	3.0945	2.5365	2.411	1.6245	1.756	1.1975	1.3685	2.745	0.64	0.8365
7157	1.2695	1.49	1.8805	1.397	0.8805	1.5075	1.029	1.245	1.05	1.5035	0.952	1.4335	1.406	1.41	1.0565	1.95	1.2205	1.2315	1.058
7160	1.417	1.5765	1.8935	1.378	1.0265	1.711	1.004	1.2405	1.085	1.516	1.134	1.4615	1.5335	1.332	1.102	1.7305	1.053	1.298	1.076
7183	2.77	3.5505	3.736	3.6605	1.355	1.8265	1.9595	2.502	2.361	2.912	0.2975	0.312	3.0645	2.7505	3.443	3.0115	2.189	2.6035	2.775
7198	2.54	2.19	2.237	2.307	1.173	2.367	1.5355	2.0035	2.2595	1.991	1.743	2.154	1.357	2.045	2.1805	2.2035	2.06	2.309	2.0415
7204	1.1315	1.8105	1.835	1.105	1.074	2.454	0.7225	0.915	1.013	1.4325	0.907	1.341	1.554	1.2925	2.1255	1.3335	1.813	2.0545	1.614
7249	1.3265	1.793	1.746	2.6295	0.9355	1.077	1.436	2.0195	1.725	1.6105	1.492	1.455	2.0685	2.081	2.3715	1.779	1.5125	1.639	1.684
7250	2.446	2.948	2.8745	2.5415	2.0305	2.905	2.5335	2.316	2.002	1.7435	1.973	1.745	2.112	1.9325	2.1025	2.306	1.216	2.5825	2.557
7323	3.307	2.7675	2.2065	2.228	1.1655	2.182	1.259	1.8765	1.981	2.2385	1.62	1.374	1.835	2.1365	2.3475	2.082	1.8015	1.335	1.448
7337	3.0165	3.2425	3.629	2.981	2.665	3.1385	2.721	2.995	3.1565	3.251	2.411	2.704	2.8855	2.8795	2.931	3.2535	3.636	3.179	2.2105
7391	1.34	0.8015	1.7025	0.6415	0.94	1.8025	1.4	1.975	0.5945	1.5585	1.225	1.342	0.513	0.579	0.564	2.093	1.1135	0.734	1.3585
7410	0.836	0.2155	0.5805	0.524	0.2955	0.341	0.3495	0.607	0.454	0.213	1.11	0.664	0.279	0.3575	1.0005	0.853	0.9695	0.5685	0.5735
7506	1.311	2.039	1.9575	1.5035	1.069	1.5355	1.07	1.2595	1.101	1.646	1.1025	1.525	1.53	1.887	1.3205	2.0015	1.1755	1.1995	1.166
7530	3.005	2.4365	2.026	2.306	2.149	3.0885	2.6675	2.4985	2.558	2.782	2.3495	1.769	2.925	2.502	2.1485	3.0245	2.421	2.4865	2.1955
7630	3.0665	3.7855	3.306	2.923	2.2335	3.131	1.382	2.4645	2.1775	3.6595	2.6035	2.843	2.208	1.9815	3.009	2.9215	2.0765	2.5985	1.841
7781	3.286	2.359	2.208	0.6005	1.223	2.323	0.6715	0.637	1.1515	1.3595	1.7285	2.1645	1.3085	2.556	0.7115	2.2845	3.3775	1.5285	1.8595
7799	1.8375	2.025	2.036	1.706	1.1235	1.9105	1.129	1.4595	1.6325	1.7175	1.325	1.7475	1.4555	1.6685	2.153	1.7685	1.83	1.466	1.442
7864	2.463	1.409	1.5935	1.346	0.872	1.7775	0.972	1.26	1.185	1.486	1.087	1.3855	1.2555	1.63	1.485	1.5605	1.806	1.486	1.4055
8204	1.2485	0.8175	2.1735	0.716	0.579	0.7475	2.4325	2.6705	0.6175	0.855	0.6715	0.572	0.849	0.7465	0.633	2.646	1.8565	1.656	2.0845
8344	1.364	2.4075	2.1475	2.5355	2.024	2.295	0.907	1.437	1.732	3.182	2.3675	1.653	1.8985	2.1475	2.445	1.809	1.893	2.08	2.017
8349	3.5255	4.3072	3.6485	3.9405	3.501	3.889	3.1415	3.781	3.4055	3.6255	3.7075	3.7535	3.7915	3.579	3.992	2.374	1.7235	3.5425	3.6525
8383	1.62	1.2735	1.612	0.578	0.958	2.164	0.9095	1.5315	1.149	2.006	0.8375	2.016	2.06	2.6	0.6195	1.8015	1.75	1.0935	1.264
8477	3.442	3.036	3.673	2.8495	1.9145	2.769	2.1845	3.059	2.0755	2.798	1.742	2.6505	2.1885	2.9995	2.682	2.7285	3.341	3.1935	2.7055
8482	2.411	2.2335	2.7385	3.242	1.23	2.23	1.782	1.841	1.582	2.1635	1.38	1.566	1.6365	2.5045	2.017	2.0425	2.8675	2.327	2.1765
8585	0.781	0.23	0.68	0.5955	0.3075	0.33	0.373	0.583	0.3325	0.2195	0.733	0.515	0.2675	0.3255	0.528	0.6225	1.1915	1.719	1.009
8706	2.729	3.5895	2.925	3.2985	2.424	2.8175	1.686	2.526	2.0985	3.6495	2.441	2.4175	2.6345	2.627	2.6705	2.656	2.329	2.3255	2.3975

Table 8.3 B. Raw ELISA OD values from 4 month convalescent (C) time-point

	7045C3	7530C3	7069C3	7799C3	7116C3	7864C3	7157C3	8204C3	7183C3	8344C3	7198C3	8349C3	8383C3	8472C3	8477C3	8482C3	8618C3	8706C3	8585C3
6387	2.27	1.7325	2.8175	3.0795	3.217	0.6035	3.3525	3.3235	0.987	1.443	3.4785	3.081	2.475	2.32	1.757	2.5165	2.936	0.571	0.57
6408	1.3315	2.8905	2.651	2.844	2.573	0.4905	3.118	3.2395	2.8535	2.879	2.4325	3.1675	2.065	2.421	2.0845	2.512	2.375	0.4375	0.5055
6429	1.055	3.1685	3.639	3.456	3.412	0.2505	3.157	1.869	2.4505	3.237	3.6595	2.9595	2.7935	1.9205	1.735	1.8205	3.299	0.234	0.235
6430	1.6605	2.7765	3.351	2.814	3.1025	0.798	3.34	2.9085	3.411	3.05	3.493	3.026	2.0785	2.995	2.703	3.032	3.041	0.501	0.538
6433	1.567	3.1565	3.149	3.0955	2.825	0.366	3.2495	3.6055	3.185	3.7025	3.051	3.1415	1.519	1.518	1.415	1.6555	1.7665	0.4	0.4
6485	1.1875	1.5265	1.554	2.416	1.1155	0.4015	2.0705	1.6055	0.647	0.7195	1.1405	0.946	1.6015	0.7305	0.563	0.989	1.1975	0.447	0.4865
6964	1.652	1.6255	1.508	1.9095	1.4705	0.1905	1.9045	1.05	0.873	1.06	2.225	1.438	0.882	0.636	0.619	0.7805	1.069	0.173	0.194
7045	0.7147	0.1175	0.6565	0.9845	0.929	0.13	1.026	0.901	0.7545	0.5035	1.161	1.045	0.421	0.29	0.2125	0.3085	0.322	0.1075	0.1095
7069	0.7455	2.086	2.6615	2.9865	2.1595	0.2405	2.6375	2.126	1.441	2.3375	2.67	2.025	1.1457	0.833	0.8323	0.8837	1.2267	0.2685	0.2718
7116	0.673	1.0795	1.0605	1.877	1.594	0.3395	2.0125	2.0395	0.9765	1.098	2.0325	2.02	0.9115	0.797	0.3905	1.008	0.7825	0.2735	0.284
7134	1.2015	1.0335	1.0405	1.282	2.2495	0.497	1.2505	1.362	1.103	1.215	1.2075	0.921	0.7995	0.524	0.737	1.0225	0.697	1.083	0.366
7157	0.7855	0.847	0.863	1.2225	0.8625	0.2215	1.118	0.936	0.647	0.7925	1.0405	0.945	0.7095	0.668	0.5445	0.8075	0.845	0.1555	0.1495
7160	0.91	0.7905	0.844	1.132	0.951	0.1945	1.175	0.7845	0.7945	0.8185	1.2355	0.988	0.9765	0.699	0.625	0.7685	0.9775	0.1585	0.154
7183	0.669	2.589	2.5095	3.063	2.8295	0.2025	2.553	1.6035	1.682	2.795	3.3975	2.7665	2.978	2.2365	1.8375	2.2765	3.3645	0.3175	0.378
7198	0.5745	1.7185	1.5155	2.7185	2.3975	0.351	2.096	2.245	0.9595	1.2485	3.022	2.268	0.99	0.808	0.7945	0.764	0.7155	0.701	0.876
7204	2.036	1.348	2.0485	2.057	2.3015	0.2115	1.951	1.028	1.3415	1.685	2.7655	1.594	0.732	0.56	0.42	0.575	0.8715	0.1965	0.221
7249	2.2875	1.393	2.267	2.3395	2.1365	0.1845	2.011	1.089	1.6605	1.7505	2.922	1.573	0.9425	0.806	0.639	0.7575	1.1115	0.179	0.161
7250	2.713	2.419	1.9585	2.885	3.5275	0.459	2.5335	1.2695	0.7805	0.9965	2.4675	1.9115	1.028	0.9687	0.7805	1.4125	1.2825	0.2625	0.2175
7323	0.5615	1.453	1.8835	2.518	1.617	0.2215	1.99	1.9625	1.1795	1.7505	2.0335	1.74	0.8595	0.767	0.693	0.723	0.586	0.748	0.821
7337	3.1235	2.913	2.133	2.861	1.327	0.4005	3.05	2.1125	2.0945	2.311	2.6435	2.366	1.1175	2.1855	1.7735	2.2755	2.061	0.3255	0.0655
7391	0.997	1.043	1.376	2.296	0.681	0.391	0.8265	0.7135	0.4785	0.529	1.1365	0.779	1.684	0.686	0.5115	0.803	1.6455	0.398	0.438
7410	0.301	0.591	0.2965	0.4735	0.405	0.524	0.314	0.593	0.463	0.636	0.745	0.8575	0.2395	0.2445	0.2195	0.2465	0.222	0.201	0.2075
7506	1.2345	1.0635	1.0955	1.261	1.0525	0.159	1.3965	0.8875	0.714	0.9615	1.465	1.13	1.071	0.759	0.6175	0.7715	1.21	0.142	0.1485
7530	0.7375	0.736	0.8125	1.702	0.8355	0.339	1.1635	1.293	0.523	0.8955	1.5105	1.5905	1.059	0.7795	0.9925	1.6925	1.9015	0.1895	0.168
7630	2.717	1.6235	2.7405	2.8335	2.731	0.2525	2.558	1.4965	1.9045	2.137	3.68	2.105	1.7335	1.078	0.9235	1.1165	2.163	0.17	0.1725
7781	1.5695	1.7595	2.1675	3.1635	1.4445	0.85	2.122	2.4155	2.0235	2.2805	1.451	1.358	1.76	0.8225	0.6775	1.288	1.889	0.437	0.458
7799	1.228	0.982	1.2005	1.369	1.2625	0.1635	1.5655	1.0325	0.8885	0.8675	1.453	0.915	0.9855	0.7105	0.688	0.973	1.217	0.1725	0.1645
7864	0.389	1.2245	1.1095	2.3145	1.252	0.261	1.5015	1.776	0.901	0.9405	1.5605	1.499	0.242	0.259	0.2685	0.2605	0.26	0.2745	0.28
8204	1.676	2.258	2.4955	3.198	2.3885	0.893	2.451	2.5755	2.427	2.333	1.572	1.485	1.4425	1.122	0.539	1.2465	0.741	0.4015	0.4075
8344	3.042	2.134	2.7365	2.332	2.483	0.171	2.3745	1.372	2.0105	2.1005	3.2305	1.8575	0.9325	0.7945	0.5715	0.758	1.1015	0.16	0.1635
8349	1.113	3.624	3.983	3.9265	3.8595	0.2865	3.7015	2.613	3.122	3.7755	3.954	3.4975	3.399	3.2015	3.24	3.1105	3.5675	0.3065	0.0585
8383	0.842	1.191	1.24	2.174	1.1205	0.3765	2.1035	1.7805	0.6435	0.7145	1.3095	1.5555	1.2535	0.9055	0.4635	0.837	0.83	0.239	0.2645
8477	1.1065	2.4125	2.3085	3.122	2.8115	0.732	2.7765	2.662	1.9565	2.261	2.689	2.3695	0.721	0.6455	3.634	0.5985	0.589	0.6025	0.635
8482	0.721	1.75	1.937	2.8205	1.928	0.3685	3.295	2.022	1.252	1.471	2.181	1.953	0.337	0.3145	0.373	1.378	0.3725	0.378	0.394
8585	0.468	0.8805	0.437	0.5725	0.5165	0.771	0.439	0.7135	0.4745	0.7125	0.767	0.8685	0.1965	0.2005	0.1875	0.1945	0.183	0.186	0.821
8706	1.168	2.203	2.8155	3.132	2.725	0.294	2.261	1.7365	1.967	2.571	3.41	2.5285	2.9035	2.111	1.8735	2.0785	3.1095	0.8415	0.2395

end Result Report

FP

ASKalfa 3050ci

mware Version 2LC_2F00.004.023 2012.09.07

18/11/2013 10:49
[2LC_1000.007.003] [2K9_1100.002.001] [2LC_7000.004.019]

No.: 003145 Total Time: -°--'--" Page: 001

rror Type : Server

ument: **doc00314520131118104910**

Date and Time	Destination	Times	Type	Result	Resolution/ECM
18/11/13 10:49	**jjemutai**	-°--'--"	E-mail	ERROR	300x300/-

[N2Q3327887]